2017

Investigation on the Performance of a Long Breathing Lean NOx Trap Using n-Butanol

Christopher Aversa
University of Windsor

Follow this and additional works at: https://scholar.uwindsor.ca/etd

Investigation on the Performance of a Long Breathing Lean NO$_x$ Trap Using n-Butanol

by

Christopher Aversa

A Thesis
Submitted to the Faculty of Graduate Studies
through Mechanical, Automotive, and Materials Engineering
in Partial Fulfillment of the Requirements for
the Degree of Master of Applied Science at the
University of Windsor

Windsor, Ontario, Canada

Investigation on the Performance of a Long Breathing Lean NO_x Trap Using n-Butanol

by

Christopher Aversa

APPROVED BY:

_____

X. Xu

Department of Civil and Environmental Engineering

_____

J. Tjong

Department of Mechanical, Automotive, and Materials Engineering

_____

M. Zheng, Advisor

Department of Mechanical, Automotive, and Materials Engineering

_____

G. Reader, Advisor

Department of Mechanical, Automotive, and Materials Engineering

10 April 2017

AUTHOR'S DECLARATION OF ORIGINALITY

I hereby certify that I am the sole author of this thesis and that no part of this thesis has been published or submitted for publication.

I certify that, to the best of my knowledge, my thesis does not infringe upon anyone's copyright nor violate any proprietary rights and that any ideas, techniques, quotations, or any other material from the work of other people included in my thesis, published or otherwise, are fully acknowledged in accordance with the standard referencing practices. Furthermore, to the extent that I have included copyrighted material that surpasses the bounds of fair dealing within the meaning of the Canada Copyright Act, I certify that I have obtained a written permission from the copyright owner(s) to include such material(s) in my thesis and have included copies of such copyright clearances to my appendix.

I declare that this is a true copy of my thesis, including any final revisions, as approved by my thesis committee and the Graduate Studies office, and that this thesis has not been submitted for a higher degree to any other University or Institution.

ABSTRACT

As regulations for nitrogen oxide (NO_x) emissions continue to be tightened, the need for both alternative fuels and intensive exhaust after-treatment will increase. n-Butanol as an alternative fuel has demonstrated the potential to reduce both NO_x and particulate matter (PM) emissions, simultaneously. The use of n-butanol in a compression ignition (CI) engine was studied on an engine test bench, at low and medium load. Engine-out NO_x emissions were reduced with the application of exhaust gas recirculation (EGR), although, they were not low enough to meet emission regulations, indicating that further NO_x reduction in the exhaust would be required. Lean NO_x trap (LNT) experiments were conducted on an after-treatment flow bench using simulated exhaust conditions. n-Butanol proved to be a more effective reductant than diesel for regeneration at 3% exhaust oxygen concentration, due to a higher hydrogen production, although at 0% exhaust oxygen concentration, diesel was slightly more effective than n-butanol. The long breathing n-butanol LNT strategy of this work proved to be capable of reducing the fuel penalty associated with an LNT by nearly 90% compared to the conventional LNT operating schemes, while simultaneously achieving ultra-low NO_x emissions.

DEDICATION

This thesis is dedicated to my parents, Domenic and Kirsty Aversa.

Dad, thank you for your continued encouragement and constant emphasis on the importance of education.

Mom, thank you for your loving support and useful advice in everything that I do.

I couldn't be where I am today without you both.

Love,

Your son,

Christopher

ACKNOWLEDGEMENTS

TABLE OF CONTENTS

LIST OF TABLES

LIST OF FIGURES

LIST OF NOMENCLATURE

Abbreviations

ATR	Autothermal Reforming	[-]
CA	Crank Angle	[°]
CA50	Crank Angle of 50% Cumulative Heat Release	[°CA]
CAI	California Analytical Instruments	[-]
CAFE	Corporate Average Fuel Economy	[mpg]
CARB	California Air Resources Board	[-]
CCEL	Clean Combustion Engine Laboratory	[-]
CI	Compression Ignition	[-]
CLD	Chemiluminescence Detector	[-]
CNG	Compressed Natural Gas	[-]
DEF	Diesel Exhaust Fluid	[-]
DI	Direct Injection	[-]
DME	Dimethyl Ether	[-]
DOC	Diesel Oxidation Catalyst	[-]
DPF	Diesel Particulate Filter	[-]
DR	Dry Reforming	[-]
EGR	Exhaust Gas Recirculation	[-]
EPA	Environmental Protection Agency	[-]
FPGA	Field Programmable Gate Array	[-]
FTIR	Fourier Transform Infrared Spectrometer	[-]
FSN	Filter Smoke Number	[-]

GHG	Greenhouse Gas	[-]
HCCI	Homogenous Charge Compression Ignition	[-]
HDD	Heavy-Duty Diesel	[-]
HFID	Heated Flame Ionization Detector	[-]
HSV	Hourly Space Velocity	$[hr^{-1}]$
ICE	Internal Combustion Engine	[-]
IMEP	Indicated Mean Effective Pressure	[bar]
LNG	Liquid Natural Gas	[-]
LNT	Lean NO_x Trap	[-]
LPG	Liquefied Petroleum Gas	[-]
LTC	Low Temperature Combustion	[-]
MAF	Mass Air Flow	[g/s]
NDIR	Nondispersive Infrared	[-]
NI	National Instruments	[-]
NSR	NO_x Storage/Reduction	[-]
PC	Personal Computer	[-]
p_{inj}	Injection Pressure	[bar]
PM	Particulate Matter	[-]
PO_x	Partial Oxidation	[-]
ppm	Parts per Million	[ppm]
PWM	Pulse Width Modulation	[-]
SCR	Selective Catalytic Reduction	[-]
SI	Spark Ignition	[-]

SR	Steam Reforming	[-]
TWC	Three-Way Catalyst	[-]
UHC	Unburned Hydrocarbon	[-]
WGS	Water Gas Shift	[-]
λ	Excess Air Ratio	[-]

Chemical Formulae

Al_2O_3	Aluminum Oxide
$BaCO_3$	Barium Carbonate
$Ba(NO_2)_2$	Barium Nitrite
$Ba(NO_3)_2$	Barium Nitrate
BaO	Barium Oxide
$C_1H_{1.8}$	Equivalent Diesel Chemical Formula
C_3H_6	Propene
$C_4H_{10}O$	Butanol
CeO_2	Ceria
CH_4	Methane
$CO(NH_2)_2$	Urea
CO	Carbon Monoxide
CO_2	Carbon Dioxide
H_2	Hydrogen
H_2O	Water
N_2	Nitrogen
N_2O	Nitrous Oxide

NH_3	Ammonia
NO	Nitrogen Monoxide
NO_2	Nitrogen Dioxide
NO_x	Oxides of Nitrogen
O_2	Oxygen
Pt	Platinum
Rh	Rhodium
Si	Silicon

CHAPTER 1: INTRODUCTION

1.1   Motivation

Each year, global automotive consumers' demands consistently challenge automotive engineers and suppliers to devote extensive time on the research of an efficient, cost effective, and environmentally friendly means of transportation. Currently, the most common fuels used in modern on-road vehicles are liquid carbon based fossil fuels such as diesel and gasoline. Compression ignition (CI) diesel engines are typically highly fuel efficient compared to spark ignition (SI) gasoline engines, due to their high compression ratios and lean air fuel operation [1]. Internal combustion engines (ICEs), however, produce harmful exhaust pollutants that can be damaging to both the environment and human health. These exhaust pollutants include: carbon dioxide (CO_2), oxides of nitrogen (NO_x), particulate matter (PM), carbon monoxide (CO), and unburned hydrocarbons (UHC).

In order to minimize the overall quantity of harmful pollutants emitted from ICE vehicles, government bodies such as the United States Environmental Protection Agency (EPA) and the California Air Resources Board (CARB) have implemented exhaust emission regulations for gasoline and diesel engines for various automotive applications. Over the past several decades, exhaust emission limits have drastically reduced, in particular NO_x and PM tailpipe emissions in heavy-duty diesel (HDD) vehicles. The trend of the reduction of NO_x and PM allowed in heavy-duty diesel vehicles from 1988 to 2017 is displayed in Figure 1.1. NO_x emissions allowed in heavy-duty diesel exhaust has reduced from 14.3 g/kW·hr in 1988 to 0.268 g/kW·hr in 2007 [2]; a 98.1% total reduction over 19 years.
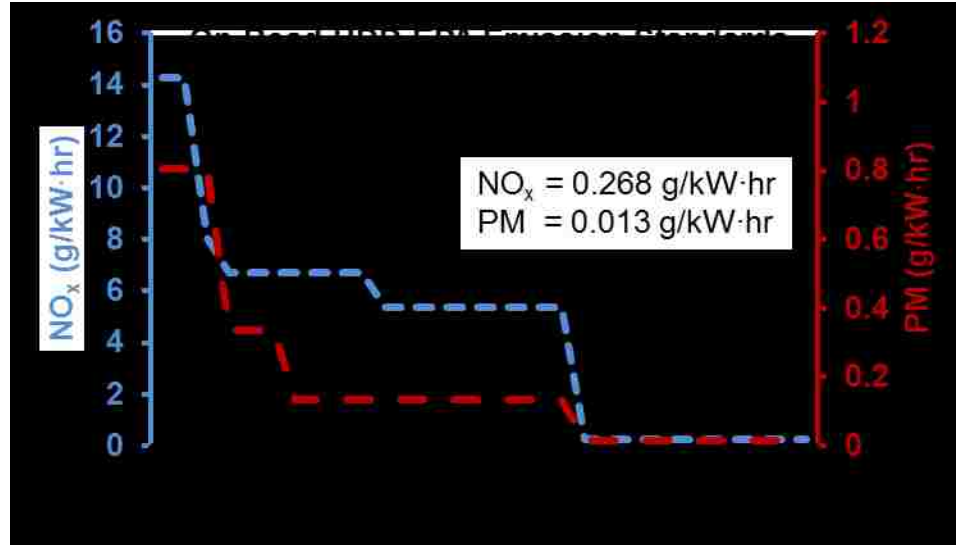
Figure 1.1 – EPA Heavy-Duty Diesel Emission Standards [2]

Regulated NO_x emissions include both nitrogen dioxide (NO_2), and nitrogen monoxide (NO), which can readily oxidize into NO_2 in the atmosphere [3]. The pollutant NO_2 can react with various compounds in the air to produce acid rain, which can damage forests and cause lakes and streams to become acidic, and smog, which can lead to lung damage and reduction in lung function in humans [4].

In conventional direct injection (DI) diesel engine operation, diffusion combustion typically dominates for the heterogeneous in-cylinder charge, which can lead to high temperature locally stoichiometric and fuel rich zones that contribute to NO_x and PM formation. Lean operations of DI diesel engines, however, provide abundant oxygen within the cylinder, which assists in oxidizing a portion of the PM formed. The formation of NO_x is accelerated at high temperatures (i.e. ~2000°C and above), which may occur when the flame site is not adequately lean or diluted. Abundant oxygen in the exhaust also makes it difficult to reduce NO_x back into inert N_2 gas. Because of the conventional operation of diesel engines, NO_x emission reduction can be quite challenging, and meeting current EPA emission regulations often requires both in-cylinder and exhaust

after-treatment NO_x reductions. With CARB's implementation of the "Mobile Source Strategy" in the state of California, NO_x emission standards can potentially reduce by up to another 80% within the next 15 years, indicating that more intensive NO_x reduction from gasoline and diesel vehicles will be required in the future [5, 6].

Aside from NO_x emissions, the EPA also plans to enforce regulations on greenhouse gas (GHG) emissions for heavy-duty diesel vehicles, beginning in the year 2021 [7]. These GHG emissions include carbon dioxide (CO_2), methane (CH_4), and nitrous oxide (N_2O). Since CO_2 is inherently formed during hydrocarbon fuel combustion, the amount of CO_2 produced will be proportional to the amount of fuel burned. Therefore, CO_2 emissions are governed via a vehicle's fuel economy, and thus regulated by corporate average fuel economy (CAFE) standards.

In order to meet current and future emission regulations, automotive manufacturers are required to implement numerous emission reduction strategies. The emission reduction strategies most commonly used in modern vehicles can be divided into two categories: in-cylinder, and exhaust after-treatment. The focus of this research is on the reduction of NO_x emissions, so the strategies relating to NO_x reduction will be specifically emphasized in the following sections.

1.2   In-Cylinder Emission Reduction

During combustion, the formation of regulated pollutants is inevitable. If, however, the combustion strategy or in-cylinder mixture is altered, the concentration of various emissions can be affected. The in-cylinder emission reduction strategies include: exhaust gas recirculation (EGR), advanced injection strategies, and the use of alternative fuels such as biofuels or oxygenated fuels.

The application of EGR can reduce the intake oxygen concentration as well as increase the specific heat capacity of the in-cylinder charge by recirculating a portion of the exhaust gas back into the cylinder. This, in turn, can lower the peak in-cylinder temperature, thus reducing the formation of NOx [8]. This however, reduces the concentration of oxygen available for PM oxidation. The impact of EGR on NO_x and PM emissions is displayed in Figure 1.2. The trade-off between NO_x and PM is well-documented and is often referred to as "slope 1". As the amount of EGR increases further, the ignition delay generally increases due to a lack of oxygen, which can result in more premixed combustion thereby suppressing the formation of PM; this is referred to as "slope 2". This region of simultaneously low NO_x and PM is referred to as low temperature combustion (LTC), which may eventually lower the flame temperature to ~1500°C.
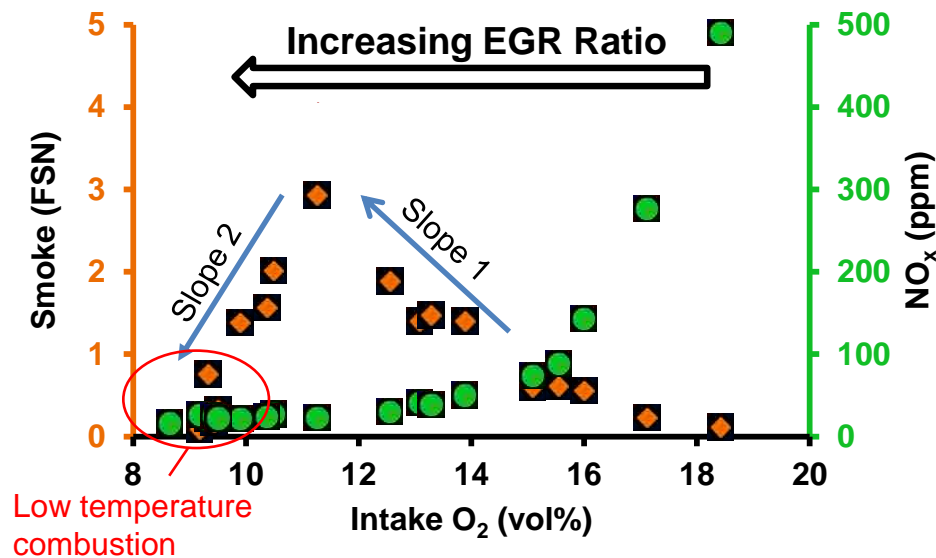
Figure 1.2 – NO_x and Smoke Emissions vs Intake O_2

Although various researchers have reported the LTC phenomenon at extensive load and operating conditions [9-11], its implementation in commercial vehicles has been

limited due to high intake pressure requirements (in order to compensate for the EGR incurred oxygen shortfall), controllability difficulties, as well as an increase in CO and UHC emissions, indicating a reduction in combustion efficiency [12].

Advanced injection strategies may also be used to reduce exhaust emissions [13]. The main objective of advanced injection strategies, such as the addition of pilot injections, is to enhance the in-cylinder mixing. An early pilot injection can increase the quantity of premixed combustion, thereby reducing PM emissions. In addition, homogenous charge compression ignition (HCCI) combustion can be achieved through the use of multiple injections, during the compression stroke, resulting in simultaneously low NO_x and soot emissions. HCCI combustion however can reduce the engine's operating range and result in a reduced combustion efficiency [14].

Another way to alter the in-cylinder combustion is to use alternative fuels. The volumetric energy density of various fuels used in ICEs is given in Figure 1.3. Compressed gases such as H_2 and compressed natural gas (CNG) have proven to allow low NO_x combustion through operation in slightly modified ICEs [15, 16]. However, they have a low volumetric energy density, and the fuel storage is a significant challenge. Dimethyl-ether (DME), liquid natural gas (LNG), and liquefied petroleum gas (LPG) also require complex fuel storage systems as they are not naturally liquids at standard temperature and pressure. Additionally, a number of different fuels have been produced from biomass sources for use in ICEs. Ethanol has been successfully used in SI engines since the mid-19th century [17]. Due to recent regulations and mandates by the EPA, over 90% of all gasoline sold in the US is blended with a minimum of 10% ethanol [18]. Because of ethanol's high volatility and poor lubricity, it is typically deemed unsuitable

for high pressure injections and therefore not traditionally used in CI diesel engines. Biodiesel and normal-butanol (n-butanol), however, have a higher potential for use in CI engines. Biodiesel is commercially available in many oil-seed producing states as B20 (20:80 biodiesel:diesel fuel blend). n-Butanol is not currently commercially available for use as a fuel for on-road vehicles, although its use in CI engines has been extensively investigated [19-22]. n-Butanol is a four carbon straight chain alcohol fuel that can be produced from biomass sources such as sugar cane, corn, or algae [23]. Compared to diesel, n-butanol has a lower volumetric energy density (30 MJ/L compared to ~43 MJ/L for diesel). Due to the relatively high kinematic viscosity of n-butanol compared to other alcohol fuels, it can be directly introduced into a diesel engine with minimal alteration (i.e. the addition of a lubricity improver). An added benefit involved with the use of biomass derived n-butanol is that it could potentially have near zero net CO_2 emissions since the biomass sources have previously absorbed CO_2 throughout their life cycle [24, 25].
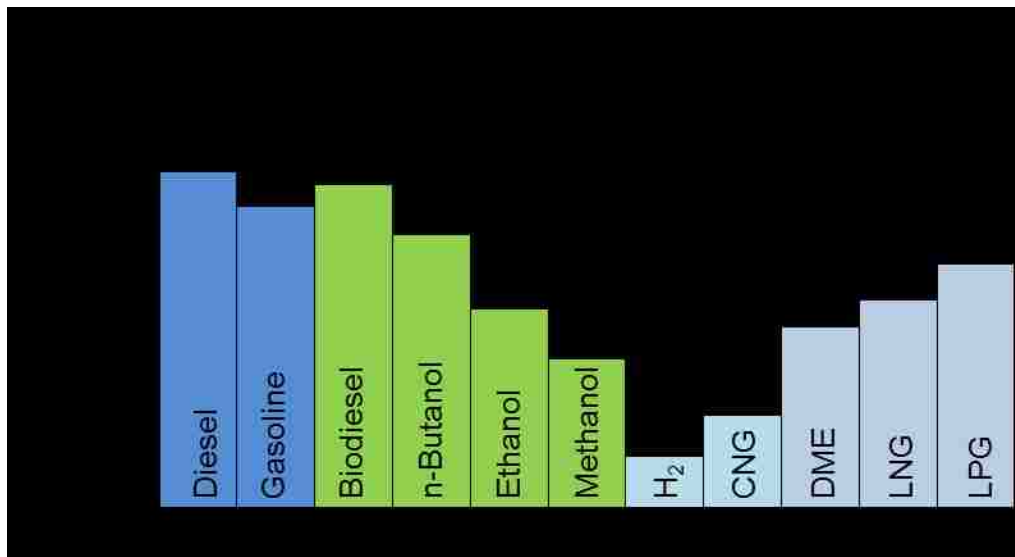
Figure 1.3 – Volumetric Energy Density of Various Energy Sources [26]

A comparison of some chemical and physical properties of n-butanol and diesel is given in Table 1.1. The main chemical properties of n-butanol that directly affect the products of combustion are: the heat of vaporization, the cetane number, and the oxygen content. n-Butanol has a higher heat of vaporization than diesel. This means that more energy must be absorbed from the in-cylinder charge in order to evaporate the fuel. This may result in a lower combustion temperature, which can help to reduce the formation of NO_x. The cetane number of a fuel is inversely proportional to ignition delay. Since n-butanol has a lower cetane number than diesel fuel, it will therefore produce a longer ignition delay. This can result in better in-cylinder mixing and thus reduce PM emissions. The oxygen content of n-butanol can also help to supress the PM formation.

Table 1.1 – Various Fuel Properties of Diesel and n-Butanol

	Diesel	n-Butanol	Remarks
Formula	$C_nH_{1.8n}$	$C_4H_{10}O$	-
Density (kg/m^3)	858	810	-
Oxygen Mass (%)	0	21.6	Benefit PM oxidation
Cetane Number	43	17 - 25	Inversely proportional to ignition delay
LHV (MJ/L)	36.2	29	Lower energy output compared to diesel
$Q_{evaporation}$ (kJ/kg)	316.6	595	Reduce combustion temperature
Boiling Point (°C)	246 - 388	117.5	Enhance Mixing

Currently, DI in-cylinder combustion strategies alone are not enough to reduce emissions below EPA standards at all engine operating conditions. For this reason, exhaust after-treatment is required on on-road vehicles to further reduce emissions. Exhaust after-treatment is also expected to be required even with the use of alternative fuels.

1.3   Exhaust After-treatment

Although in-cylinder emission reduction strategies, such as EGR, are often used in conventional vehicles, reducing engine-out emissions below EPA regulations for a wide range of conditions can be especially challenging. Therefore, further treatment of the exhaust gas is required before it can be released from the vehicle's tailpipe. This is often achieved with the use of exhaust filters and/or catalysts. Conventional SI engines, for example, use a three-way catalyst (TWC) to alternately oxidize CO, and UHC into CO_2 and H_2O, and reduce NO_x into N_2 [27]. Due to the inherent lean operation of diesel engines, the concentration of oxygen in diesel engine exhaust is much higher than in conventional SI engines, and therefore, a TWC cannot be employed as an effective emission reduction catalyst in diesel vehicles. Instead, the reduction of various emissions is required through multiple filters and catalytic converters rather than just one catalyst. These after-treatment devices include: diesel particulate filter (DPF), diesel oxidation catalyst (DOC), selective catalytic reduction (SCR) catalyst, and lean NO_x trap (LNT) catalyst.

1.3.1   Diesel Particulate Filter

A diesel particulate filter (DPF) is an exhaust after-treatment device that is used to trap and oxidize PM. The most common type of DPF that is employed in modern diesel engines is made from wall-flow ceramic cordierite. Figure 1.4 shows a photograph of the front face of a DPF and a schematic of the cut-out view of a DPF. For these filters, alternate channels are blocked so that the exhaust gas must flow through the porous walls, where the larger PM particles are trapped. Eventually the back pressure will increase and may trigger the stochastic regeneration of the DPF. In the case of active

regeneration, a reductant, typically a hydrocarbon fuel such as diesel is introduced into the exhaust stream in order to burn the PM that is stored on the DPF. For this active regeneration, a supplemental fuel injection is required, and can therefore result in a fuel penalty.
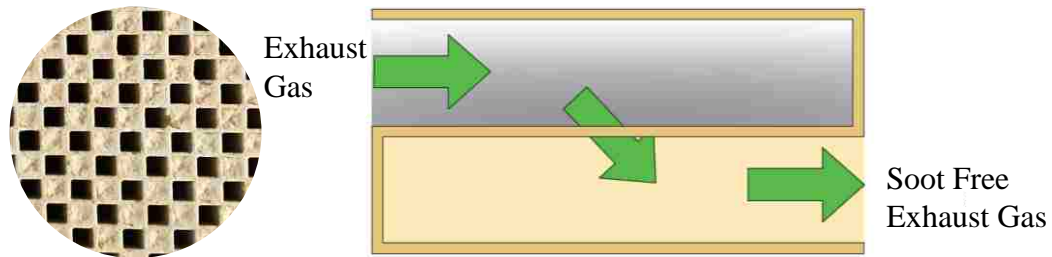
Figure 1.4 – DPF Front Face and Cut-out View Schematic

1.3.2 Diesel Oxidation Catalyst

A diesel oxidation catalyst (DOC) is a flow through catalyst that actively oxidizes CO and UHC into CO_2 and H_2O. Modern DOCs typically feature a ceramic honeycomb monolith, as shown in Figure 1.5, coated with a precious metal substrate that acts as a catalyst during oxidation reactions. Due to the generally high exhaust oxygen concentrations of conventional diesel engines, there is usually sufficient oxygen for the oxidation reactions to occur within the DOC catalyst.
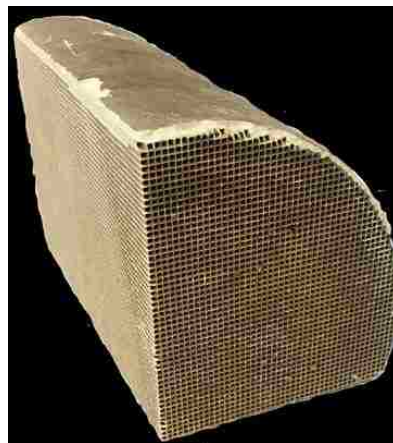
Figure 1.5 – Photograph of a Portion of a Diesel Oxidation Catalyst

9

1.3.3   Selective Catalytic Reduction Catalyst

A selective catalytic reduction (SCR) catalyst is a NO_x reduction catalyst commonly found in present heavy-duty diesel engines. For these devices, a ceramic honeycomb monolith is coated in a base metal oxide catalyst such as vanadium, molybdenum, or tungsten. In principle, the stoichiometric chemical reaction for the reduction of NO_2 over the SCR catalyst is given in Equation 1.1.

$$2NO_2 + 4NH_3 + O_2 \longrightarrow 3N_2 + 6H_2O \qquad \text{(Equation 1.1)}$$

Since ammonia (NH_3) is generally the active reductant for selective NO_x reduction, a constant supply of ammonia, in accordance with the concentration of NOx in the exhaust, is required. In an on-vehicle application, ammonia storage is challenging. In practice, a water-urea (67.5% deionized water, 32.5% $(NH_2)_2CO$) mixture is introduced into the exhaust stream prior to the catalyst. This water-urea mixture, referred to in the industry as diesel exhaust fluid (DEF), is then converted into ammonia and CO_2 (Equation 1.2). The ammonia then reduces the NOx emissions over the SCR catalyst into N_2 and H_2O, through a number of chemical reaction schemes.

$$(NH_2)_2CO + H_2O \longrightarrow 2NH_3 + CO_2 \qquad \text{(Equation 1.2)}$$

There are a number of challenges involved with the use of an SCR catalyst. Some types of zeolite based catalysts demonstrate deactivation in the presence of steam, which can be found in diesel exhaust [28]. Silver aluminum oxide ($Ag\text{-}Al_2O_3$) SCR catalysts can utilize HCs as a reductant, thereby eliminating the need for an external reductant such as urea; however, they are more sensitive to temperature than zeolite or vanadium SCR catalysts [29]. Classic SCR catalytic systems have certain issues such as the storage of urea, difficulty in control, and packaging. The storage and availability of the water-urea

mixture within a vehicle becomes difficult under low environment temperatures as this mixture has a freezing point of -11°C. In order to eliminate this challenge, a heater is often installed in the urea storage tank. Since transient engine operation can result in rapid fluctuations of engine-out NO_x concentrations, the concentration of ammonia supplied can potentially be insufficient or in excess. Excess ammonia can readily be converted into NO_x, so an ammonia slip catalyst is often required downstream of the SCR catalyst. This creates an issue with the packaging of an SCR after-treatment system especially in light-duty diesel vehicles.

1.3.4 Lean NO_x Trap Catalyst

The lean NOx trap (LNT) catalyst is another device used for NO_x reduction in diesel and lean burn gasoline vehicles. Other widely used names for an LNT are: NO_x adsorber catalyst, deNO$_x$ trap, NO_x storage catalyst, or NO_x storage/reduction (NSR) catalyst. The main function of an LNT catalyst is to store and subsequently reduce NO_x into N_2 gas by periodically cycling between lean and rich exhaust conditions. An LNT is typically a monolithic ceramic substrate coated in a high surface area refractory oxide washcoat, such as aluminum oxide (Al_2O_3), with an alkali- or alkaline-earth metal oxide adsorber, and precious metal catalysts that may facilitate the redox reactions required for operation of the LNT. One of the most common formulations of an LNT features platinum (Pt), with barium oxide (BaO) supported on Al_2O_3. This type of LNT is often referred to as a Pt/Ba/Al$_2$O$_3$ LNT. The LNT catalyst is similar in external appearance to the DOC shown in Figure 1.5.

During typical exhaust conditions, the bulk exhaust gas flows through the channels of the monolithic substrate, and the NO_x and reducing agents in the exhaust gas

react in the presence of the catalysts on the washcoat. The LNT catalyst reduces NO_x through periodic cycling of two modes of operation: lean adsorption and rich regeneration.

The lean adsorption takes place during lean exhaust conditions. This is also referred to as the storage period. During the storage period, NO molecules are oxidized over a platinum catalyst (Equation 1.3), and stored on the barium oxide adsorbent as barium nitrate ($Ba(NO_3)_2$) as shown in Equation 1.4 [30]. The storage process is shown in Figure 1.6.

$$NO + \frac{1}{2}O_2 \longrightarrow NO_2 \qquad \text{(Equation 1.3)}$$

$$3NO_2 + BaO \longrightarrow Ba(NO_3)_2 + NO \qquad \text{(Equation 1.4)}$$
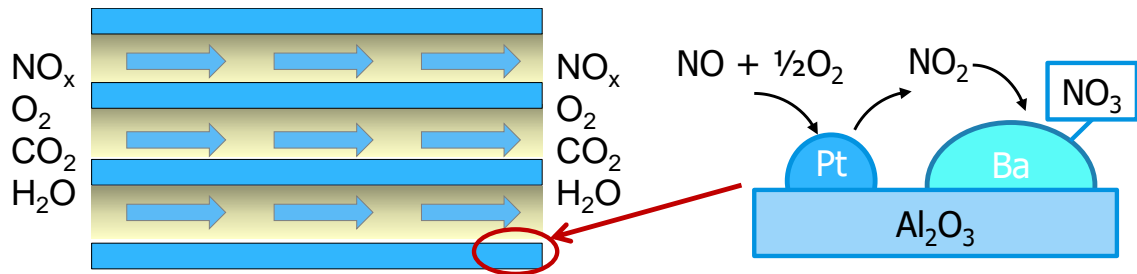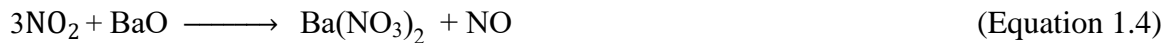
Figure 1.6 – LNT Adsorption Process. Adapted from [31]

The NO_x storage capacity of an LNT is limited, and reduces as the number of BaO sites available for NO_x storage reduces. After a specified saturation of the LNT catalyst is achieved, the rich regeneration period must begin.

Usually, the regeneration of an LNT requires a fuel rich and oxygen deficient environment. The reductant for LNT regeneration is typically introduced on conventional vehicles through an injection of fuel into the exhaust, or a post combustion in-cylinder injection. The regeneration triggers the release of NO_x and consequently reduces the NO_x

into N_2 through various chemical mechanisms that can be summarized by Equation 1.5 – Equation 1.8. The regeneration process is shown in Figure 1.7.

$$5C_1H_{1.8} + 2.9Ba(NO_3)_2 \longrightarrow 4.5H_2O + 5CO_2 + 2.9BaO + 2.9N_2 \qquad \text{(Equation 1.5)}$$

$$8H_2 + Ba(NO_3)_2 \longrightarrow 2NH_3 + BaO + 5H_2O \qquad \text{(Equation 1.6)}$$

$$8CO + Ba(NO_3)_2 + 3H_2O \longrightarrow 2NH_3 + BaO + 8CO_2 \qquad \text{(Equation 1.7)}$$

$$10NH_3 + 3Ba(NO_3)_2 \xrightarrow{\text{Pt}} 8N_2 + 3BaO + 15H_2O \qquad \text{(Equation 1.8)}$$
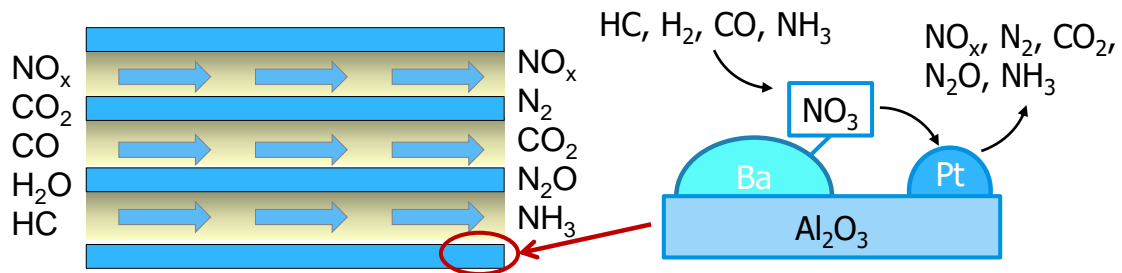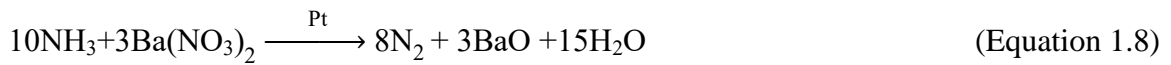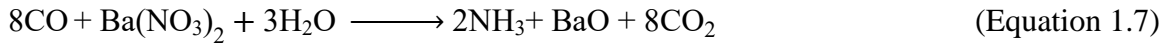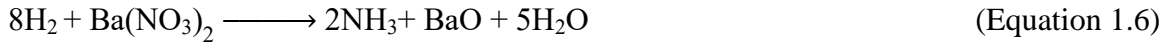
Figure 1.7 – LNT Regeneration Process. Adapted from [31]

Conventional LNT operates by continuously cycling between lean adsorption and rich regeneration. Since a supplementary fuel, or equivalent, is required for the regeneration, a fuel penalty is associated with the LNT. For this reason, the use of an LNT in conventional diesel vehicles is limited. A more detailed study of LNT catalyst operation is provided in Chapter 2.

An additional advantage of an LNT catalyst is its H_2 reforming characteristics. Since a precious metal catalyst is often coated on the LNT washcoat, H_2 can be produced through various chemical reactions [30]. These H_2 reforming reactions will be elaborated on in Chapter 2.

1.4 Long Breathing Lean NO$_x$ Trap Strategy

In typical on-vehicle LNT operation, the adsorption period could be about one minute long and the regeneration period could be around 5-10 seconds [30]. A long breathing LNT features a long adsorption period, basing on a conventional LNT flow bed. Diesel engine-out NO$_x$ emissions can be as high as 1000 ppm, under conventional high temperature combustion [1], and can quickly saturate an LNT, requiring frequent regenerations. However, if the engine-out NO$_x$ emissions can be reduced to 100 ppm or lower, by lowering the in-cylinder flame temperature, the adsorption period can be significantly longer, while still maintaining a low concentration of outlet NO$_x$ throughout the adsorption phase [32]. A concentration of 100 ppm engine-out NO$_x$ is an achievable target for various engine load levels, and would still meet current emission standards at high load even if the storage efficiency of the LNT was low (i.e. below 70%). The advantage of a long breathing LNT strategy is, since the adsorption phase is longer, the time between regenerations will therefore be longer. Assuming that a low pressure injection of the same quantity of fuel is used for each regeneration period, this will therefore reduce the fuel penalty associated with a long breathing LNT, compared to a conventional LNT. The latter would require a regeneration every minute or so, depending on the engine load and speed. A conceptual diagram of the long breathing lean NO$_x$ trap concept compared to the conventional operation of an LNT is shown in Figure 1.8.
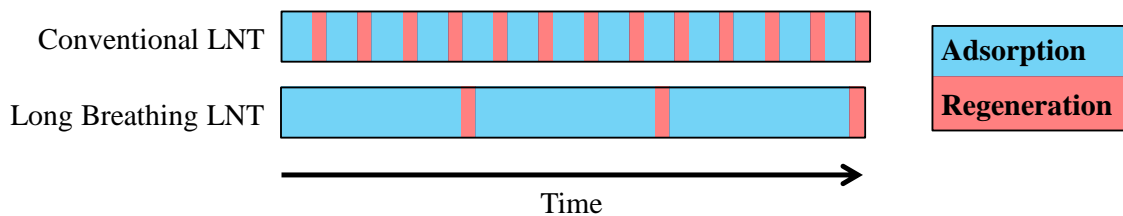
Figure 1.8 – Conventional LNT vs. Long Breathing LNT

In order to achieve low engine-out NO_x emissions, an in-cylinder strategy, such as EGR, must be applied. If however, EGR is the in-cylinder strategy used to reduce NO_x, the PM emissions may increase because of the NO_x-soot trade-off. Due to the operation of the DPF, high PM emissions can possibly result in a fuel penalty due to an increase in the exhaust back pressure and necessity for frequent DPF regenerations [33]. For this reason, an indicated engine-out PM limit of 0.036 g/kW·hr was used for this research, in order to minimize the required DPF filtration efficiency to meet current and proposed future regulations. Although the filtration efficiency of a conventional DPF can be as high as 98%, the DPF tolerance limit selected for this study would still satisfy the current regulations with a much lower DPF filtration efficiency (i.e. below 70%). Thus, engine-out emissions may be classified within the long breathing region if NO_x emissions are at or below 100 ppm and PM emissions are at or below 0.036 g/kW·hr.

1.5   Objectives of this Research

Previously, LNT after-treatment systems had been studied extensively both on an independent flow bench, as well as coupled to an engine exhaust system [34-56], however have only been used sparingly in on-vehicle applications due to their associated fuel penalty and sometimes inconsistent conversion efficiency. As NO_x emission regulations in CI engines continue to tighten, the use of biofuels in CI engines may be identified as a viable option for NO_x reduction. Many different adsorption and regeneration strategies for LNT NO_x reduction have been extensively reported in literature [34-56]; whereas the use of an alternative fuel such as n-butanol to regenerate an LNT catalyst for potential application in CI engine systems has not been extensively tested. The study of n-butanol post-injection has been initiated to reveal the possibility of

incorporating an LNT device in the exhaust [34]; however, the actual regeneration of the LNT using n-butanol has not been reported. Park et al [35] investigated the use of DME in an after-treatment system featuring an LNT and a H_2 reforming catalyst; although, according to the author's search, no other literature was found featuring a reductant other than propene (C_3H_6), CO, H_2, or diesel as a reductant for LNT regeneration. Thus, the main objective of this study is to investigate the use of n-butanol as a reductant in an LNT after-treatment catalyst, mainly the release and conversion of NO_x, as well as the H_2 reforming characteristics. The secondary objective of this study is to reduce the fuel penalty associated with an LNT by applying a long breathing strategy through the combination of EGR and n-butanol DI combustion. The strategy that is proposed in this research is summarized in Figure 1.9.

n-Butanol Combustion   +   Exhaust Gas Recirculation   +   Lean NO_x Trap

- Low PM emissions
- Low net CO_2 emissions

- Lower engine-out NO_x emissions

- Long adsorption period
- Infrequent regeneration
- Reduced fuel penalty
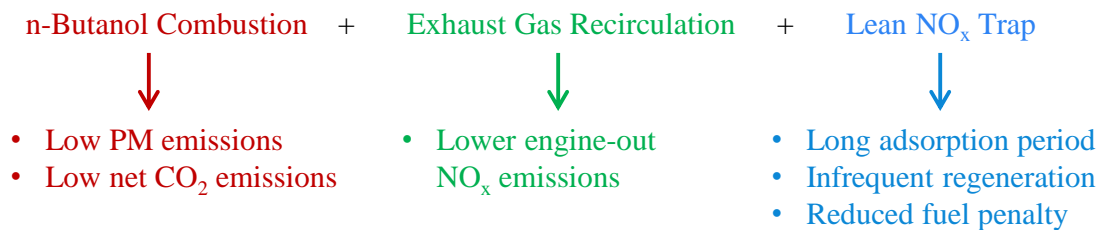
Figure 1.9 – Proposed Strategy for Reduced PM, NO_x, and Fuel Penalty

This study is divided into three parts. The first part of the study focuses on engine tests conducted in order to achieve long breathing LNT exhaust conditions; and subsequently, flow bench tests focusing on the schemes of the LNT for these engine-out NO_x conditions. Engine tests involved the application of EGR in a DI n-butanol CI engine at various engine loads. The second part of the study is to observe the hydrogen generation with n-butanol or diesel on the after-treatment flow bench. The final portion focuses on the regeneration of the LNT. Regeneration was carried out with both diesel

and n-butanol fuel. The flow-bench tests were conducted in different phases to study the storage characteristics of the LNT, the H_2 reforming capability of the LNT, as well as the regeneration of the LNT, individually.

1.6   Structure of the Thesis

The structure of the thesis is as follows:

Chapter 1 is an introduction to CI diesel engine emissions and the current and future emission control strategies.

Chapter 2 is a detailed description of the current state of LNT research and an introduction to H_2 reforming to aid LNT regeneration.

Chapter 3 is a description of the experimental setup at the Clean Combustion Engine Laboratory (CCEL). A detailed breakdown of the engine dynamometer setup and the after-treatment flow bench setup is provided in this chapter.

Chapter 4 elaborates on the engine test results with n-butanol and diesel fuel in the single cylinder research engine at the CCEL. The engine test conditions were recreated on the after-treatment flow bench in order to validate the adsorption concept of the LNT.

Chapter 5 discusses the H_2 generation within the after-treatment flow bench setup using diesel and n-butanol injections into the exhaust stream.

Chapter 6 explains the results from the after-treatment flow bench tests focusing on the regeneration of an LNT catalyst with different gas compositions, and a comparison of diesel and n-butanol as a reductant.

Chapter 7 summarizes the main conclusions of this thesis and provides recommendations for future studies.

CHAPTER 2: LEAN NO$_X$ TRAP CATALYSTS

The LNT catalyst has proven to be an effective NO$_x$ reduction after-treatment device in lean burn diesel engines; however, due to strict CAFE standards, has only been used sparingly in automotive diesel vehicles. It has been relatively phased out due to the increasing popularity of the SCR catalyst, and the wide availability of DEF. The LNT has two main modes of operation: lean NO$_x$ adsorption, and regeneration. This chapter provides a review on the status of LNT research, along with some qualitative analyses.

2.1 Lean NO$_x$ Adsorption

The removal of NO$_x$ emissions from the exhaust during lean exhaust conditions is one of the most attractive operational advantages of the LNT catalyst. The chemical mechanisms involved with NO$_x$ storage are well established in literature. Throughout the storage period, the adsorption sites will eventually become occupied, and the NO$_x$ concentration downstream of the LNT (NO$_x$ slip) will gradually increase, eventually triggering the need for regeneration. The efficiency of the lean NO$_x$ storage is greatly affected by the exhaust temperature, exhaust gas composition, storage duration, and the LNT catalyst material [36-40].

Mazhoul et al [36] investigated the NO$_x$ storage characteristics of multiple Pt/BaO/Al$_2$O$_3$ catalysts, with various formulations, under different gas concentrations on an after-treatment flow bench. The storage capacity of each LNT was increased as the oxygen concentration in the feed gas increased from 0% to 3%. There was no noticeable effect as the oxygen concentration increased above 3%. The maximum storage capacity was achieved for each catalyst at 350°C. High Ba and Pt density LNT formulations also resulted in a high NO$_x$ storage capacity.

Svedberg et al [37] compared the NO$_x$ storage at low temperatures in different types of LNT catalysts. Results showed that effective NO$_x$ storage was achieved at temperatures as low as 100°C in a Pt/BaO/Al$_2$O$_3$ LNT, while the removal of BaO, and the addition of ceria (CeO$_2$) reduced the storage capacity. It was also found that H$_2$O did not significantly affect the NO$_x$ storage performance.

Lindholm et al [38] investigated the effect of H$_2$O and CO$_2$ on the NO$_x$ storage in a Pt based LNT. Three different LNT catalysts were tested: Pt/BaO/Al$_2$O$_3$, Pt/Al$_2$O$_3$, and Pt/Silicon (Si), in a flow reactor. The Pt/BaO/Al$_2$O$_3$ catalyst exhibited the greatest storage capacity of the LNTs tested. H$_2$O and CO$_2$ had a negative effect on the storage of NO$_x$ in all the catalysts tested at temperatures of 200°C and 400°C, and a minimal reduction in storage capacity at temperatures of around 300°C. CO$_2$ had a greater effect than H$_2$O on the Pt/BaO/Al$_2$O$_3$ LNT tested.

Various adsorption phase durations have also been reported in literature. Jeftić et al [39] experimented with various NO$_x$ feed rates into an LNT catalyst on an after-treatment flow bench. A NO$_x$ feed rate of 110 ppm took 11.3 minutes until a NO$_x$ concentration of 20 ppm downstream of the LNT was observed, while a NO$_x$ feed rate of 50 ppm took over 50 minutes to reach the same slip downstream. This strategy effectively reduced the LNT fuel penalty below 1%. Abdulhamid et al [40] experimented with a 40 minute adsorption period with 500 ppm NO$_x$ and used a 5 minute regeneration with H$_2$, CO, or C$_3$H$_6$; thereby after only 4 minutes of adsorption, the NO$_x$ concentration downstream exceeded 400 ppm, indicating a low storage efficiency.

In classical LNT operations, the adsorption period is followed by a transition into rich exhaust conditions, to begin the regeneration of the LNT catalyst.

2.2 LNT Regeneration

In conventional LNT systems, a fuel rich regeneration period is produced through the addition of hydrocarbons in the exhaust. These fuel rich conditions are typically produced by (1) an in-cylinder post injection or (2) a low pressure fuel injection into the exhaust stream. Depending on driving conditions, the rich regeneration period is on average 5-10 seconds. The purpose of the regeneration is to release the NO$_x$ that was stored on the LNT during the adsorption period, and subsequently reduce it to N$_2$. Since the release and reduction of NO$_x$ occur simultaneously, they are difficult to decouple, and thus a portion of NO$_x$ slip is usually observed at the onset of the regeneration period, as shown conceptually in Figure 2.1. By reducing the total NO$_x$ slip, the conversion of NO$_x$ into N$_2$ may potentially be improved.
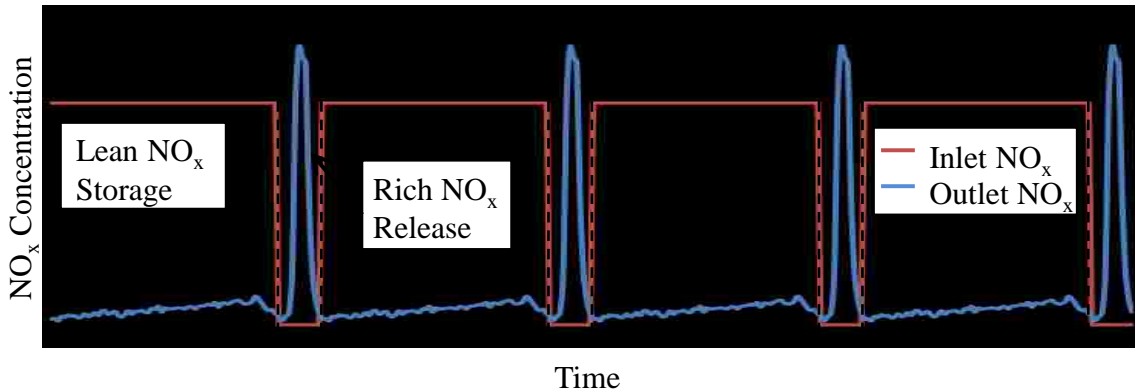
Figure 2.1 – Conceptual Diagram of LNT Periodic Operation – Adapted from [30]

The chemical reaction route by which NO$_x$ is released and reduced during LNT regeneration is less understood than the NO$_x$ storage mechanisms that take place during adsorption. The release of NO$_x$ has generally been attributed to: an increase in temperature due to reductant oxidation, which causes a reduction in stability of surface nitrates [41, 42]; a shift in equilibrium due to a lack of oxygen [43]; and the presence of

CO_2, which can form barium carbonate ($Ba(CO_3)_2$) species in place of surface nitrates [44]. The reaction route of the conversion of NO_x into N_2 is typically summarized by Equation 1.5 – Equation 1.8. The general process of NO_x reduction during LNT regeneration is shown conceptually in Figure 2.2, and can be summarized by the main pathways initially proposed by Clayton et al [45]:

1. Reductant releases NO_x and directly reduces it to nitrous oxide (N_2O) and N_2

2. Reductant reacts with released and stored NO_x to form NH_3 which reacts in the following ways:

    a. NH_3 reacts with released and stored NO_x to form N_2 and N_2O

    b. NH_3 is oxidized to produce N_2, N_2O, and NO

    c. NH_3 decomposes to N_2 and H_2, or is released downstream of the catalyst
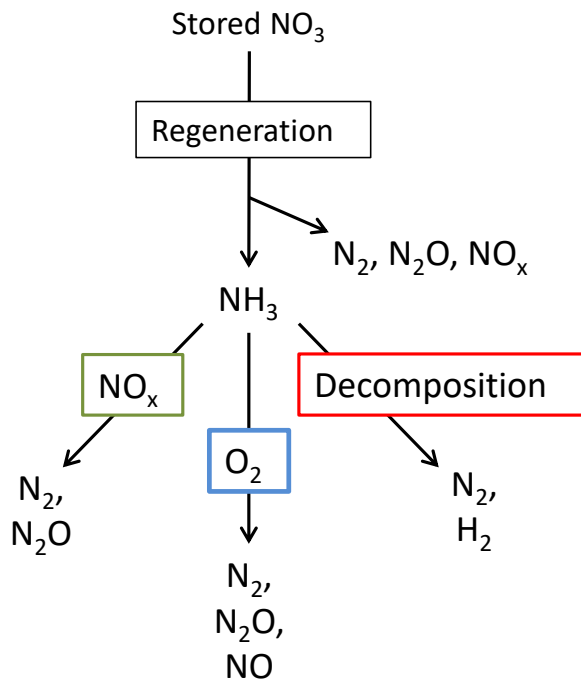
Figure 2.2 – NO$_x$ Reduction Pathways in an LNT – Adapted from [46]

This reaction pathway indicates the existence of a regeneration front that propagates along the LNT flow bed during regeneration. Since NH$_3$ is utilized for NO$_x$ reduction, it is usually observed downstream of the catalyst after the initial peak in NO and N$_2$O, simultaneously with reductant breakthrough. More detail into the chemical reactions can be found in literature [47-49].

Many factors, such as gas composition, reductant type, and regeneration duration can affect the conversion and selectivity of LNT regeneration. Jozsa et al [50] compared the effectiveness of regeneration using different reductants such as CO, C$_3$H$_6$, and H$_2$. The amount of NO$_x$ released during the regeneration was compared using 0.18% C$_3$H$_6$, 1.6% CO, or 1.6% H$_2$, with 5% CO$_2$ and balance N$_2$. The mass of NO$_x$ stored remained constant for each test, and the storage was conducted at three temperatures of 60, 80 and 100°C. The regeneration using H$_2$ as the reductant proved to have the lowest quantity of NO$_x$ released, and also provided the greatest reduction to N$_2$, especially at low temperatures.

Poulston et al [51] investigated the use of H$_2$ or CO as a NO$_x$ reduction agent in an LNT in combination with C$_3$H$_6$. The storage phase was maintained constant, and the storage efficiency was compared following each regeneration. The H$_2$ regeneration was much more effective at regenerating the LNT, evidenced by a high storage efficiency following regeneration. It was also demonstrated that a high concentration of H$_2$ with N$_2$ balance was not completely effective at regenerating the catalyst, and only when a more representative engine-out exhaust mixture was used, including CO$_2$, was the regeneration highly effective.

Wang et al [46] investigated the effect of regeneration conditions on the conversion of NO$_x$ into N$_2$, NH$_3$, and N$_2$O during regeneration of a Pt-Rh/BaO/Al$_2$O$_3$ LNT. Results showed that with CO and H$_2$ as the reductant, selectivity to NH$_3$ increased with increasing regeneration duration, reductant quantity, and space velocity. With C$_3$H$_6$ as a reductant the selectivity to NH$_3$ increased with increasing temperature. This relationship was assumed to be due to the steam reforming reaction, as the NH$_3$ increased with increasing H$_2$ generation.

Kong et al [52] used a dual LNT exhaust system on a heavy-duty diesel engine test setup. The after-treatment system featured a diesel reformer upstream of the dual LNT system which would produce an H$_2$ rich gas for regeneration. The dual LNT system featured a switch valve allowing for one LNT to regenerate while the other LNT would continue with the adsorption of NO$_x$. The H$_2$ regeneration results were compared with regeneration using a low pressure diesel injection into the exhaust. H$_2$ regeneration proved to out-perform diesel regeneration resulting in a higher conversion efficiency as well as a reduced associated fuel penalty.

Park et al [35] utilized a combined H$_2$ reformer and LNT catalyst system to study the NO$_x$ reduction capabilities of DME. A 5 second rich period of 0.7% DME, 5% H$_2$O, and 5% CO was able to produce significant H$_2$, which increased with increasing temperature, and resulted in NO$_x$ conversion of 80% through a copper Al$_2$O$_3$ LNT. When the reformer was removed the conversion of NO$_x$ was less than 60%.

Although the rich regeneration is conventionally around 5 seconds, a number of researchers have experimented with both short regeneration periods [54], and long regenerations periods [55, 56]. Yuejin et al [54] investigated the effect of various

lean/rich durations on the conversion of NO$_x$ in an LNT. Results demonstrated that at temperatures between 250-400°C, there was a strong relationship between the NO$_x$ conversion and the balance of lean/rich timing. Longer adsorption times resulted in a reduced NO$_x$ conversion unless the rich time was also increased. The results were repeated with CO and H$_2$, where the same trend was observed, although the CO reductant regeneration achieved the best performance.

2.3   On-Board Hydrogen Generation

Although H$_2$ can benefit LNT regeneration, it may be difficult to supply H$_2$ to an on-vehicle after-treatment application. H$_2$ can be stored on a vehicle as a compressed gas in a gas cylinder, or as a liquid in a cryogenic storage tank. H$_2$ can also be found in small concentrations in the engine-out exhaust gas.   Engine conditions that result in H$_2$ emissions can also result in high UHC emissions, which may also benefit LNT regeneration; however, these conditions generally result in a reduced combustion efficiency [57]. Another attractive way to supply H$_2$ to an on-board after-treatment system is through H$_2$ reforming within the exhaust.

Generation of hydrogen is a well-established industrial process and has the potential to occur over precious metal catalysts [30]. Hydrogen can be produced through various chemical reactions such as: partial oxidation (PO$_x$), steam reforming (SR), autothermal reforming (ATR), dry reforming (DR), and the water gas shift (WGS) reaction.

Partial oxidation of diesel fuel yields carbon monoxide and hydrogen gas as shown in Equation 2.1. It is an exothermic reaction that typically produces temperatures

above 1200°C, although this temperature can be reduced to around 800 - 900°C when a catalyst is used.

$$C_1H_{1.8} + 0.5O_2 \longrightarrow CO + 0.9H_2 \hspace{4cm} \text{(Equation 2.1)}$$

Partial oxidation of an oxygenated hydrocarbon will also result in CO and H$_2$, as shown with n-butanol in Equation 2.2. Although PO$_x$ of n-butanol is still exothermic, it is slightly less exothermic than diesel [58, 59]. The partial oxidation of diesel fuel or n-butanol is not considered to be efficient because it is an exothermic process, and the resulting H$_2$ produced has a lower volumetric energy density than the fuel used for partial oxidation [60].

$$C_4H_{10}O + 1.5O_2 \longrightarrow 4CO + 5H_2 \hspace{3.5cm} \text{(Equation 2.2)}$$

The steam reforming reaction has been extensively studied and used in industrial practice. SR results in H$_2$ and CO being produced when a hydrocarbon fuel reacts with high temperature steam. This chemical reaction is shown with diesel in Equation 2.3. The potential H$_2$ yield is greater for steam reforming than partial oxidation.

$$C_1H_{1.8} + H_2O \longrightarrow CO + 1.9H_2 \hspace{3.5cm} \text{(Equation 2.3)}$$

The efficiency of the SR reaction can potentially be favourable if abundant oxygen is present in the exhaust. The oxidation of hydrocarbons is inherently exothermic, and thus the heat of combustion may be used to promote the SR reaction. Although the process is still endothermic, steam reforming of oxygenated hydrocarbons can occur at much lower temperatures compared to diesel fuel. SR of n-butanol, for instance, can occur at temperatures as low as 200°C, compared to for diesel at 500°C [61]. The SR reaction of n-butanol is given in Equation 2.4.

$$C_4H_{10}O + 3H_2O \longrightarrow 4CO + 8H_2 \qquad \text{(Equation 2.4)}$$

Autothermal reforming is a combination of partial oxidation and steam reforming. The exothermic partial oxidation reaction produces the energy required for steam reforming resulting in a net overall exothermic reaction. Since this reaction is a combination of PO$_X$ and SR, a hydrocarbon, such as diesel fuel, reacts with both oxygen and high temperature steam to produce CO and H$_2$, as shown in Equation 2.5. If oxygen is unavailable, this reaction will become the steam reforming reaction, and if high temperature steam is not available, this reaction will become partial oxidation. Ideally, the products CO and H$_2$ should be prevented from burning.

$$C_1H_{1.8} + 0.5H_2O + 0.25O_2 \longrightarrow CO + 1.4H_2 \qquad \text{(Equation 2.5)}$$

Limited research is available on the ATR of n-butanol (Equation 2.6); however, the reaction has been utilized at temperatures as low as 500°C over a rhodium (Rh) catalyst [62], while diesel is less effective at temperatures below 700°C on an Rh catalyst [63].

$$C_4H_{10}O + H_2O + O_2 \longrightarrow 4CO + 6H_2 \qquad \text{(Equation 2.6)}$$

Another H$_2$ generating chemical reaction involving a hydrocarbon fuel is the dry reforming reaction. This reaction yields CO and H$_2$ from a hydrocarbon and CO$_2$ (Equation 2.7). This reaction is endothermic and thus requires an input of energy. The DR reaction of n-butanol is given in Equation 2.8.

$$C_1H_{1.8} + CO_2 \longrightarrow 2CO + 0.9H_2 \qquad \text{(Equation 2.7)}$$

$$C_4H_{10}O + 3CO_2 \longrightarrow 7CO + 5H_2 \qquad \text{(Equation 2.8)}$$

The final hydrogen generation reaction that will be discussed in this thesis is the water gas shift reaction. This reaction does not involve a HC fuel. Instead, CO and high temperature steam react to form H_2 and CO_2. This reaction is shown in Equation 2.9.

$$CO + H_2O \longrightarrow CO_2 + H_2 \hspace{4cm} \text{(Equation 2.9)}$$

It may be noticed that for each of the H_2 reforming reactions, n-butanol produces a slightly higher yield of H_2 per mole of carbon. This is because n-butanol has a higher gravimetric content of H_2 (13.5 wt%) compared to diesel (13.35 wt%). It has also been shown that the activation energy required to break the carbon-carbon (C-C) bond in oxygenated hydrocarbons is lower than that required for alkanes [64]. Thus it appears that n-butanol may have better qualities for H_2 generation in a precious metal catalyst.

In summary, the LNT has proven to be an effective catalyst for NO$_x$ reduction in CI engine vehicles. The materials of the LNT as well as the operating temperature both have a major effect on the storage, release and reduction of NO$_x$. The gas composition and the type of reductant used also play a major role on the conversion of NO$_x$. H_2 has proven to be one of the most effective reductants for LNT regeneration; however it has also shown to increase the selectivity to undesired products of regeneration such as N_2O, and NH_3. Thus, the H_2 reforming characteristics of an LNT can improve the performance of an LNT, but can also reduce the conversion efficiency. This study therefore intends to investigate the effect of n-butanol as a reductant on H_2 reforming and LNT regeneration, as well as attempts to improve the reduced storage efficiency associated with long adsorption periods.

CHAPTER 3: EXPERIMENTAL SETUP

This chapter will describe the setups for the experiments conducted for this research. Engine tests and after-treatment flow bench tests were conducted separately on independent test setups. The main purpose of the engine tests was to identify exhaust gas compositions at various engine operating conditions. These exhaust gas compositions were then simulated on the after-treatment flow bench.

3.1   Engine Test Setup

Engine tests were conducted on a 4-cylinder, 4-stroke Ford Duratorq diesel engine converted into a single cylinder engine with the three remaining cylinders used for motoring. The engine is connected to an eddy current dynamometer. The specifications for this engine are listed in Table 3.1 and a schematic of the engine test bench is shown in Figure 3.1. The intake pressure was supplied via an external air compressor. An optical high precision encoder is mounted on the engine crank and is used to determine the crank position and angular velocity. The encoder resolution is 0.1°CA. The research engine is equipped with a high pressure common rail fuel injection system using a solenoid injector mounted in the cylinder head. The common rail pressure, injection timing, and injection duration of the fuel were controlled by an independent real-time controller with embedded field-programmable gate arrays (FPGA). This injection system is capable of using either diesel or n-butanol with an added lubricity improver. In-house built algorithms operating on a LabVIEW 2010 software interface were used to control injection events. Four EFS IPoD solenoid injector drivers were used to drive the DI injectors of the engine. The exhaust gas from the research cylinder is routed through a diesel oxidation catalyst and into the exhaust gas surge tank. An exhaust backpressure

valve along with an EGR valve were used to control the flow of EGR which is cooled and introduced into the intake, downstream of the intake surge tank.

Table 3.1 – Test Engine Specifications

Displacement Volume	1998 cm^3
Bore x Stroke	86 mm x 86 mm
Compression Ratio	18.2:1
Maximum Cylinder Pressure	180 bar
Injection System	DI Common Rail
Maximum Injection Pressure	~1600 bar
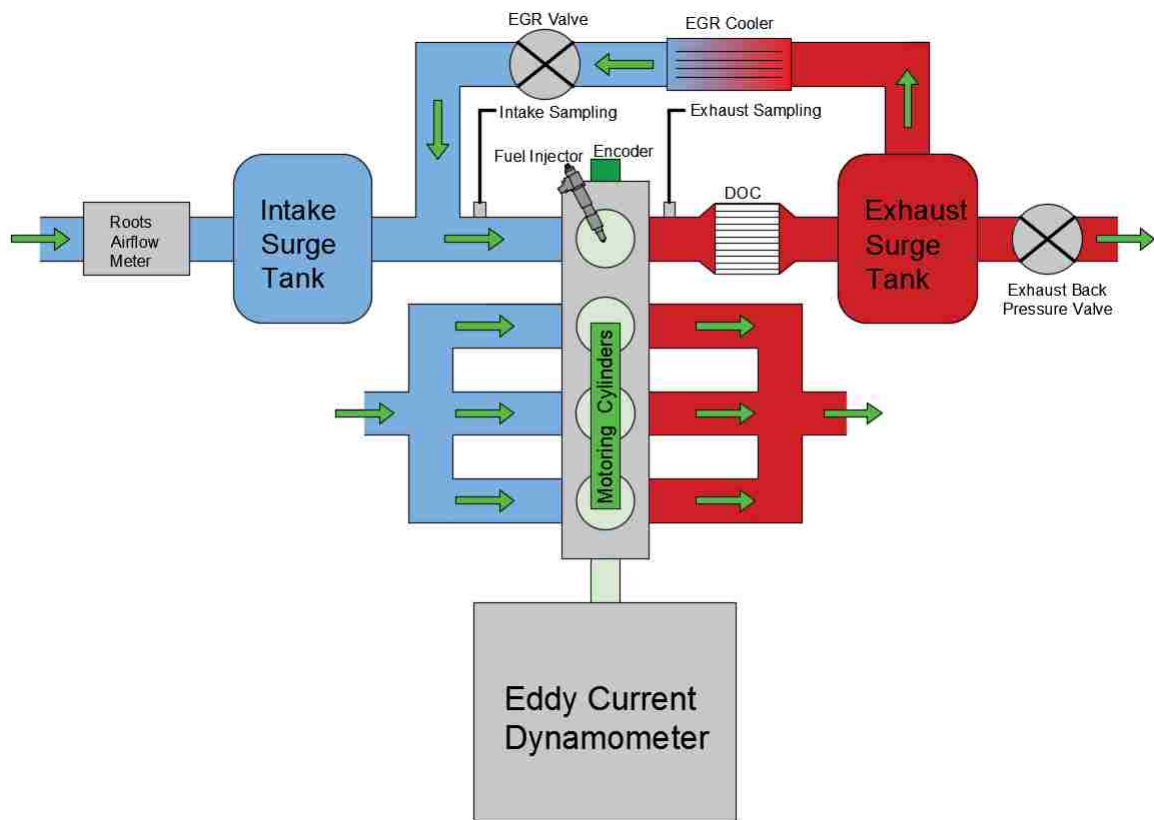
Figure 3.1 – Schematic of Engine Test Setup

Gas sampling is implemented on the engine immediately before the intake manifold and immediately after the exhaust manifold. A heated pump draws the intake and exhaust sampling gas to an in-house built conditioning unit featuring a heated filter

29

and chiller unit in order to remove any PM or water particles from the gas. The sample gas is then fed to a dual-bank emission analyzer system, which was instrumented for this engine and is displayed in Figure 3.2. One bank is for the exhaust emissions (NO_x, UHC, CO, CO_2, O_2), and the other bank is used to measure the intake gas concentration (NO_x, CO_2, O_2). The O_2 is measured with a paramagnetic oxygen detector; CO and CO_2 are measured with nondispersive infrared (NDIR) detectors; NO_x is measured with a chemiluminescence detector (CLD); UHC concentration is measured with a heated flame ionization detector (HFID); and the smoke concentration is measured with an AVL 415S smoke meter which indicates the smoke emissions by filter smoke number (FSN). Further details of the engine test setup are provided in [65].

Figure 3.2 – California Analytical Instruments Dual Bank Analyzers

3.2   After-treatment Flow Bench Setup

After-treatment tests were performed on an off-engine flow bench used to simulate engine exhaust conditions. The LNT catalyst used for flow bench experiments featured a BaO washcoat with a CeO_2 catalyst promoter and a Pt catalyst, on an Al_2O_3 support. A scanning electron microscope image produced from a local laboratory shows the LNT surface washcoat in Figure 3.3. The LNT catalyst was purchased from Volkswagen, and had a diameter of 144 mm and a length of 152 mm. The cell density of the LNT catalyst is 625 cells per square inch. For proper installation in the after-treatment flow bench, a 2-inch diameter sample was cut from the LNT. The DOC monolith used for flow bench tests was the same size as the LNT, and both had a volume of 0.234 L. The catalysts were wrapped in a thermal insulating ceramic fibre mat, and placed in separate 2 inch diameter stainless steel pipes installed on the flow bench.
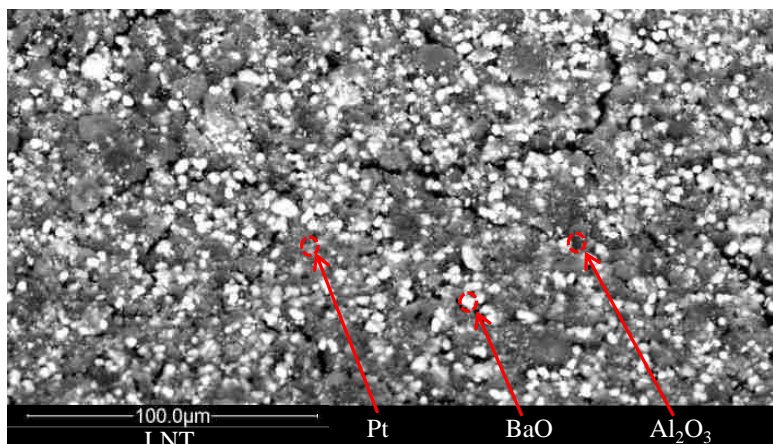
Figure 3.3 – Scanning Electron Microscope Image of LNT Catalyst

The schematic diagram of the after-treatment flow bench is given in Figure 3.4. Four pressurized Praxair gas bottles supplied NO, CO, CO_2, and N_2 directly to the inlet of the flow bench. The flow was controlled through multiple pressure regulators to provide specific concentrations, and steady flow to the flow bench. Compressed air from a

pressure regulated air line was supplied to an Environics Series 2000 Multi-Component

Gas Mixer to regulate flow as well as control the oxygen concentration. The gas mixer

was connected to a Windows 7 personal computer (PC) through an RS232 serial

connection. An open source terminal emulation program called "Tera Term" was used to

control the gas mixer. More information on the operation of the Environics Gas Mixer is

available in Appendix A. The flow rate of air was varied and the N_2 gas supply pressure

was increased or decreased accordingly in order to adjust the oxygen concentration. A

low concentration of oxygen was essential for fuel-rich regeneration of the LNT. A

Leister LE 10000s Electric Hot Air Tool heater, capable of achieving outlet gas

temperatures up to 650°C, was used to heat the gaseous flow. A Bosch model

0281002619 mass air flow (MAF) sensor was installed upstream of the heater for a

secondary measurement of the mass flow rate. All catalyst canisters featured four Omega

K-type thermocouples evenly spaced apart.
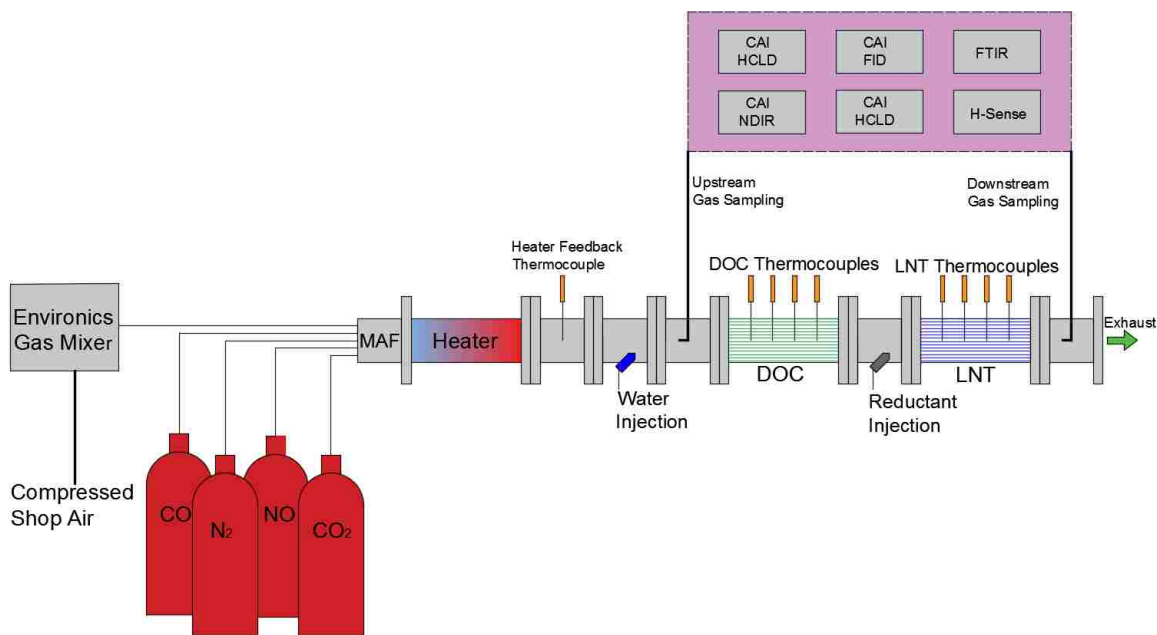
Figure 3.4 – Schematic of the After-treatment Flow Bench

Fuel and water were supplied to the flow-bench using two low pressure solenoid pintle type 4-hole injectors that were mounted on stainless steel sections on the flow bench. An encompassing water cooled jacket was fabricated around each of the injectors in order to prevent damage to the sealing o-rings from the heat of the gas flowing through the flow bench. In-house built pump carts were used to supply water and diesel or n-butanol to the injectors at a constant pressure of 2.5 bar gauge. A photograph of the flow bench setup complete with the water and fuel pump carts is shown in Figure 3.5.
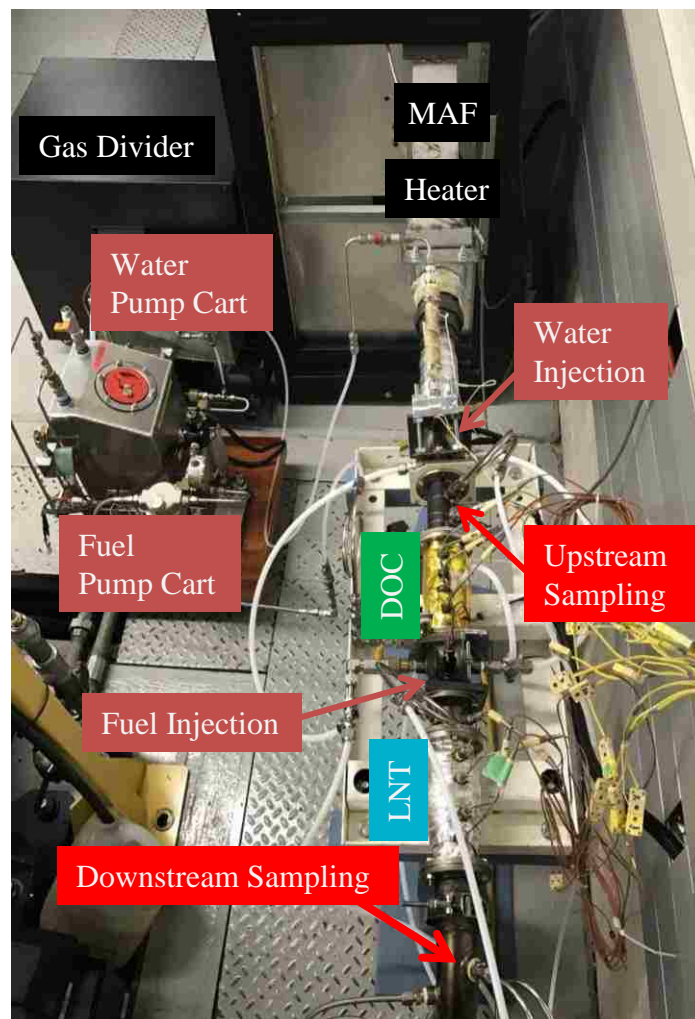
Figure 3.5 – After-treatment Flow Bench Photograph

Measurement data from the flow bench tests were collected using a National Instruments (NI) PCI 6220 data acquisition card. Signals harvested from thermocouples were transmitted to an NI SCXI-1102 thermocouple module through an NI SCXI-1303 terminal block. The NI SCXI-1102 thermocouple module has 32 analog-channels for thermocouple reading acquisition. An SCXI-1302 module was used to acquire the measurement from a MAF sensor. The transfer function for the MAF sensor was obtained from the manufacturer's datasheet to convert the measured voltage signal (V) to mass flow rate (g/s).

The user interface for data sampling and injection control was developed under the LabVIEW 2010 programming environment and is shown in Figure 3.6.
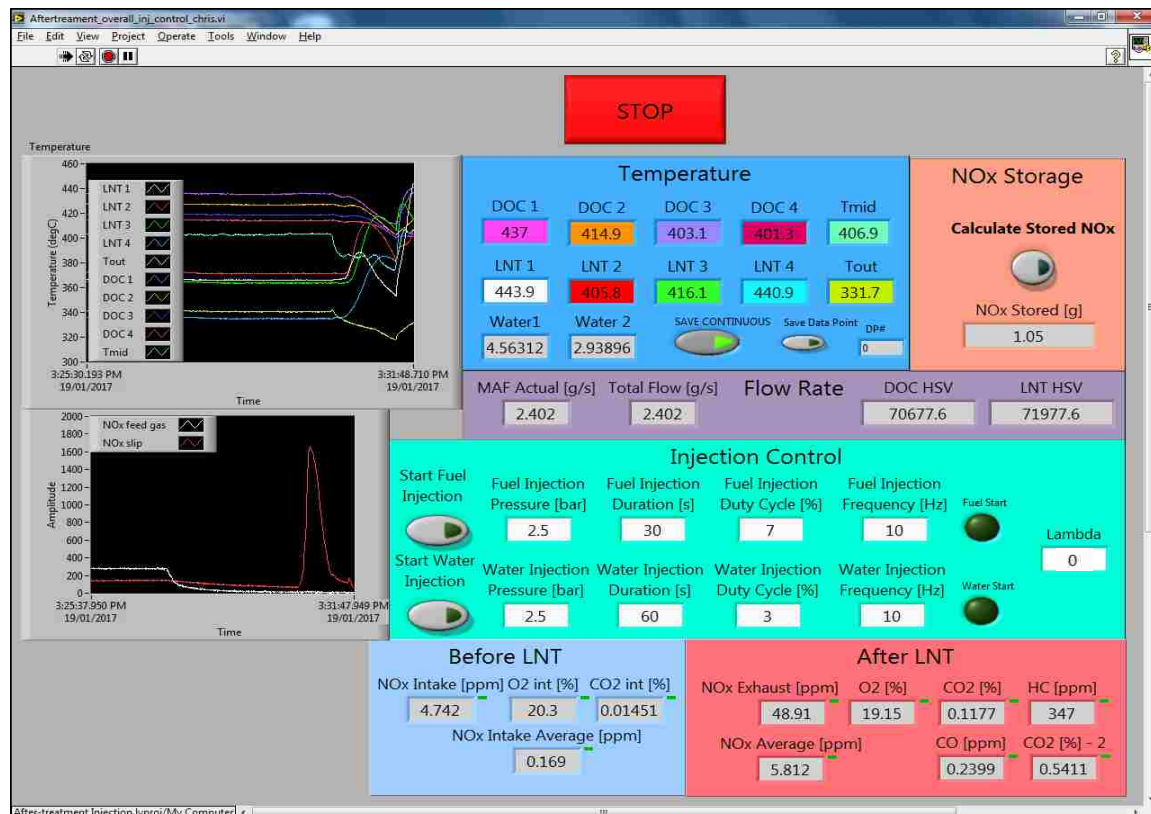
Figure 3.6 – After-treatment Control LabVIEW Front Panel

The user interface provides temperature information sampled from various thermocouples, the mass air flow rate from the MAF sensor, and emission measurement from the CAI emission analyzers. The program also supports real-time control of the injectors mounted on the after-treatment test bench. In this study, the injection pressure was maintained constant at 2.5 bar gauge. The injection command signal was generated as a pulse-width modulation (PWM) signal. The length, frequency, and duty cycle of the PWM signal can be controlled by the user so as to organize the quantity of water or reductant desired for various test conditions. The injection command was sent from the host personal computer (PC) to an NI PXI-8110 real-time computer. Based on the received instructions, an NI PXI-7853R FPGA module, which was connected to the real-time computer through a PXI communication protocol, generated the desired PWM control signal. The injection signal was then sent to an in-house built injector driver circuit. For the H_2 reforming and the LNT regeneration tests, the total PWM command signal duration and the signal frequency were set to 30 seconds, and 10 Hz, respectively, amounting to 300 total injections per 30 seconds. In order to vary the quantity of injected reductant, the duty cycle of the reductant injection signal was varied from 1% to 7%, corresponding to pulse widths of 1 ms and 7 ms, respectively (Figure 3.7).
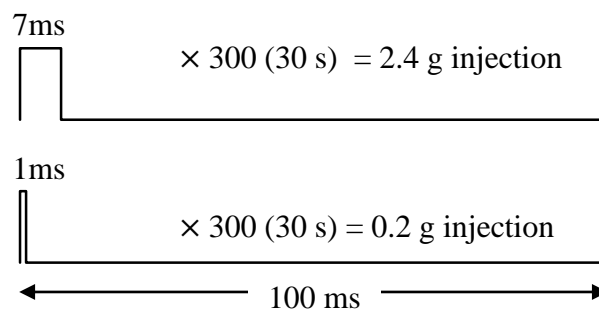
Figure 3.7 – PWM Signal Representation

Gas sampling was available upstream and downstream of the LNT catalyst as shown in Figure 3.4. The sample gas was then fed to the CAI dual-bank emission analyzer bench shown in Figure 3.2. A MKS 2030-HS Fourier transform infrared (FTIR) spectrometer (Figure 3.8) and a V&F Q7000 hydrogen analyzer (Figure 3.9) were also utilized for downstream measurement of H_2, NH_3, N_2O, NO_x, and UHCs.

Figure 3.8 – MKS Fourier Transform Infrared Spectrometer

Figure 3.9 – V&F H-Sense Hydrogen Analyzer

CHAPTER 4:ENGINE TEST AND ADSORPTION FLOW BENCH RESULTS

This portion of the thesis pertains to engine test experiments and after-treatment adsorption flow bench tests. The engine experiments were conducted in order to collect a baseline for the exhaust makeup at targeted engine operating conditions, as well as to test the achievable engine-out NO_x levels of diesel and n-butanol combustion. As was previously mentioned, the application of EGR can reduce the concentration of engine-out NO_x emissions, thereby lengthening the adsorption period of an LNT, and reducing the fuel penalty associated with the LNT. The engine test conditions are outlined in Table 4.1. EPA emission regulations are enforced on a brake-specific basis; however, this chapter reports emission levels on an indicated basis, and thus a lower indicated emission level could be required to satisfy the regulations.

Table 4.1 – Engine Test Conditions

Test	Fuel	Intake Pressure (bar absolute)	p_{inj} (bar)	Target IMEP (bar)	Intake O_2 (%)	CA50 (°CA)
1	Diesel	2.0	1200	6.0	11-18.5	364
2	n-Butanol	2.0	900	6.0	21	364
3	Diesel	1.9	1400	10.0	13.5-19.5	369
4	n-Butanol	2.0	900	10.0	14.9-18	369

For the following engine test results, the engine load was defined using indicated mean effective pressure (IMEP) given in Equation 4.1, where p is the cylinder pressure, V is the cylinder volume, and V_S is the total piston swept volume. For this study, a low engine load was defined between 0-6.9 bar, a moderate engine load was defined between 7-11.9 bar, and a high engine load was defined as 12 bar and above.

$$IMEP = \frac{1}{V_S} \oint pdV$$
(Equation 4.1)

4.1 Low Load Engine Tests

Engine tests were performed on a single cylinder research engine at the Clean Combustion Engine Laboratory at the University of Windsor, in order to see the effect of EGR on NO_x and PM emissions at low and medium load levels. The specifications for this engine can be found in Table 3.1. The first engine test was conducted at a low engine load of 6.0 bar IMEP using diesel as a fuel. In order to achieve this load level, the commanded injection duration was 465 μs and a constant injection pressure of 1200 bar was used. The injection timing was varied in order to maintain CA50 (50% mass fraction of fuel burned) at 364°CA, as this was the best efficiency case for these testing conditions. The intake pressure was boosted to 2.0 bar absolute. The engine speed was 1500 rpm. The NO_x and PM emissions throughout the EGR sweep for the diesel engine test are shown in Figure 4.1. The 100 ppm long breathing NO_x emission target is marked by the red dashed line.
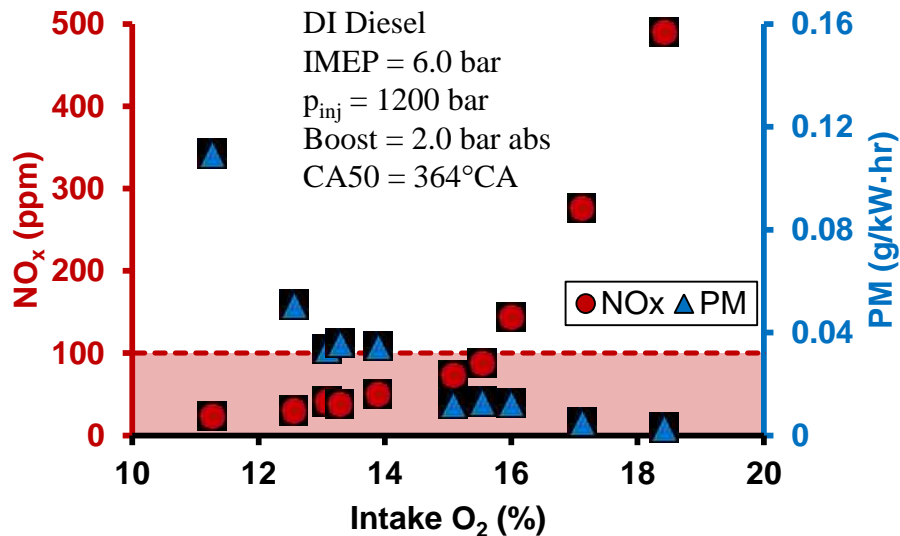
Figure 4.1 – Low Load Diesel EGR Sweep NO_x and PM Emissions

Initially, at a minimal EGR level, the engine-out NO_x was almost 500 ppm. With increasing EGR and decreasing intake O_2 concentration, the NO_x emissions gradually reduced, eventually to below 100 ppm at around 15.5% intake O_2. This resulted in an indicated NO_x level of 0.24 g/kW·hr, only marginally meeting the current EPA standard. PM emissions followed the opposite trend to NO_x, as was expected. Initially, PM levels were minimal, below the current EPA regulation; however, as the EGR ratio was further increased, the NO_x emissions continued to decrease, while the PM emissions increased. This was evidence of the well-documented NO_x-soot trade-off. Therefore, although the NO_x emissions continued to decrease, as low as 30 ppm when the intake O_2 concentration was reduced below 13%, the indicated PM emissions increased to more than 0.1 g/kW·hr. This exceeded the set DPF tolerance limit of 0.036 g/kW·hr and would thereby increase the fuel penalty associated with the DPF. Thus this condition produced emissions outside the range of feasible long breathing LNT application.

The next engine test was conducted with n-butanol as the DI fuel. Because of n-butanol's high viscosity, it could be fully implemented in a conventional diesel engine with minimal alteration. For this engine, a lubricity improver was added to the n-butanol fuel so that the fuel delivery system would be adequately lubricated. In order to achieve a low load of 6.0 bar IMEP, a single direct injection of n-butanol was used with an injection pressure of 900 bar. The combustion phasing was maintained so that the CA50 occurred at 364°CA. Intake pressure and speed of the engine were 2.0 bar absolute, and 1500 rpm, respectively. For this load, EGR was not necessary as at 21% intake O_2 concentration, the NO_x was already well below the long breathing engine-out target of

100 ppm, about 34 ppm, while PM emissions were negligible. This amounted to an indicated NO_x level of just 0.09 g/kW·hr, well below the current standard.

Therefore, both diesel and n-butanol were able to achieve low engine-out NO_x emissions at low engine load as shown in Figure 4.2. n-Butanol was able to achieve below 100 ppm without the application of EGR. PM emissions were also very low (below the AVL 415S smoke meter was able to measure) for n-butanol, and thus would not require further filtration in the exhaust. It was also found that although the application of EGR pushed diesel engine-out NO_x emissions into the long breathing region, excessive application of EGR increased the PM emissions beyond the DPF tolerance limit, thereby moving the engine-out conditions outside of the long breathing LNT region.
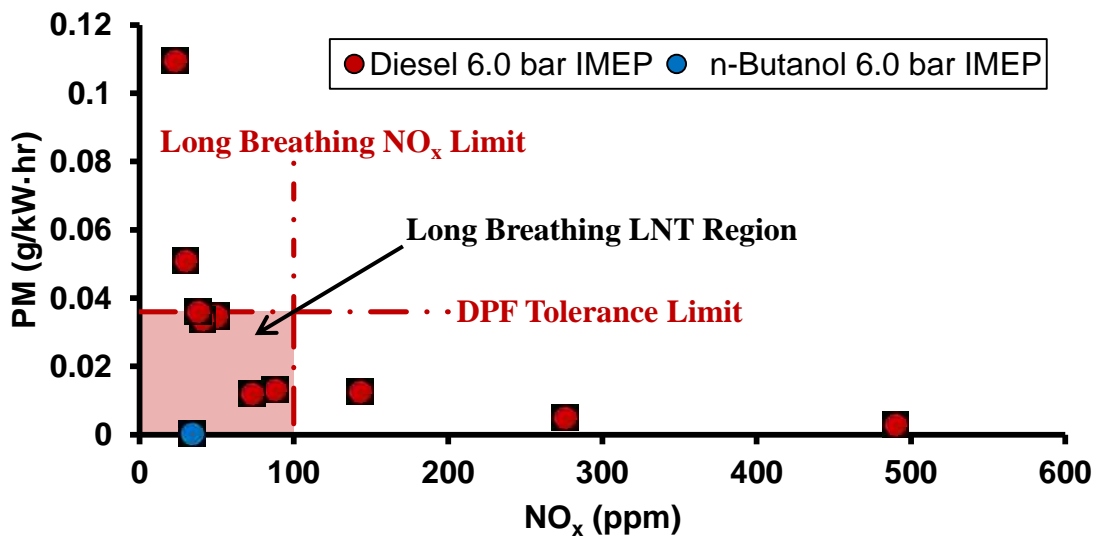
Figure 4.2 – Long Breathing LNT Region for Low Load Diesel and n-Butanol

4.2   Medium Load Engine Tests

The purpose of the next set of tests was to examine the engine-out NO_x emissions with an increase in the engine load for both diesel and n-butanol. Typically, to increase the engine load, the fuel injected per cycle must be increased. In order to increase the

quantity of fuel injected for the engine test with diesel, the injection duration was increased from 465 μs, at low load, to 600 μs. The injection pressure was also increased to 1400 bar. The combustion phasing was retarded from 364°CA to 369°CA. The engine speed was maintained at 1500 rpm, and the intake pressure was 1.9 bar absolute. Figure 4.3 shows the NO_x and PM emissions of an EGR sweep with intake O_2 concentration reduced from 19.5% to 13.5%.
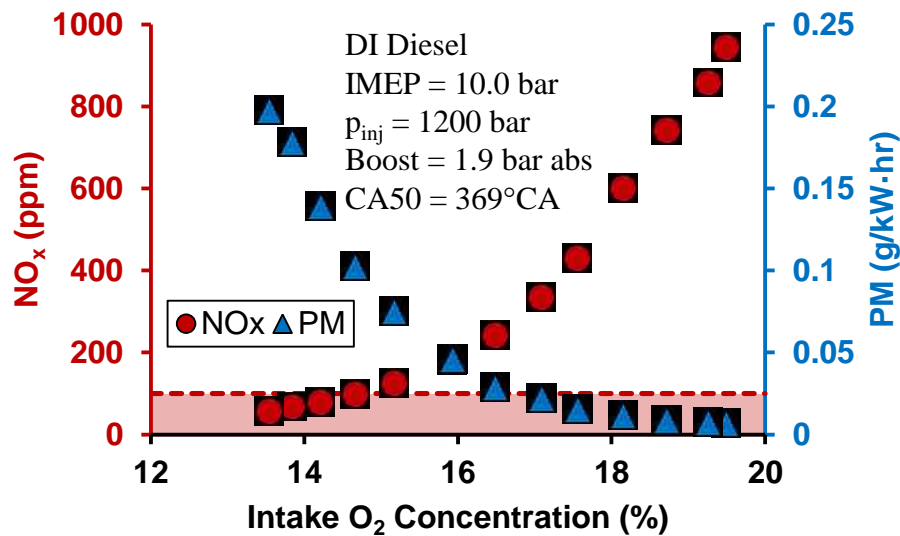
Figure 4.3 – Diesel EGR Sweep NO_x and PM emissions

At about 19.5% intake O_2, with minimal EGR application, the NO_x emissions were fairly high, above 800 ppm. With decreasing intake O_2 concentration, the NO_x emissions slowly reduced, eventually reaching below 500 ppm once the concentration of intake O_2 was below 18%. The NO_x emissions did not reduce below the long breathing LNT engine-out NO_x limit until approximately 14.5% intake O_2. This was in contrast to the low load diesel case, where NO_x emissions were below 100 ppm at 15.5% intake O_2. Initially, indicated PM emissions were below the EPA regulation, until 500 ppm NO_x was reached, and then the PM began to increase above the regulated limit. The NO_x-soot

trade-off was clearly evident, as PM increased while NO_x decreased, as the intake O_2 concentration decreased. For a DPF tolerance limit of 0.036 g/kW·hr, the lowest engine-out NO_x achievable was about 200 ppm, for this engine load and injection parameters. Therefore, the long breathing LNT region was not achievable at medium load with DI diesel, for the tested engine conditions. Other fueling strategies could be viable for engine-out emission reduction during medium load diesel combustion but were beyond the scope of this research.

In order to verify the effect of EGR on the reduction of NO_x emissions with n-butanol fuel, engine tests were conducted with DI n-butanol at a medium load level. In order to maintain a load level of 10 bar IMEP, multiple injections were required, so as to reduce the pressure rise rate associated with n-butanol combustion. Combustion phasing of 369°CA CA50 was maintained. The timing for the two injections was 343°CA and 362°CA at an injection pressure of 900 bar. The intake pressure was 2.0 bar absolute. The engine speed was 1500 rpm. The NO_x and PM emissions throughout the n-butanol EGR sweep are shown in Figure 4.4.
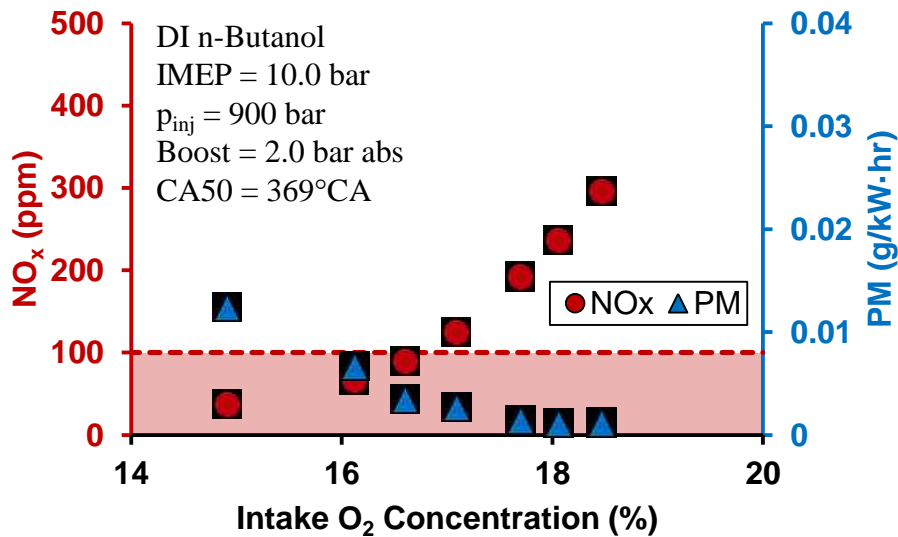
Figure 4.4 – n-Butanol EGR Sweep NO_x and PM Emissions

n-Butanol combustion showed the same trend as diesel, in that the NO_x emissions reduced with decreasing intake O_2 concentration; however, the initial NO_x exhaust emissions at the low EGR case were much lower than diesel at the same intake O_2 concentration. This was again partly due to the higher heat of vaporization of n-butanol fuel, resulting in a lower peak in-cylinder temperature, and thus suppressing the formation of NO_x emissions. Although NO_x emissions were much lower than the diesel case for these test conditions, they were still not low enough to satisfy the EPA emission regulations, unlike the low load n-butanol test. Thus EGR was required to further reduce NO_x into the long breathing region. The NO_x soot trade-off was evident in the n-butanol EGR sweep for these test conditions; however, due to the oxygen content in the n-butanol fuel, as well as the relatively longer ignition delay, PM emissions were still relatively low. The PM emissions were low enough to meet the previously set DPF tolerance limit throughout the EGR sweep as well as the EPA regulated limit throughout most of the EGR sweep, thereby potentially eliminating the need for regeneration or resulting in infrequent regenerations of the DPF during these conditions. As the intake O_2 concentration was reduced, CO and UHC emissions tended to increase. This was especially evident with n-butanol fuel, and indicated a decrease in combustion efficiency; however, the main focus of these engine tests was to decrease NO_x and PM. CO and UHC emissions can be easily oxidized in the exhaust with the use of a DOC.

4.3   Summary of Engine Test Results

For the specified engine testing conditions, both n-butanol and diesel DI combustion were able to achieve long breathing engine-out NO_x emission levels at a low load of 6.0 bar, while only n-butanol DI combustion was able to satisfy the long

breathing condition at a medium load of 10.0 bar. The limiting factor for the medium load diesel case was the PM emissions. In order to achieve long breathing LNT exhaust conditions, the DPF tolerance limit of 0.036 g/kW·hr engine-out PM must be satisfied. Because of n-butanol fuel's characteristically long ignition delay, better in-cylinder mixing was usually expected, even at a lower injection pressure. The oxygen content in n-butanol also helped the oxidation of PM emissions.

Figure 4.5 shows the overall trend of NO_x and PM emissions for the engine results conducted for this study. Each test resulted in an engine-out NO_x level below 100 ppm, however the intake O_2 concentration required and the PM emissions were different.
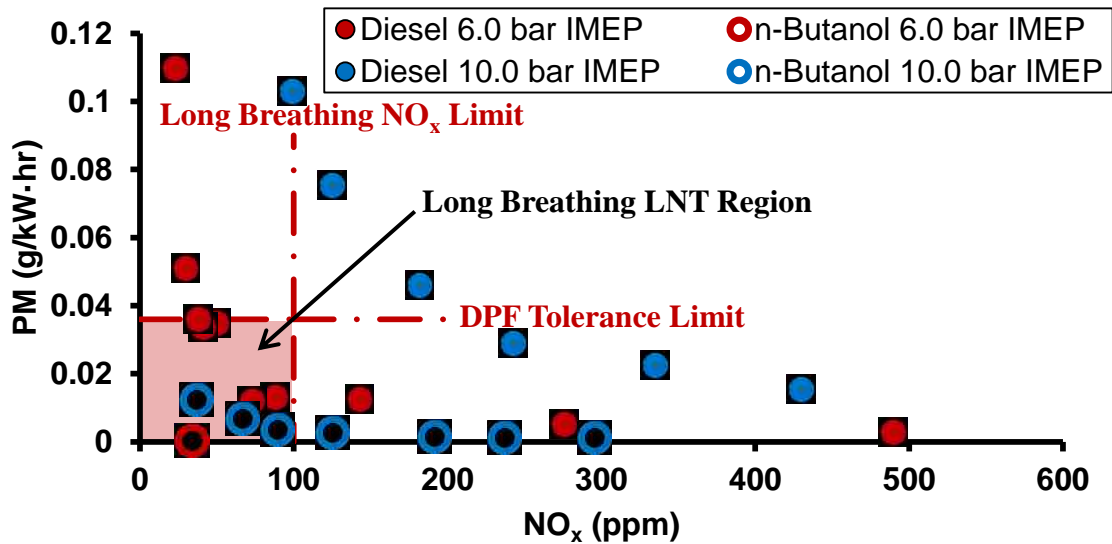
Figure 4.5 – Long Breathing LNT Region for Overall Engine Test Results

For the low load n-butanol case, the intake O_2 concentration was 21% and the PM emission level was negligible. For the low load diesel case, the engine-out NO_x reached 100 ppm at an intake O_2 concentration of 15.5%, which resulted in indicated PM emissions of 0.0132 g/kW·hr, which is right around the current EPA emission standard for PM allowed in heavy-duty diesel vehicles. The medium load n-butanol case reached

44

100 ppm at a higher intake O_2 compared to both diesel cases. An intake O_2 concentration of 16.6% resulted in a NO_x level of 90 ppm and an indicated PM level of 0.0035 g/kW·hr, for n-butanol combustion at 10.0 bar IMEP. Although the medium load diesel case was not suitable for the long breathing region, the NO_x was still reduced to below 100 ppm. However, only at a threshold of 14.7% intake O_2 did the NO_x emissions reduce below 100 ppm, by far the highest amount of EGR of all the test conditions. At this point PM emissions exceeded 0.1 g/kW·hr, which would require a DPF filtration efficiency of almost 90%, and thus an increased fuel penalty would be required to regenerate the DPF. These results are summarized in Table 4.2.

Table 4.2 – Overall Engine Test Results Summary

Test Condition	Target IMEP (bar)	Intake O_2 (%)	NO_x (ppm)	Indicated PM (g/kW·hr)
Diesel Low Load	6.0	15.5	88	0.0132
n-Butanol Low Load	6.0	21.0	34	~ 0
Diesel Medium Load	10.0	14.7	99	0.1029
n-Butanol Medium Load	10.0	16.6	90	0.0035

4.4 After-treatment Flow Bench Storage Tests

The purpose of the next portion of tests was to validate the lean NO_x trap adsorption concept. An off-engine exhaust flow-bench fitted with two low pressure liquid injectors and a DOC and LNT converter was used for these tests. Detailed schematic and specifications of this setup can be found in Chapter 3. The volume of the LNT catalyst used in the flow-bench was 0.234 L. Preliminary experiments, conducted by the author, determined that a NO_x loading of 0.85 g/L of LNT was the maximum suitable amount of NO_x until the regeneration would require a significantly higher amount of reductant. This amounted to a mass of 0.2 g of total NO_x stored on the LNT flow bed.

For these tests, NO_x gas was supplied to the flow bench from a gas bottle with a concentration of 10% NO, and balance N_2. As was mentioned previously, there are two sequential steps involved in the storage process: First, the oxidation of NO into NO_2, and second, the storage of NO_2 on BaO sites as $Ba(NO_3)_2$. This overall adsorption process was given in Equation 1.3 and Equation 1.4. Since, the supply gas was predominantly NO, the oxidation of NO was required, through the DOC or within the LNT, before adsorption. The adsorption tests were conducted at steady state conditions, with an average LNT temperature of 350°C, and an hourly space velocity (HSV) of 80,000 hr^{-1}.

An LNT temperature of 350°C was used because not only did it pertain to the exhaust temperature of both diesel and n-butanol at medium load, but it has also been reported that below temperatures of 300°C, the storage capacity of an LNT can reduce and the storage of less stable barium nitrite $(Ba(NO_2)_2)$ can dominate, which can reduce the conversion efficiency during regeneration [66]. CO_2 and H_2O were not used for the adsorption tests because they were reported to have no significant effect on the adsorption characteristics of this type of LNT between 300°C and 400°C [38], and also, during initial preliminary experiments, displayed no negative effect other than the H_2O having a cooling effect on the catalysts. The O_2 concentration was held constant at 21%, since any concentration of O_2 above 3% has no effect on the storage of NO_x [36].

In order to determine the frequency of regenerations required for various NO_x concentrations, the NO_x inlet concentration was varied for each adsorption phase from 60 to 1000 ppm (60, 100, 200, 300, 500, 750, and 1000). The time from initial NO_x dosing into a freshly regenerated catalyst until a mass of 0.2 g of NO_x was stored on the catalyst

was recorded, and defined as the adsorption time. These test conditions are summarized in Table 4.3.

Table 4.3 – Adsorption Flow Bench Test Conditions

Test	LNT Temp.	Hourly Space Velocity	NO_x Inlet Concentration	O_2	CO_2	H_2O
	(°C)	(hr^{-1})	(ppm)	(%)	(%)	(%)
5	350	80,000	1000	21	0	0
	350	80,000	750	21	0	0
	350	80,000	500	21	0	0
	350	80,000	300	21	0	0
	350	80,000	200	21	0	0
	350	80,000	100	21	0	0
	350	80,000	60	21	0	0

The adsorption time results collected for each specified inlet concentration are presented in Figure 4.6. As the NO_x inlet concentration decreased, the adsorption time increased. This was expected as the mass flow rate of NO into the LNT was lower for lower NO_x concentrations since the overall flow rate was maintained.
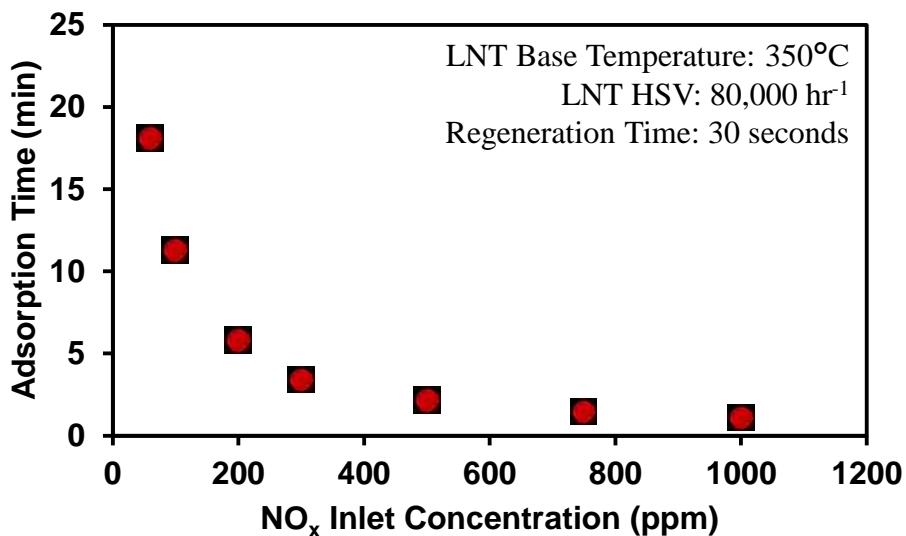
Figure 4.6 – Adsorption Time vs. NO_x Inlet Concentration

As the long breathing region is defined as engine-out NO_x concentrations below 100 ppm, the 100 ppm and 60 ppm NO cases were considered to be in the long breathing region. The 100 ppm inlet concentration resulted in an adsorption time over 11 minutes, while the 60 ppm inlet concentration case had an adsorption time of about 18 minutes.

As the adsorption time was increased, a reduction in the storage capacity of the LNT was observed. Depending on the NO inlet concentration, this could potentially decrease the instantaneous NO_x trapping efficiency of the LNT. The definition of the instantaneous NO_x trapping efficiency, by volume or by mole, is given in Equation 4.2, while the definition of the storage efficiency for an LNT is given in Equation 4.3. The instantaneous NO_x trapping efficiency is the difference between the concentration of NO_x upstream of the catalyst ($[NOx_{in}]$) and the concentration of NO_x downstream of the catalyst ($[NOx_{out}]$), divided by $[NOx_{in}]$ at a specified point in time during adsorption. The storage efficiency is usually observed after the adsorption period is finished, and is the difference between the total cumulative mass of NO_x into the catalyst ($m_{NOx\ in}$) and the total cumulative mass of NO_x slip downstream of the catalyst ($m_{NOx\ out}$) throughout adsorption, divided by $m_{NOx\ in}$.

$$NO_x \text{ Trapping Efficiency} = \frac{[NOx_{in}] - [NOx_{out}]}{[NOx_{in}]} \qquad \text{(Equation 4.2)}$$

$$\text{Storage Efficiency} = \frac{m_{NOx\ in} - m_{NOx\ out}}{m_{NOx\ in}} \qquad \text{(Equation 4.3)}$$

Figure 4.7 shows the NO_x upstream of the LNT and NO_x downstream of the LNT throughout the 100 ppm adsorption cycle. It can be seen that throughout the entire storage period, the concentration of NO_x downstream of the LNT, was very low (below 2 ppm). The NO_x trapping efficiency was over 98% throughout the adsorption period.

48
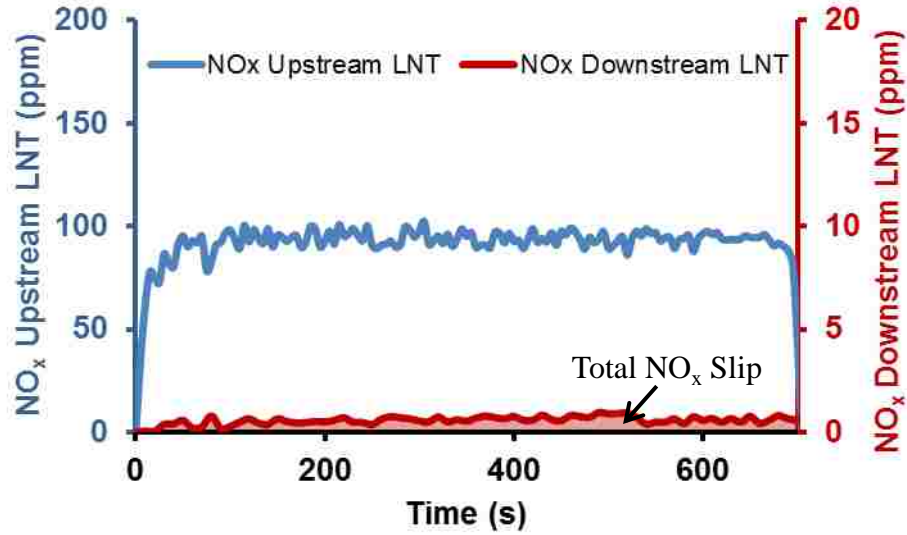
Figure 4.7 – LNT Adsorption with 100 ppm NO_x Inlet Concentration

The 1000 ppm NO_x inlet concentration case is shown in Figure 4.8. At initial NO_x dosing, the concentration of NO_x slip downstream of the LNT was very low; however, after approximately 10 seconds, the NO_x slip began to rapidly increase, reaching a maximum NO_x slip of 30 ppm by the end of the tested adsorption period. Although the NO_x trapping efficiency reduced, it was still 97% at the end of the adsorption period.
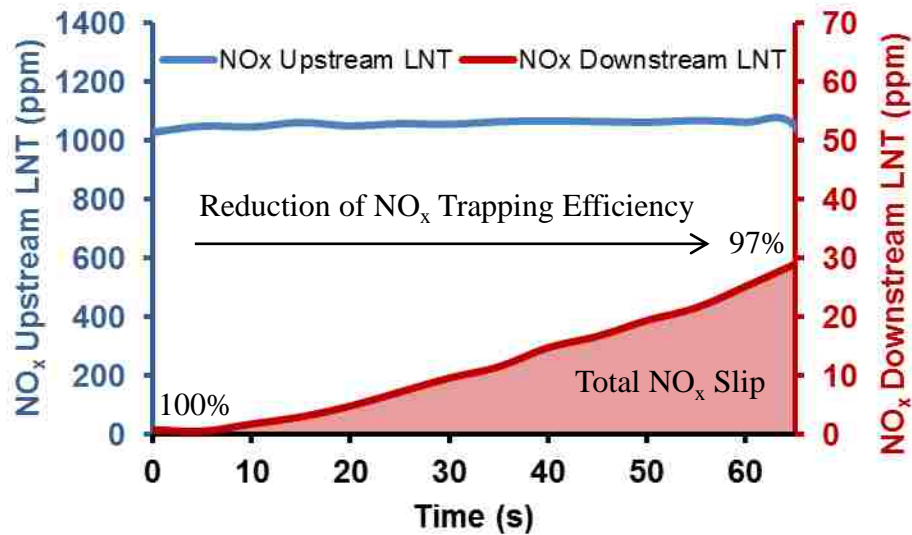
Figure 4.8 – LNT Adsorption with 1000 ppm NO_x Inlet Concentration

The NO_x emissions upstream and downstream of the LNT were sampled throughout the adsorption period for all NO_x inlet concentrations tested. Initially, the NO_x downstream of the LNT was very low for all cases, indicating a high instantaneous trapping efficiency, similar to the 1000 ppm case shown in Figure 4.8. The peak NO_x slip concentration occurred at the end of the adsorption period for each case, and reduced with reducing NO_x inlet concentration, even though the adsorption duration increased. The 60 ppm case had the lowest peak NO_x slip of less than 1.5 ppm.

A summary of the cumulative mass of NO_x slip values for the different NO_x inlet concentrations is given in Figure 4.9. As the NO inlet concentration reduced, the cumulative mass of NO_x slip also reduced, even though the total adsorption duration was longer. The lowest mass of NO_x slip was for the 60 ppm NO case, while the greatest mass of NO_x slip was observed at the highest NO inlet concentration tested, 1000 ppm. At low NO_x inlet concentrations, the NO_x slip was extremely low throughout the entire adsorption period, and even below 2 ppm for the 60 ppm case. For every case, the testing results indicated that the majority of the NO_x slip downstream of the LNT throughout the adsorption period was NO_2, sometimes as much as double the concentration of the NO. This was especially the case at the initiation of the adsorption period.
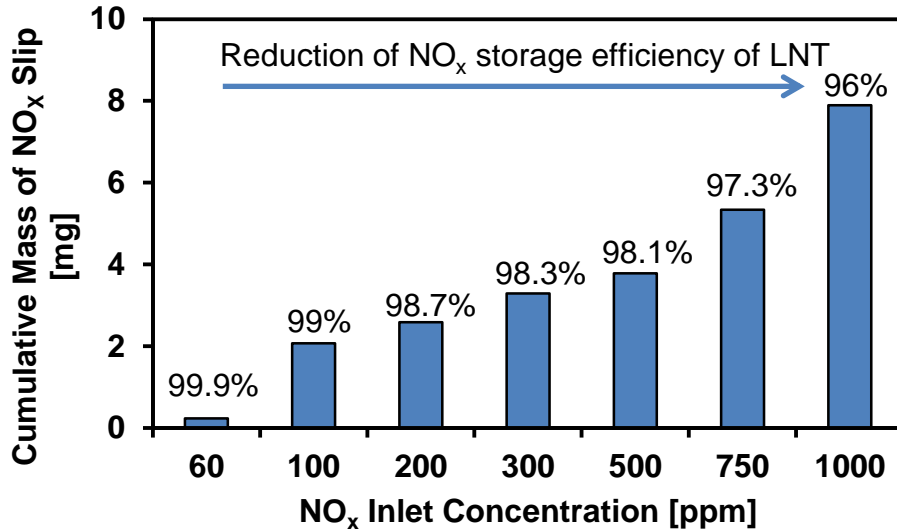
Figure 4.9 – Cumulative Mass of NO_x Slip vs. NO_x Inlet Concentration

The adsorption test results demonstrated that by lowering the engine-out NO_x, the inlet concentration of NO_x into the LNT was reduced, thereby increasing the adsorption time, while maintaining a high storage efficiency above 99%. A reduced inlet NO concentration also resulted in a longer total adsorption period, thereby requiring less frequent regenerations, and potentially reducing the fuel penalty associated with the LNT.

CHAPTER 5:HYDROGEN REFORMING EXPERIMENTAL RESULTS

The presence of hydrogen in the exhaust can greatly benefit the regeneration characteristics of an LNT. This chapter will focus on the reforming of diesel and n-butanol through an LNT monolith. The conditions for the H_2 reforming tests are outlined in Table 5.1. For these tests, the reductant was injected immediately before the LNT on the after-treatment flow bench, thus allowing for hydrogen generation through the LNT monolith. The purpose of these tests was to identify the regeneration conditions, to be used in Chapter 6, in order to compare the hydrogen reforming characteristics of diesel and n-butanol through an LNT catalyst, so as to potentially predict which reductant, diesel or n-butanol, may better suit H_2 reforming in an after-treatment system. Tests 6 and 7 aimed to investigate the reforming of H_2 in the presence of 3% exhaust oxygen, while tests 8 and 9 involved H_2 reforming with CO in an oxygen deficient environment.

Table 5.1 – Hydrogen Reforming Test Outline

Test	Reductant	LNT Temp (°C)	Hourly Space Velocity (hr^{-1})	Total Inj. Time (s)	Reductant Quantity (g)	O_2 (%)	H_2O (%)	CO (%)
6	Diesel	350	45,000	30	0.2	3	6	0
		350	45,000	30	0.6	3	6	0
		350	45,000	30	1.3	3	6	0
		350	45,000	30	2.4	3	6	0
7	n-Butanol	350	45,000	30	0.2	3	6	0
		350	45,000	30	0.6	3	6	0
		350	45,000	30	1.3	3	6	0
		350	45,000	30	2.4	3	6	0
8	Diesel	350	50,000	30	0.2	0	6	1.5
		350	50,000	30	0.6	0	6	1.5
		350	50,000	30	1.3	0	6	1.5
		350	50,000	30	2.4	0	6	1.5
9	n-Butanol	350	50,000	30	0.2	0	6	1.5
		350	50,000	30	0.6	0	6	1.5
		350	50,000	30	1.3	0	6	1.5
		350	50,000	30	2.4	0	6	1.5

Most of the H_2 reforming reactions are sensitive to temperature, and the reductant oxidation in the exhaust during rich conditions can cause significant fluctuations in temperature. Hence, the temperature of the LNT during H_2 reforming was of interest. The temperatures of the LNT were measured along the central line of the flow bed with four evenly spaced thermocouples, mounted to the LNT pipe, as shown in Figure 5.1.
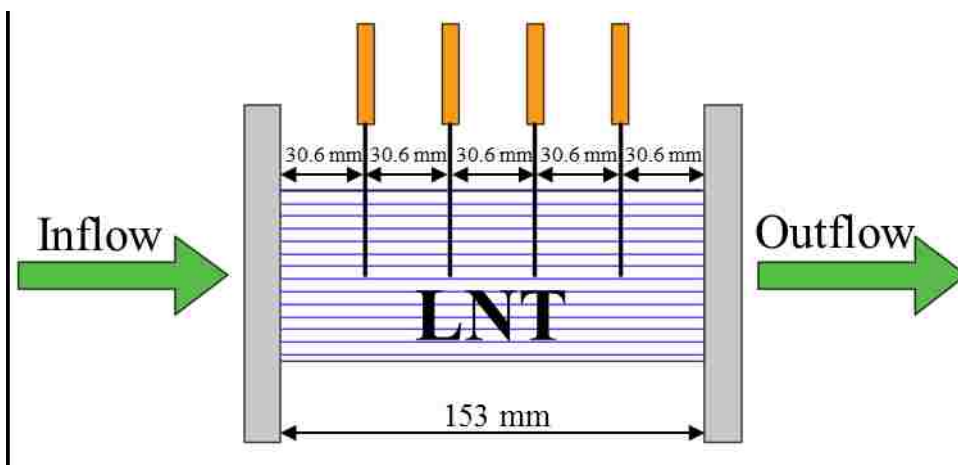
Figure 5.1 – LNT Thermocouple Layout

5.1   Hydrogen Generation with 3% Exhaust Oxygen

For the hydrogen generation experiments, a rich mixture was produced in the flow bench to simulate an LNT regeneration environment, except no NO_x was loaded on the catalyst. The yields of hydrogen from four different injection quantities of n-butanol were compared to the yields of hydrogen from the same quantities of diesel injected. Because of the greater hydrogen content of n-butanol as well as the lower activation energy for the breaking of C-C bonds in oxygenated hydrocarbons, the total H_2 yielded from n-butanol can potentially be greater than diesel. n-Butanol can also experience thermal decomposition at lower temperatures, producing a higher amount of light hydrocarbons, which can further react with O_2, CO_2 or H_2O to produce H_2.

53

The conditions for the H_2 generation tests at 3% O_2 are shown in Table 5.1 and the flow bench set-up is given in Figure 3.4. A wide range of test conditions, which were thought to be suitable for LNT regeneration, were explored. Both tests 6 and 7 were conducted with a flow of 3% O_2 and a balance of N_2. The effect of oxygen was of interest for the H_2 reforming tests, and 3% was the lowest achievable oxygen concentration for this flow bench setup. This gas composition resulted in an average LNT HSV of about 45,000 hr^{-1}. The temperatures of the DOC and LNT as well as the injection pressure of diesel and n-butanol were kept constant for each test and testing reductant. The total injection time was 30 seconds for each case. The injection duty cycle commanded was varied to alter the quantity of reductant injected for each case. To achieve a 6% concentration of H_2O, a 2.5 bar gauge injection of water was utilized upstream of the DOC and LNT. Tests 6 and 7 each had four data points involving one injection of reductant. The lowest injected quantity produced a lean mixture, and with each subsequent increase in injected reductant quantity, the mixture became slightly richer.

The hydrogen generation test results for the 3% exhaust oxygen case are shown in Figure 5.2. The results showed that with a greater quantity of reductant injected, a greater mass of hydrogen was produced, for both diesel and n-butanol. By injecting a greater quantity of reductant, each mixture became richer, allowing for a greater portion of the reductant injected to be used for hydrogen reforming. At the lowest reductant injection quantity of 0.2 g, n-butanol produced a peak H_2 concentration of about 300 ppm, resulting in a mass of about 0.3 mg of H_2. The same injection quantity of diesel did not produce any H_2. During the oxidation of the 0.2 g of diesel injected, the temperature increased to about 430°C, which may have been insufficient for the endothermic H_2

reforming reactions to occur with diesel. Although the quantity of H_2 yield increased with diesel and n-butanol injection, the increase was much more pronounced with n-butanol. With the increase in reductant from injection 3 to injection 4 (1.3 g to 2.4 g), n-butanol had a much greater increase in the total mass of H_2 yield, compared to diesel. This was also true for the peak concentration produced; diesel had an increase from 3,150 ppm to 3,200 ppm, or about 1.6%, while n-butanol had an increase from 11,500 ppm to 17,500 ppm, about a 50% increase, with the 85% increase in reductant quantity. The richest mixture of n-butanol yielded over 8 times the total mass of H_2 as the richest mixture of diesel (16.4 mg of H_2 from n-butanol, 1.9 mg of H_2 from diesel). Thus, in the presence of 3% oxygen, it was observed that by mass, n-butanol produces more H_2 than diesel.
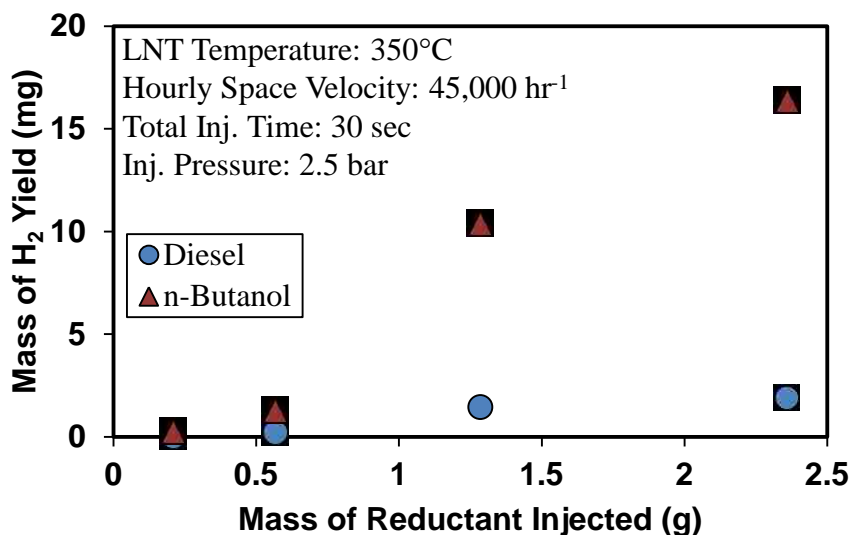
Figure 5.2 – Mass of H_2 Yield (3% Exhaust O_2)

The gravimetric energy density of n-butanol (33 MJ/kg) is lower than that of diesel (43 MJ/kg). So, in order to compare the quantity of H_2 produced by each reductant, while taking into account the different energy densities of diesel and n-butanol, the total mass of H_2 yielded per kilojoule (kJ) of reductant injected was of interest. This

relationship was plotted against the total energy of reductant injected, as shown in Figure 5.3 and Figure 5.4. Because the diesel and n-butanol injections were the same on a mass basis, the n-butanol not only injected a lower quantity of energy, but also created a leaner mixture than diesel. For the diesel reductant reforming tests, it was clear that as the exhaust mixture became richer, the H_2 yield per kJ of reductant injected increased, reaching a maximum value of 0.026 mg/kJ of reductant when a mass of 1.3 g of diesel (56 kJ) was injected, and then dropping again as the mixture became richer for a 2.4 g diesel (103 kJ) injection. For the n-butanol reforming tests, the initial increase as the exhaust mixture became richer was evident, reaching a maximum value of 0.245 mg/kJ of reductant from the 1.3 g n-butanol (43 kJ) injection, and, similar to the diesel case, dropping again as the mixture became richer. This showed that n-butanol was much more efficient at H_2 generation, producing nearly ten times the amount of H_2 per kJ of reductant.
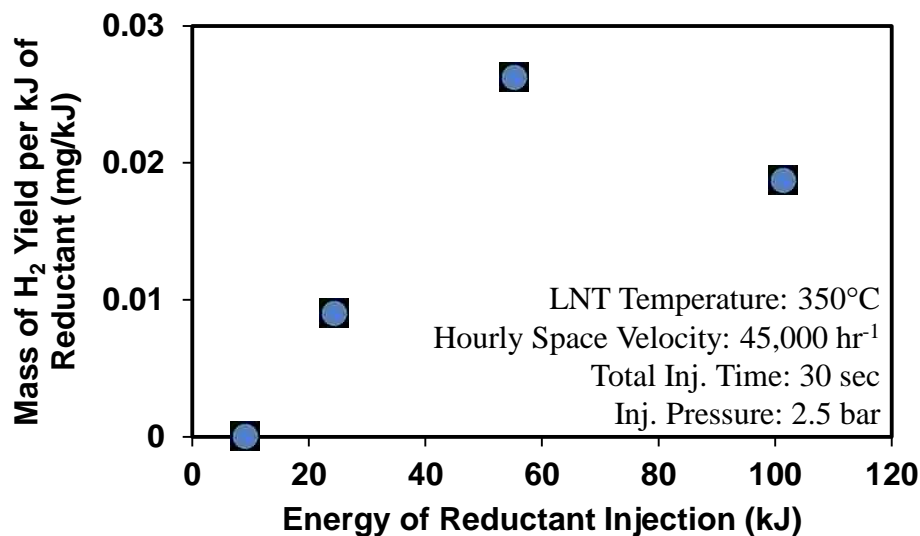
Figure 5.3 – H_2 Yield per kJ of Diesel (3% Exhaust O_2)
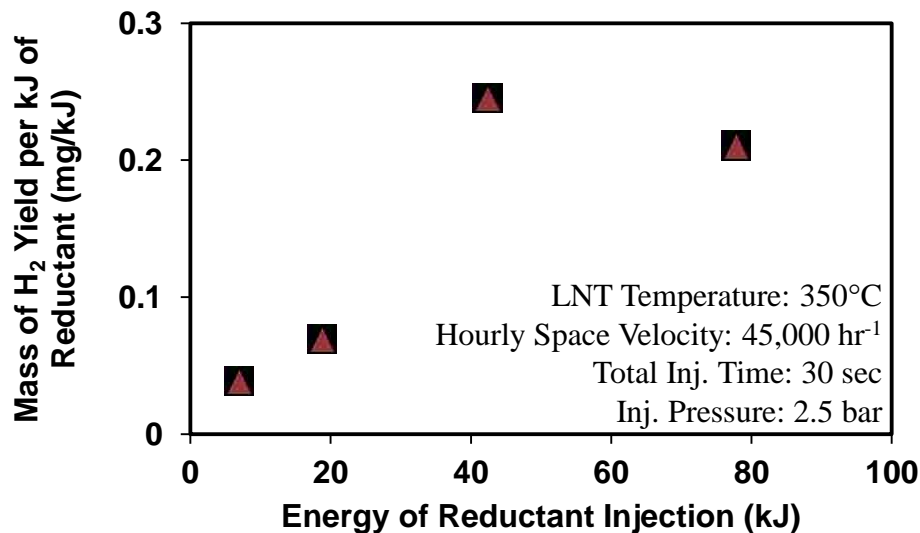
Figure 5.4 – H_2 Yield per kJ of n-Butanol (3% Exhaust O_2)

5.2   Hydrogen Generation with 0% Exhaust Oxygen

The presence of oxygen in the exhaust during regeneration can consume a portion of the injected reductant, thereby reducing the amount of reductant available for H_2 generation, NO_x release, and NO_x reduction. This can therefore result in the need for a greater quantity of reductant to be injected for efficient regeneration of the LNT, thus increasing the fuel penalty associated with the overall operation of the LNT. The purpose of the next set of H_2 generation tests was to determine the optimal quantity of reductant for efficient generation of H_2 in the exhaust in the absence of oxygen. One disadvantage of a lack of oxygen is that combustion in the exhaust will not occur, and therefore the temperature will not increase, potentially limiting the endothermic H_2 reforming reactions.

The conditions for tests 8 and 9 are shown in Table 5.1. In order to achieve an oxygen concentration of 0%, N_2 gas was used in combination with 1.5% CO. The addition of CO increased the HSV to about 50,000 hr^{-1}. With a lack of oxygen in the

exhaust, the majority of CO can be used for the water gas shift reaction (Equation 2.9). First, in order to verify how much H_2 can be produced from just the WGS reaction alone, a 2.5 bar water injection was added to produce an H_2O concentration of 6% within the exhaust. Preliminary experiments demonstrated that 8000 ppm of H_2 was yielded from just CO and H_2O due to the WGS reaction through both the DOC and the LNT, totalling 12 mg of H_2. With the absence of O_2, CO will not be oxidized into CO_2 through the DOC, potentially decreasing the yield of H_2 from the dry reforming reaction. Tests 8 and 9 involved the addition of reductant through a low pressure injection of 2.5 bar for a total injection time of 30 seconds.

Figure 5.5 and Figure 5.6 show a comparison of peak concentration of H_2 generated and the total mass of hydrogen yielded, respectively, for both n-butanol and diesel. The peak hydrogen produced did not always indicate the greatest production of total hydrogen yielded throughout the reforming test, because for some cases the peak was only reached for a short duration. Initially, at the lowest quantity of reductant injected, diesel produced a higher peak concentration of H_2. As the quantity of n-butanol injection increased, the peak concentration of H_2 generated steadily increased, and then tapered off at the highest reductant injection. This could also be seen as a linear increase in the mass of hydrogen yielded with reductant injection. The peak H_2 yield of diesel was not much greater than the yield of H_2 from the WGS reaction. Since the lack of oxygen meant minimal or no increase in temperature, many of the endothermic hydrogen reforming reactions may not have occurred. n-Butanol yielded a greater mass of H_2 than diesel throughout the reductant injection sweep.
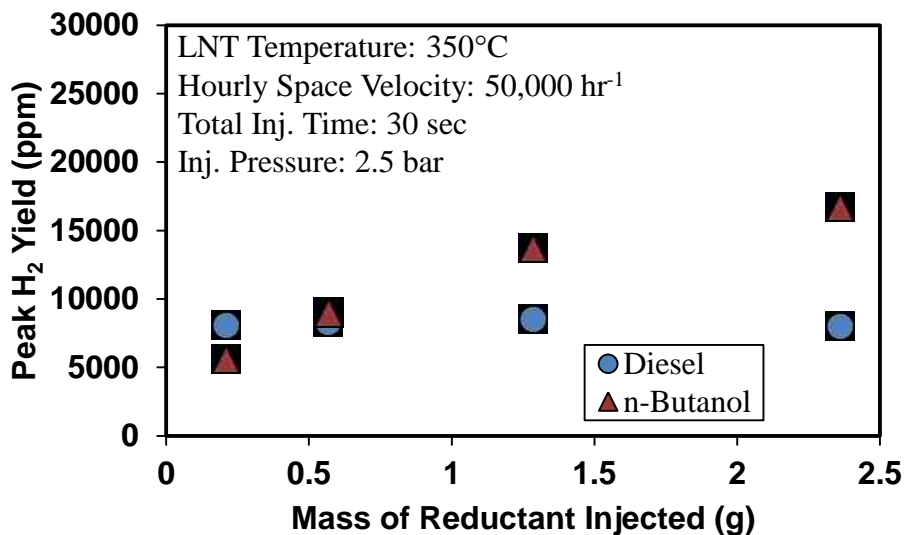
Figure 5.5 – Peak H_2 Yield (0% Exhaust O_2)
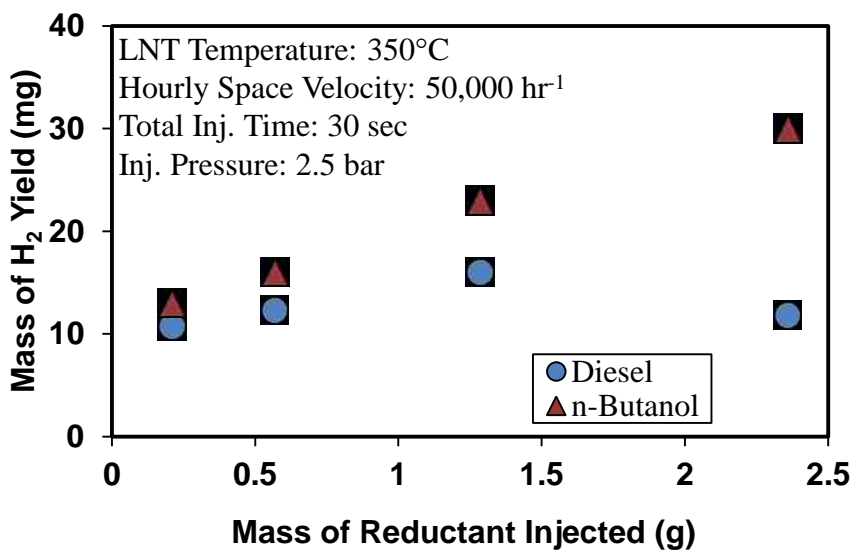
Figure 5.6 – Mass of H_2 Yield (0% Exhaust O_2)

Again, since the mass of reductant injection was the same with tests 8 and 9, a lower energy of n-butanol was injected. The trend for the mass of hydrogen yielded per kJ of reductant against the energy of reductant injected is shown in Figure 5.7. As the reductant injection increased, the mass of H_2 yielded per kJ of reductant injected decreased for both n-butanol and diesel. This was contrary to the 3% exhaust oxygen

concentration tests, when the mass of H_2 produced per kJ of reductant increased with reductant injection. Initially, at low quantity reductant injections, it appeared that n-butanol was almost 50% more efficient at generating H_2 compared to diesel, even though the mass of H_2 produced was less than 30% greater for n-butanol than diesel. Although the mass of H_2 produced per kJ of reductant reduced with increasing reductant injection for both diesel and n-butanol, n-butanol was almost 50% more effective in production of H_2, even with a lower total energy injection. This also includes the H_2 yielded from the WGS reaction.
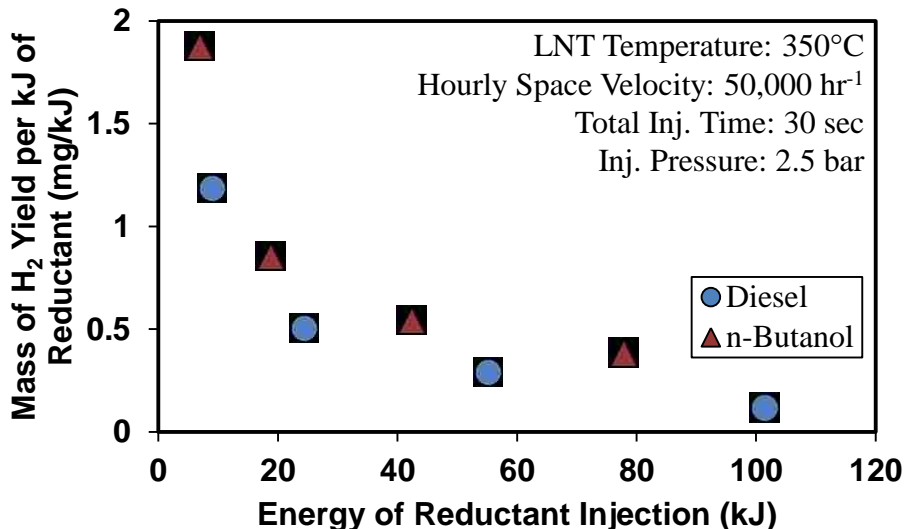
Figure 5.7 – H_2 Yield per kJ of Diesel and n-Butanol (0% Exhaust O_2)

5.3   Summary of Hydrogen Generation Test Results

Table 5.2 and Table 5.3 show the overall H_2 reforming test results, for the 3% oxygen and 0% oxygen concentration tests, respectively, while Figure 5.8 shows the total mass of H_2 for tests 6 through 9, respectively. Comparing the 3% O_2 concentration and 0% O_2 concentration experimental results, it was observed that with no oxygen, n-butanol and diesel yielded much higher H_2 concentrations at identical conditions to the 3% O_2

concentration. One major reason for this was the addition of CO. Preliminary experiments showed that without reductant injection, CO and H_2O reacted to produce a peak H_2 concentration of 8000 ppm totalling about 12 mg of H_2. Diesel injection at 0% O_2 did not significantly contribute to H_2 production. It was also observed that the CO emissions downstream of the LNT were at a higher concentration with n-butanol than with diesel. CO is a product of the steam reforming reaction, and thus a higher concentration of CO may signify effective steam reforming of n-butanol.

Table 5.2 – Hydrogen Reforming Results at 3% Exhaust O_2

Reductant	Mass of Reductant Injected	Energy of Reductant Injected	Peak H_2 Concentration	Mass of H_2 Produced	Max Temp
Diesel	0.2 g	8.6 kJ	0 ppm	0 mg	430°C
Diesel	0.6 g	25.8 kJ	550 ppm	0.22 mg	530°C
Diesel	1.3 g	55.9 kJ	3150 ppm	1.45 mg	560°C
Diesel	2.4 g	103.2 kJ	3200 ppm	1.9 mg	560°C
n-Butanol	0.2 g	6.9 kJ	340 ppm	0.27 mg	400°C
n-Butanol	0.6 g	19.8 kJ	1870 ppm	1.3 mg	465°C
n-Butanol	1.3 g	42.9 kJ	11500 ppm	10.4 mg	530°C
n-Butanol	2.4 g	79.2 kJ	17500 ppm	16.4 mg	540°C

Table 5.3 – Hydrogen Reforming Results at 0% Exhaust O_2

Reductant	Mass of Reductant Injected	Energy of Reductant Injected	Peak H_2 Concentration	Mass of H_2 Produced	Max Temp
Diesel	0.2 g	8.6 kJ	8070 ppm	10.7 mg	350°C
Diesel	0.6 g	25.8 kJ	8300 ppm	12.3 mg	350°C
Diesel	1.3 g	55.9 kJ	8500 ppm	16.0 mg	350°C
Diesel	2.4 g	103.2 kJ	8000 ppm	11.8 mg	350°C
n-Butanol	0.2 g	6.9 kJ	5600 ppm	13.0 mg	350°C
n-Butanol	0.6 g	19.8 kJ	9000 ppm	16.0 mg	350°C
n-Butanol	1.3 g	42.9 kJ	13700 ppm	23.0 mg	350°C
n-Butanol	2.4 g	79.2 kJ	16700 ppm	30. mg	350°C
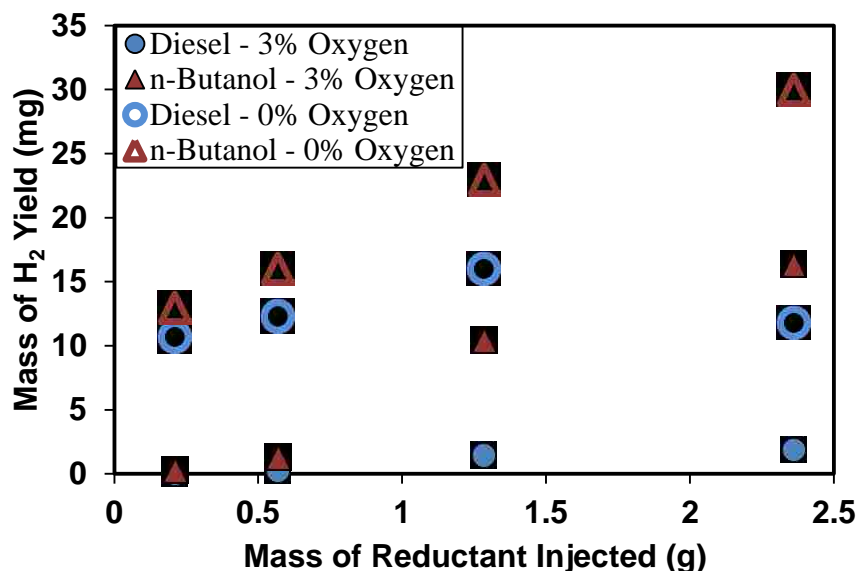
Figure 5.8 – Summary of Mass of H_2 Yielded for Tests 6-9

It was noticed that for the 3% O_2 tests, more CO_2 was measured downstream of the LNT during diesel reforming than for the n-butanol test at the same conditions. This potentially indicates that CO_2 formed during n-butanol hydrogen generation could have reacted with methane or other light hydrocarbons in the dry reforming reaction. This would explain the low CO_2 sampled downstream of the LNT, and may also be another reason for the greater quantity of hydrogen produced by n-butanol.

The total mass of H_2 yield per kJ of reductant for tests 6 through 9 is shown in Figure 5.9. The mass of H_2 yielded from the WGS reaction in tests 8 and 9 was 12 mg. In order to estimate the diesel or n-butanol contribution to H_2 reforming, 12 mg was subtracted from the total H_2 yield of test 8 and 9, for this comparison. Thus, the mass of H_2 yield per kJ of reductant increased with reductant injection with both diesel and n-butanol at 0% and 3% exhaust oxygen concentration. Again, the highest yield of H_2 per reductant injection was observed at the 1.3 g reductant injection case for both diesel and n-butanol.
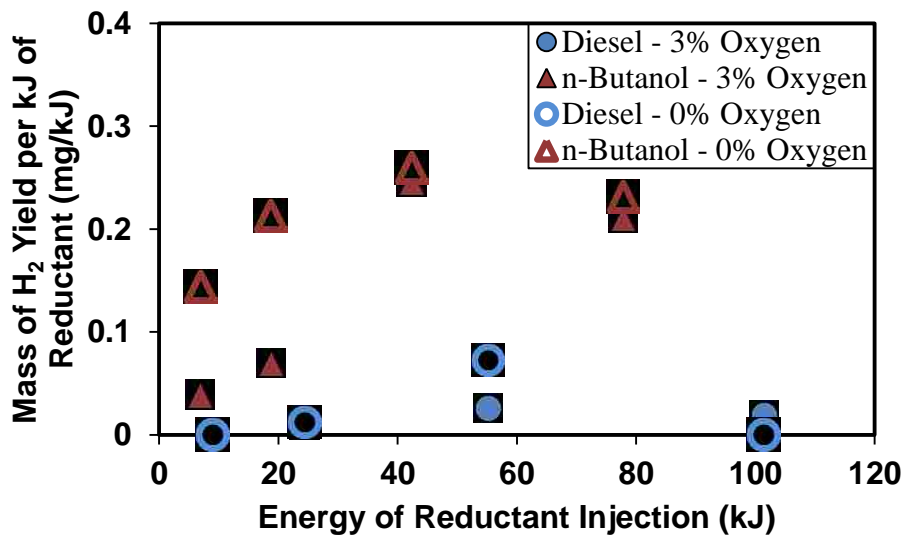
Figure 5.9 – Summary of Mass of H_2 Yielded per kJ of Reductant for Tests 6-9

Thus, it is clear that n-butanol can potentially produce more H_2 from the same mass of reductant as diesel, at either an oxygen concentration of 3% or 0%. This potentially means that the regeneration of an LNT through an n-butanol injection into the exhaust compared to a diesel injection, can have a greater benefit. However, it has also been shown that excess H_2 during regeneration can result in high NH_3 emissions [30, 38, 46, 48, 49, 66].

CHAPTER 6:LNT REGENERATION EXPERIMENTAL RESULTS

This chapter focuses on the LNT regeneration experiments conducted on the after-treatment flow bench. The conditions used for the regeneration experiments are outlined in Table 6.1, and are similar to the hydrogen generation experiment conditions. The main purpose of the regeneration experiments was to compare the release and reduction of NO_x from n-butanol and diesel regeneration at different exhaust oxygen concentrations and reductant quantities. The flow bench schematic was given in Figure 3.4.

Table 6.1 – LNT Regeneration Test Conditions

Test	Reductant	LNT Temp (°C)	NO_x Stored (g)	Hourly Space Velocity (hr^{-1})	Total Inj. Time (s)	Reductant Quantity (g)	O_2 (%)	H_2O (%)	CO (%)
10	Diesel	350	0.2	45,000	30	0.2	3	6	0
		350	0.2	45,000	30	0.6	3	6	0
		350	0.2	45,000	30	1.3	3	6	0
		350	0.2	45,000	30	2.4	3	6	0
11	n-Butanol	350	0.2	45,000	30	0.2	3	6	0
		350	0.2	45,000	30	0.6	3	6	0
		350	0.2	45,000	30	1.3	3	6	0
		350	0.2	45,000	30	2.4	3	6	0
12	Diesel	350	0.2	50,000	30	0.2	0	6	1.5
		350	0.2	50,000	30	0.6	0	6	1.5
		350	0.2	50,000	30	1.3	0	6	1.5
		350	0.2	50,000	30	2.4	0	6	1.5
13	n-Butanol	350	0.2	50,000	30	0.2	0	6	1.5
		350	0.2	50,000	30	0.6	0	6	1.5
		350	0.2	50,000	30	1.3	0	6	1.5
		350	0.2	50,000	30	2.4	0	6	1.5

In conventional LNT operations, the regeneration phase is followed immediately by an adsorption period, which is again followed by a regeneration period, and so on. For these experiments, a purge period, using only 1.5% CO, 6% H_2O, and balance N_2, was

added following LNT regeneration. This added purge period was used to release any NO_x still remaining on the LNT after the regeneration. A high NO_x release during the purge period would indicate that the regeneration was ineffective.

6.1   LNT Regeneration with 3% Exhaust Oxygen

Each regeneration of the LNT was conducted at steady state conditions, and only the quantity and type of reductant was altered. In order to fairly compare the use of n-butanol and diesel, the same quantity of NO_x was loaded onto the LNT catalyst prior to the regeneration. Preliminary tests showed that the regeneration of the LNT was fairly independent of the NO_x adsorption period, as long as the quantity of NO_x stored on the LNT was maintained constant. In order to reduce the overall test time, a nominal inlet NO_x concentration of around 200 ppm was used for each test until 0.2 g of NO_x (0.85g/L of catalyst) was stored on the LNT. This resulted in an adsorption time of about 5 minutes. This was consistent with the adsorption tests discussed in Chapter 3. During adsorption, only air and NO were used.

An average LNT temperature of 350°C was maintained throughout the adsorption period. Once 0.2 g of NO_x was stored on the catalyst, the NO feed gas was shut off, and the regeneration mode was enabled. Similar to the hydrogen generation tests, two different regeneration conditions were applied. Each test compared the effect of the reductant quantity on the regeneration of the LNT. The rich condition used for regeneration tests 10 and 11 was achieved with an air flow rate of 10 L/min, with a balance of N_2 gas to create an exhaust oxygen concentration of around 3%. Once the conditions were stable, a water injection was initiated to produce an H_2O concentration of 6%. The water injection was upstream of the DOC and the LNT. These exhaust

conditions produced an LNT HSV of about 45,000 hr^{-1}. Test 10 featured four separate diesel regenerations that provided four different oxygen-based λ values (1.6, 0.6, 0.3, and 0.2). Test 11 featured four separate n-butanol regenerations that provided four different oxygen-based λ values (2.3, 0.9, 0.4, and 0.2). The same quantity of reductant of diesel and n-butanol resulted in different λ values because diesel and n-butanol have different chemical compositions.

Gas sampling was available both upstream and downstream of the LNT. The downstream sampling was fed to the CAI analyzers and to the FTIR. The FTIR was used to measure NO, NO_2, various light hydrocarbon species, N_2O, and NH_3. Although the release and reduction of NO_x occurs simultaneously during LNT regeneration, these next two subsections will observe these processes separately.

6.1.1   Release of NO$_x$

In order to activate the regeneration of the LNT, a low pressure reductant injection was utilized upstream of the LNT catalyst while a simultaneous low pressure water injection was employed upstream of the DOC catalyst. As the reductant was introduced, it began to oxidize due to the oxygen present in the exhaust flow. This in turn created an oxygen depleted rich regeneration front that propagated through the LNT catalyst, increasing the temperature. It has been demonstrated that the quantity of NO_x slip increases with increasing temperature [30]. This potentially means that if too much reductant is injected into an oxygen rich exhaust, a greater quantity of NO_x may be released unconverted, from the LNT. At the initiation of the regeneration, a high increase in NO_x slip downstream of the catalyst was observed.

The peak NO_x slip concentration during the regeneration relative to the reductant injection quantity is given in Figure 6.1. Initially, at the lowest reductant injection, the concentration of NO_x slip was less than 60 ppm for the diesel regeneration. Since the mixture was still lean, and only a small portion of reductant was injected, the temperature did not significantly increase, thereby only releasing a small portion of NO_x. The n-butanol regeneration resulted in a significantly higher peak concentration of NO_x slip during the leanest regeneration, although it was still fairly low at only 140 ppm. This higher concentration may potentially be due to the higher H_2 concentration produced from n-butanol regeneration, as shown in Figure 5.2. For the diesel reductant regeneration tests, as the diesel injection increased, the peak NO_x concentration downstream of the catalyst increased, reaching a maximum of 370 ppm at the second richest regeneration tested. The NO_x slip then reduced below 150 ppm for the final richest condition tested. This same trend was realized for the n-butanol regeneration; however, the NO_x slip was higher than that with diesel, and had a lower variation, with only a 14% increase in NO_x slip from the 0.6 g to 1.3 g regeneration, while diesel showed over a 50% increase in NO_x slip for the same increase in reductant. One potential reason for this higher concentration of NO_x release with n-butanol regeneration is the oxygen content of n-butanol. n-Butanol contains 21.6% oxygen by mass compared to diesel which has 0% oxygen, which could potentially reduce the efficiency of the conversion of NO_x.
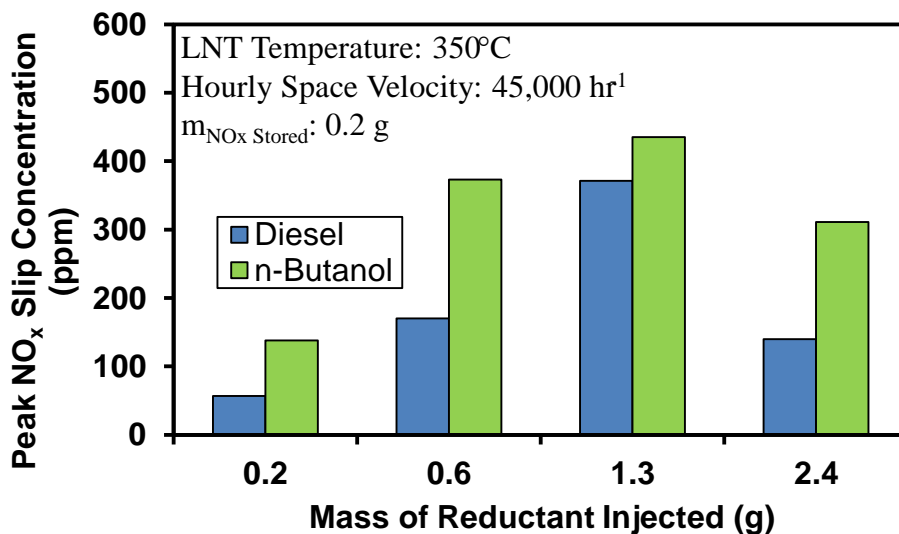
Figure 6.1 – Peak NO_x Slip During LNT Regeneration (3% Exhaust O_2)

Although the reductant was injected for 30 seconds, the release of NO_x generally began at the onset of the injection, and reduced to zero after about 10-20 seconds. The duration of NO_x release varied for each regeneration, indicating that a higher peak of NO_x slip may not necessarily be associated with a higher total quantity of NO_x slip released during regeneration. Figure 6.2 shows the total percentage of NO_x stored which was released during the regeneration on a mass basis. Although each regeneration had a fairly high peak concentration of NO_x slip, the total quantity of NO_x slip never exceeded 5% of the total quantity of NO_x stored. The leanest regeneration showed the lowest quantity of NO_x slip, with both diesel and n-butanol releasing less than 0.7% of the total NO_x during regeneration.

As the reductant quantity injected per regeneration increased, the concentration was driven to richer conditions, and the total NO_x slip decreased for both diesel and n-butanol regeneration. The highest total NO_x slip occurred at the regeneration closest to a stoichiometric mixture, for both diesel (O_2-based $\lambda = 0.6$) and n-butanol (O_2-based $\lambda =$

0.9). The lowest total NO_x slip, besides the lean regeneration, occurred at the richest regeneration. Throughout the reductant quantity sweep, the diesel regeneration showed a higher total NO_x slip than n-butanol. A low release of NO_x during regeneration can indicate that the NO_x on the LNT was effectively reduced, or that the NO_x is still stored on the catalyst.
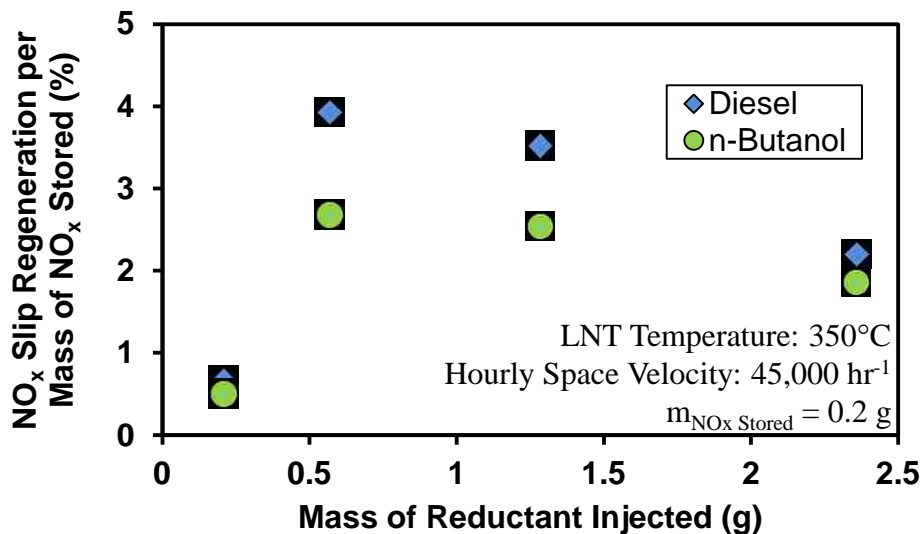
Figure 6.2 – NO_x Slip per Mass of NO_x Stored LNT Regeneration (3% Exhaust O_2)

Following each regeneration, a purge period was conducted. This was used in order to determine the quantity of NO_x remaining on the catalyst, following regeneration. An example of the inlet and outlet NO_x concentration throughout the entire process is shown with diesel regeneration in Figure 6.3 and with n-butanol regeneration in Figure 6.4. This example shows the NO_x loading period, the LNT regeneration period, and also the CO and H_2O purge. It may be noted that although the peak NO_x slip was higher for the n-butanol regeneration, the duration of the n-butanol release was slightly shorter than the diesel regeneration. This is the reason for the similar total quantity of NO_x slip as shown in Figure 6.2. As for the purge, a lower total NO_x slip during the purge indicates

that the regeneration was more effective, or less NO_x remained on the catalyst following regeneration. Similar to the regeneration, however, a lower peak concentration of NO_x slip does not necessarily coincide with a lower total quantity of NO_x slip.

Figure 6.3 – NO_x During Adsorption, Diesel Regeneration, and Purge
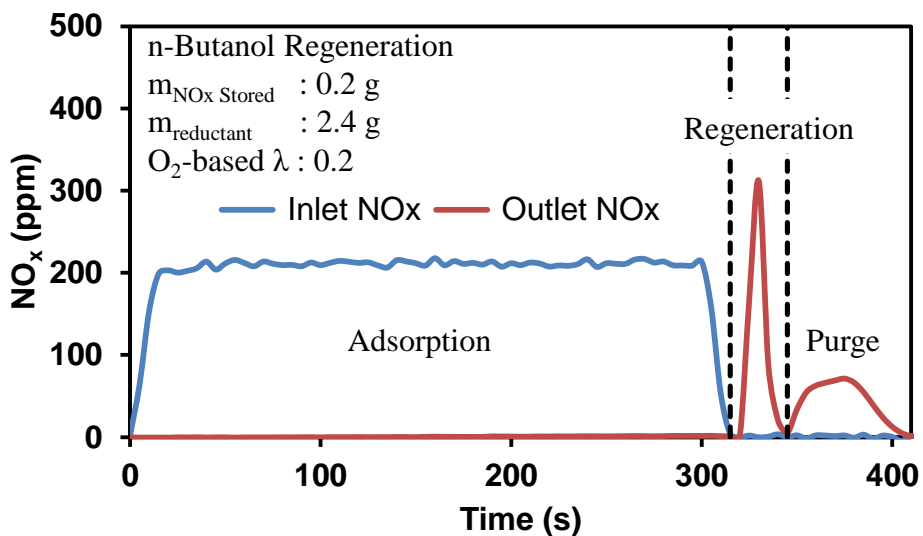
Figure 6.4 – NO_x During Adsorption, n-Butanol Regeneration, and Purge

The total cumulative mass of the inlet and outlet NO_x throughout the entire process is shown with diesel regeneration in Figure 6.5 and n-butanol regeneration in

Figure 6.6. The cumulative mass of NO_x released during the purge was significantly higher (over 60%) following the diesel regeneration of 2.4 g than following the n-butanol regeneration of 2.4 g. This indicates that the diesel regeneration was less effective at removing NO_x from the LNT than the n-butanol regeneration.
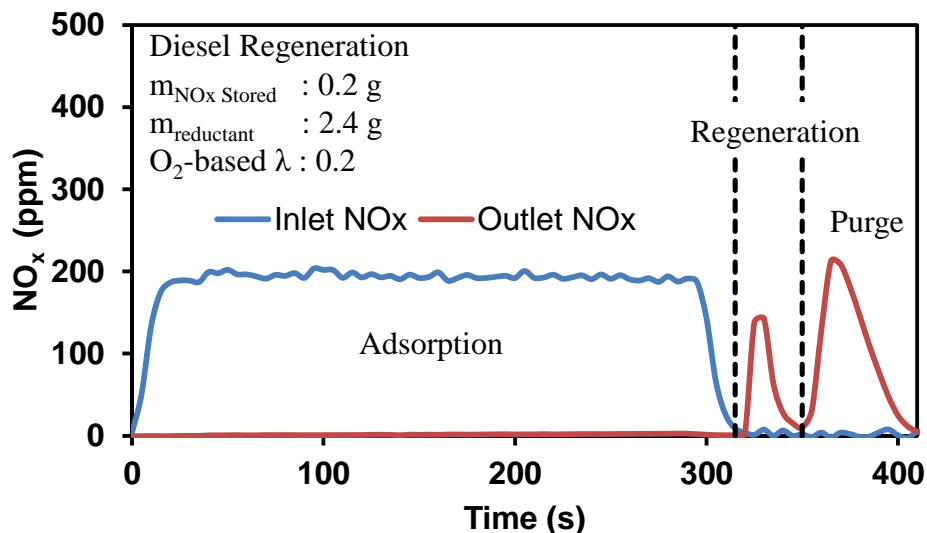

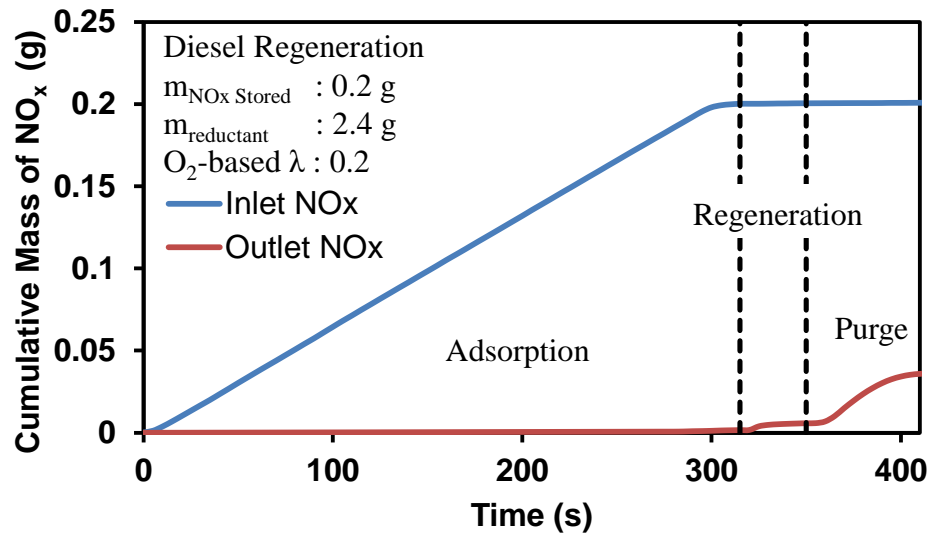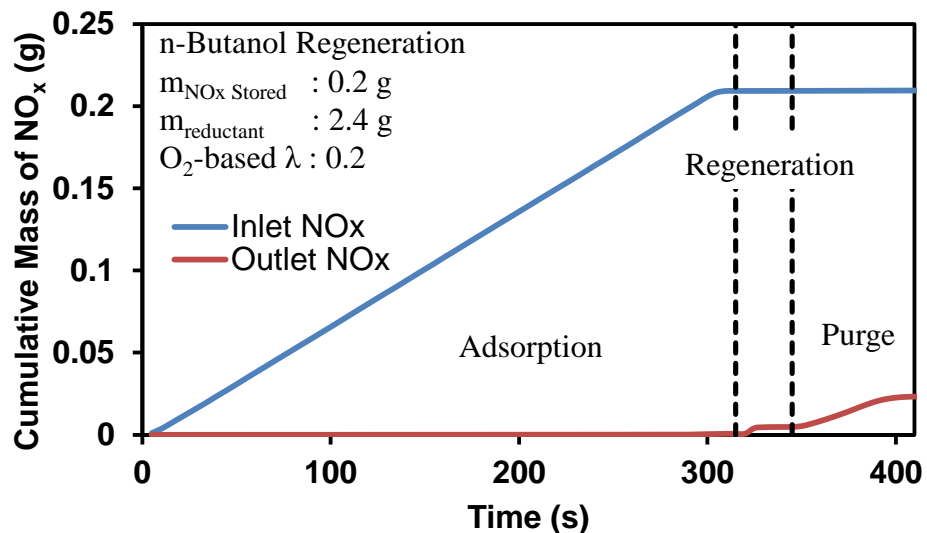Figure 6.5 – Mass of NO_x During Adsorption, Diesel Regeneration, and Purge

Figure 6.6 –Mass of NO_x During Adsorption, n-Butanol Regeneration, and Purge

The difference between the cumulative mass of NO_x stored, and the cumulative mass of NO_x released during the purge, divided by the cumulative mass of NO_x stored is defined as the regeneration effectiveness (Equation 6.1)

$$\text{Regeneration Effectiveness} = \frac{m_{\text{NOx stored}} - m_{\text{NOx released during purge}}}{m_{\text{NOx stored}}} \text{(Equation 6.1)}$$

For a regeneration to have 100% regeneration effectiveness, the regeneration must not leave any NO_x remaining on the catalyst. The effectiveness of the regeneration does not take into account the conversion of NO_x, meaning a very high cumulative mass of NO_x released during regeneration can still be quantified as an effective regeneration if the mass of NO_x released during the purge is low.

The regeneration effectiveness of both diesel and n-butanol regeneration is shown in Figure 6.7. The leanest regeneration was the most effective at over 95%. However, although the regeneration did not release significant NO_x, it was likely that a portion of the NO_x was adsorbed towards the rear of the LNT. As the reductant injection increased, initially both n-butanol and diesel were not very effective at regenerating the LNT, only about 76% effective with n-butanol and 71% with diesel. As the gas became richer with a greater injected reductant quantity, the regeneration was more effective. The greatest reductant injection was also the most effective, besides the lean regeneration; over 91% effective with n-butanol and 85% effective with diesel. Each regeneration proved that n-butanol was more effective at regenerating the LNT than diesel for the given test conditions, except for the leanest regeneration test case where the regeneration effectiveness of diesel and n-butanol was similar.
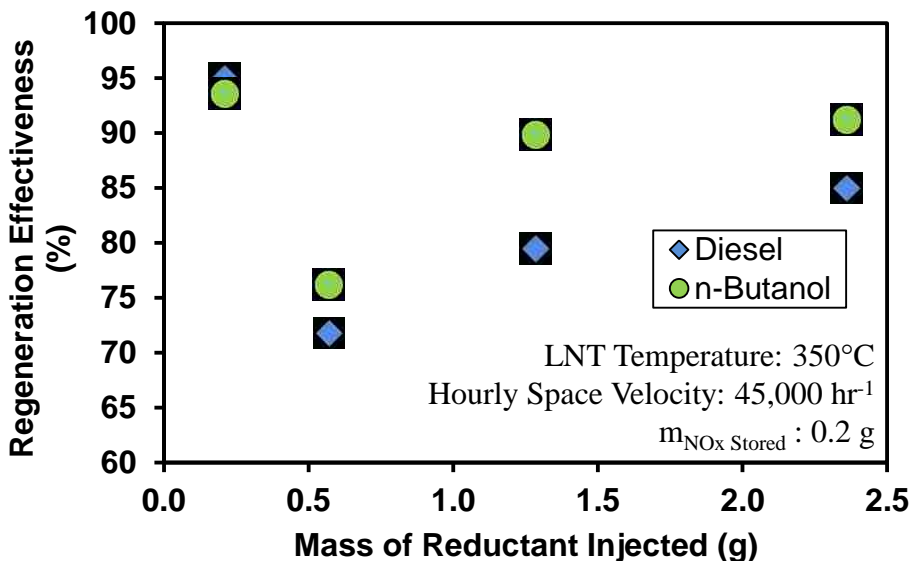
Figure 6.7 – Regeneration Effectiveness (3% Exhaust O_2)

Therefore, both the diesel and n-butanol LNT regeneration proved to effectively release NO_x, and the effectiveness appeared to increase with increasing injected reductant quantity. Although, the leanest regeneration tested regenerated the LNT effectively, preliminary investigations determined that the NO_x storage capacity of the LNT decreased during adsorption periods following regenerations where minimal H_2 was formed. Thus without the added purge, the lean regeneration condition had an adverse effect on the storage period.

6.1.2   Reduction of NO_x

The effectiveness of regeneration in terms of how well the regeneration cleared the LNT for a subsequent adsorption cycle has been shown. However, the efficiency of conversion of NO_x into N_2 has not been discussed. The N_2O and NH_3 emissions were measured during tests 10 and 11 with an FTIR analyzer. The chemical mechanism of the NO_x reduction in an LNT was discussed in Chapter 2. It was mentioned that the initial

peaks of NO_x and N_2O were observed at the beginning of regeneration, while NH_3 was released later. This trend was observed in the regeneration of the LNT with diesel as shown in Figure 6.8. The same trend was observed regardless of the type of reductant, or quantity of reductant injected, although the concentrations were different.
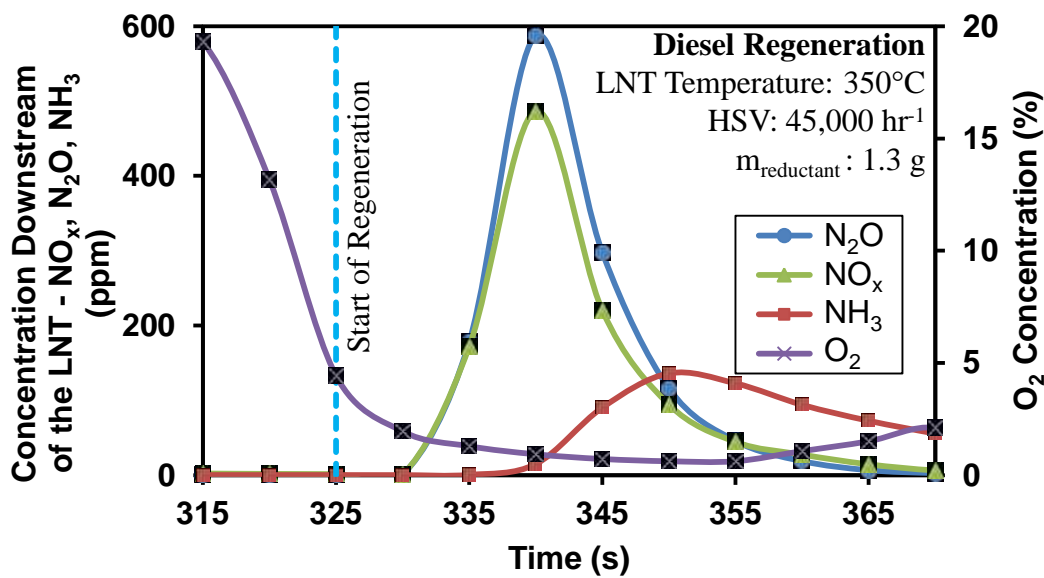
Figure 6.8 – NO_x, N_2O, and NH_3 Emissions During Regeneration with Diesel

Since N_2 emissions were not directly measured for this study, the difference between the total quantity of NO_x stored, and the total quantity of N-containing products released during the regeneration and purge was assumed to be N_2. NH_3 and N_2O were not released during the purge period. This was expected since no diesel or n-butanol was used, and the conversion of NO_x was very low, indicating that the traditional reduction reactions may not have proceeded.

The peak concentration of N_2O sampled during regeneration with n-butanol and diesel is shown in Figure 6.9. The trend of N_2O slip was somewhat similar to the concentration of NO_x release during regeneration. At low reductant quantities, the concentration of N_2O was quite low, only just above 100 ppm for both the diesel and n-

butanol regeneration. Since, the increase in reductant quantity used for regeneration resulted in an increase in temperature, the rate of NO_x release would have increased, but the rate of conversion may not have necessarily increased. This could explain the increase in N_2O concentration as the reductant quantity used for regeneration increased. The peak N_2O formed with n-butanol as the reductant was only slightly higher than the diesel case, except for the richest condition where the concentration was about equal. The highest peak N_2O formed was at the second richest regeneration.
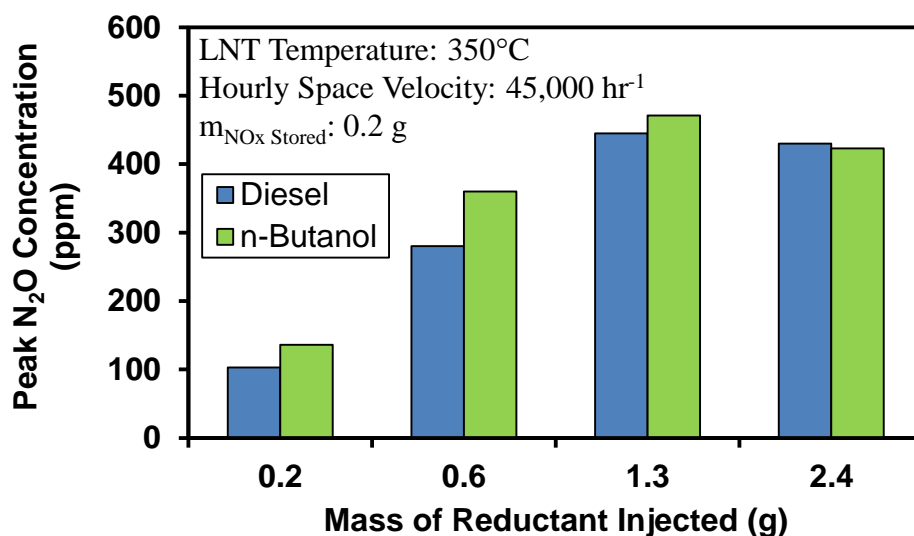
Figure 6.9 – Peak N_2O During LNT Regeneration (3% Exhaust O_2)

The amount of NH_3 slip generally depends on the type and quantity of reductant used. The peak concentration of NH_3 for tests 10 and 11 is shown in Figure 6.10. The amount of NH_3 slip increased as the quantity of reductant increased; however, the peak NH_3 released during n-butanol regeneration was significantly higher than with diesel regeneration. The highest concentration of NH_3 occurred during the richest n-butanol regeneration, and amounted to a concentration of 530 ppm, while the highest NH_3 concentration during diesel regeneration also occurred at the richest diesel regeneration,

with a concentration of about 120 ppm. The hydrogen generation results of Chapter 5 showed that n-butanol produced more H_2 than diesel for the same injected reductant quantity. The greater H_2 yield of n-butanol could explain the high peak in NH_3 formed for the n-butanol regeneration compared to the diesel regeneration.
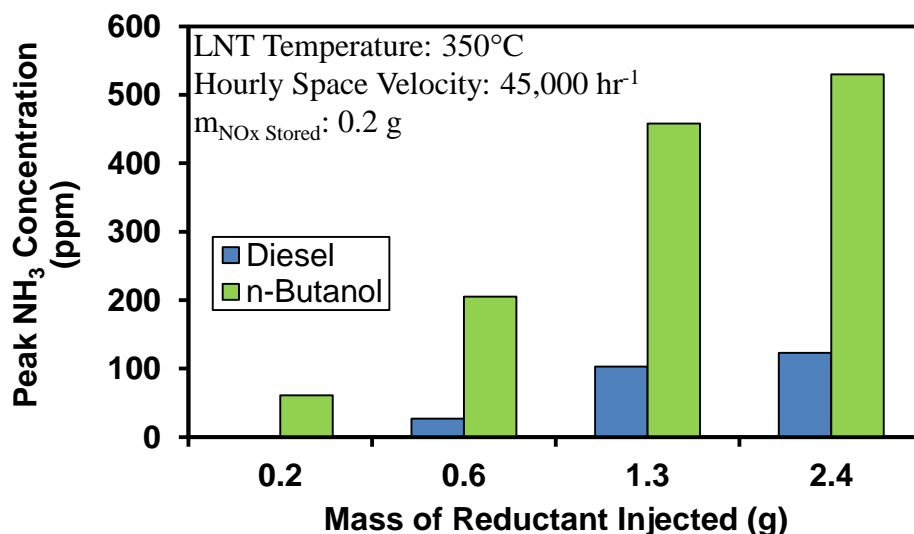
Figure 6.10 – Peak NH_3 During LNT Regeneration (3% Exhaust O_2)

Although NH_3 is generally unfavourable, it can be relatively easily reduced with the use of an ammonia slip catalyst. Also, the use of an SCR downstream of the LNT could potentially utilize the NH_3 to further reduce NO_x. The use of an LNT and SCR in series has been studied extensively [66-69].

In order to determine the conversion efficiency of the LNT during each regeneration, all nitrogen containing products formed during regeneration must be considered. This will be defined as the selectivity to N_2 (Equation 6.2). Since the main focus was to observe the conversion during the regeneration, the NO_x released during the purge is directly subtracted from the NO_x stored. Therefore the cumulative NO_x stored is represented by $[N]_{in}$, while the cumulative N_2O, NH_3 and NO_x slip are signified as $[N_2O]$,

[NH$_3$], and [NO$_x$]$_{slip}$, respectively. Since this equation is calculated on a molar basis, the quantity of N$_2$O is doubled to account for two N-atoms per molecule.

$$N_2 \text{ Selectivity} = \frac{[N]_{in} - ([2N_2O] + [NH_3] + [NO_x])_{slip}}{[N]_{in}} \qquad \text{(Equation 6.2)}$$

The selectivity to N$_2$ for each regeneration is compared in Figure 6.11. At the leanest regeneration, the highest selectivity to N$_2$ was achieved for both diesel and n-butanol. As the regeneration became richer, the diesel and n-butanol regeneration selectivity to N$_2$ initially decreased, then increased as the reductant quantity increased. The selectivity to N$_2$ with n-butanol as a reductant was consistently higher than with diesel as a reductant, although only slightly, except for the leanest regeneration. The richest regeneration tested achieved a selectivity to N$_2$ of 89% for n-butanol, and 87% for diesel.
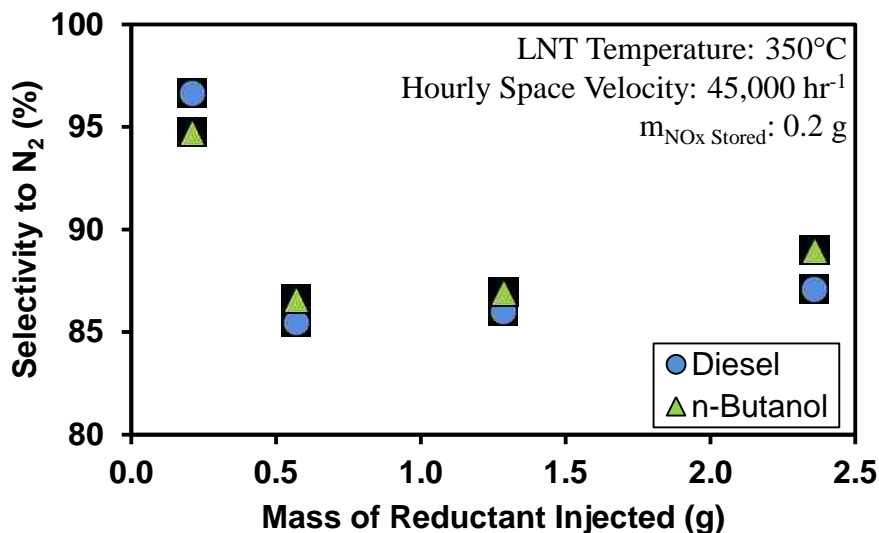

Figure 6.11 – Selectivity to N$_2$ (3% Exhaust O$_2$)

Thus it was apparent that the use of n-butanol as a reductant was highly effective in the conversion of NO$_x$ into N$_2$ during LNT regeneration at an oxygen concentration of 3%.

6.2   LNT Regeneration with 0% Exhaust Oxygen

To ensure that the entirety of reductant added during regeneration was used for LNT regeneration, an oxygen-free environment was utilized during regeneration for test 12 and test 13. This eliminated the potentially unnecessary oxidation of reductant, and allowed for observation into the exothermic nature of LNT regeneration. The specific testing conditions for tests 12 and 13 are listed in Table 6.1. Prior to regeneration, the LNT was loaded with 0.2 g of NO_x through a 5 minute adsorption period of 200 ppm NO and air at 350°C. To initiate regeneration of the LNT, the NO feed gas and air supply were shut off, and 1.5% CO and N_2 balance were supplied to the flow bench, producing an HSV of 50,000 hr^{-1}. The amount of diesel or n-butanol reductant supplied was swept from 0.2 g to 2.4 g per regeneration, similar to the 3% O_2 regeneration tests. The purge period concentration following regeneration was maintained the same as in tests 10 and 11, with 6% H_2O, 1.5% CO and balance N_2. The purpose of the purge was to release any NO_x still remaining on the LNT following regeneration. After the purge period, an air and NO mixture was introduced into the flow bench allowing for NO_x adsorption to begin again.

The gas downstream of the LNT was sampled throughout the regeneration and purge period. The CAI analyzers and FTIR were utilized for determining the concentration of various N-containing species, light HCs, CO, CO_2, and O_2. The emissions measured during the regeneration and purge allowed for analysis and quantification of the release and reduction of NO_x during LNT regeneration with diesel or n-butanol as a reductant.

6.2.1   Release of NO_x

It was previously mentioned that the release of NO_x is accelerated by an increase in temperature, since the stability of $Ba(NO_3)_2$ sites decreases. With the absence of oxygen, the reductant used for regeneration did not oxidize, and therefore no significant temperature increase was realized. It has been hypothesized that a lack of oxygen decreases the stability of nitrate species and can trigger the release of NO_x, however, in the experiments conducted for this study, no NO_x release was realized upon transition into rich conditions. In Chapter 5, under the same regeneration conditions of tests 9 and 10 without stored NO_x, hydrogen was generated in abundance with both diesel and n-butanol. Thus, the formation of H_2, as well as the decomposition of diesel or n-butanol into lighter hydrocarbons appeared to be the main cause of NO_x release during regeneration with a lack of oxygen.

The peak concentration of NO_x released during regeneration with diesel or n-butanol is given in Figure 6.12. The concentration of NO_x slip during regeneration with n-butanol appeared to directly depend on the amount of reductant used. The concentration of NO_x slip increased with increasing n-butanol injection, reaching a maximum NO_x concentration of 1200 ppm at the richest regeneration condition. The diesel regeneration, however, did not appear to follow a trend in terms of the peak concentration of NO_x released relative to the total amount of reductant injected. The peak NO_x slip occurred during the 0.6 g diesel injection, with a value of almost 700 ppm.
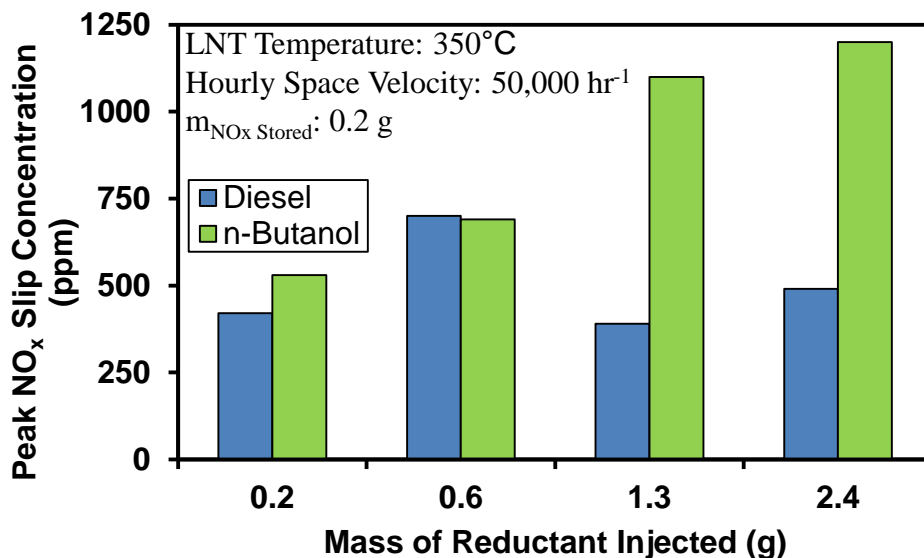
Figure 6.12 – Peak NO_x Slip During LNT Regeneration (0% Exhaust O_2)

Since the NO_x release occurred over a very short period of time for each regeneration, similar to tests 10 and 11, the peak concentration was not necessarily a true representation of the total amount of NO_x released. Instead, the mass of NO_x slip per total NO_x stored can be observed in Figure 6.13. At the lowest reductant quantity, the diesel regeneration released a slightly higher quantity of NO_x relative to the quantity of NO_x stored on the LNT. However, as the reductant quantity increased, the n-butanol regeneration released a much higher quantity of NO_x compared to the diesel regeneration at the same reductant quantity. The highest NO_x release for both diesel and n-butanol occurred at the 0.6 g regeneration. This coincided with the highest peak concentration of NO_x released during diesel regeneration; however it was not the highest peak concentration of NO_x released during n-butanol regeneration.
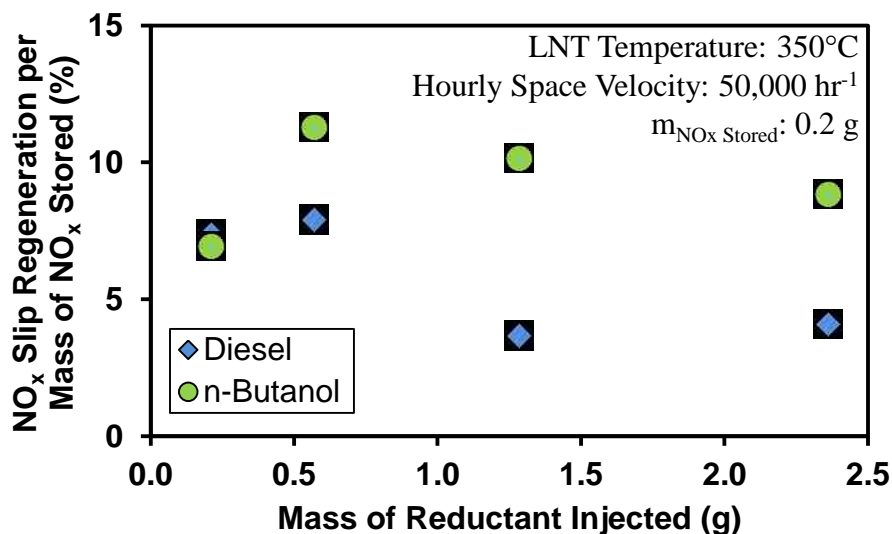
Figure 6.13 – NO$_x$ Slip per Mass of NO$_x$ Stored LNT Regeneration (0% Exhaust O$_2$)

The purge period following each regeneration at 0% oxygen showed minimal NO$_x$ release. The peak NO$_x$ slip concentration during the purge did not exceed 100 ppm for any purge following diesel or n-butanol regeneration. The NO$_x$ released during purge per gram of NO$_x$ stored is shown in Figure 6.14. Less than 2% of the total NO$_x$ stored remained on the catalyst following each of the n-butanol or diesel regenerations. However, it is clear that with the increase of reductant quantity, the diesel regeneration was more effective at regenerating the LNT. There was no apparent NO$_x$ release following the greatest quantity of diesel regeneration. This indicates that the regeneration was nearly 100% effective. The purge following n-butanol regeneration released a slightly higher quantity of NO$_x$ than the purge following diesel regeneration, except at the lowest reductant quantity where the regeneration left about the same quantity of NO$_x$ on the LNT. Again, the highest reductant quantity regeneration of n-butanol appeared to be the most effective, resulting in the lowest release of NO$_x$ during purge.
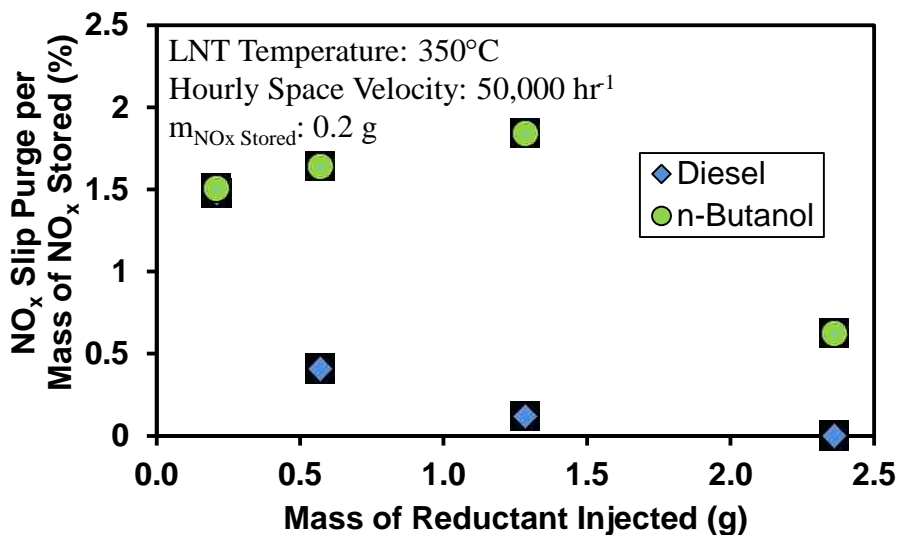
Figure 6.14 – NO$_x$ Slip Per Mass of NO$_x$ Stored LNT Purge (0% Exhaust O$_2$)

The regeneration effectiveness of each case is given in Figure 6.15. The effectiveness of each diesel and n-butanol regeneration was greater than 98%. The diesel regeneration was slightly more effective than the n-butanol regeneration at the same reductant quantity. This can potentially be attributed to the oxygen content of n-butanol. Although the majority of NO$_x$ released during regeneration was NO with both diesel and n-butanol, the n-butanol regeneration released a slightly higher amount of NO$_2$. Thus, the oxygen content of n-butanol could have oxidized NO to NO$_2$, which may have assisted adsorption further downstream in the LNT.
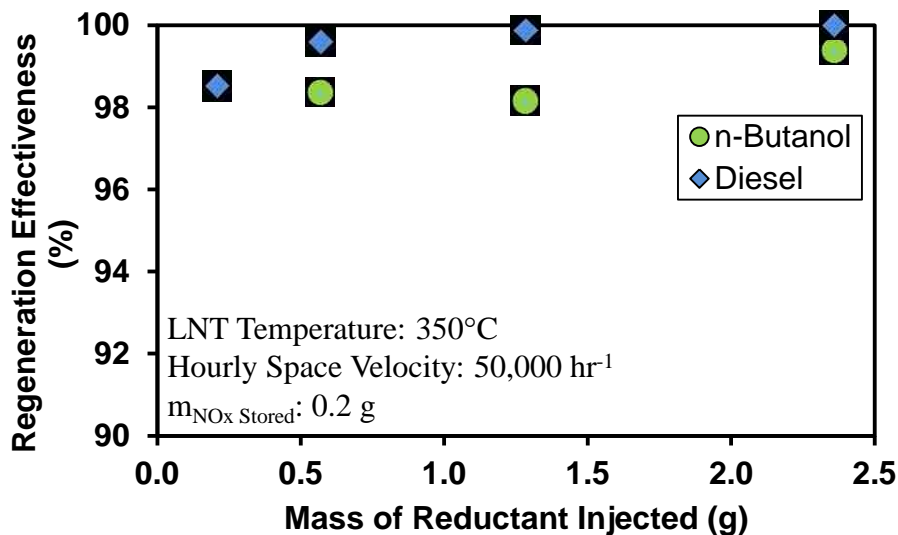
Figure 6.15 – Regeneration Effectiveness (0% Exhaust O_2)

6.2.2   Reduction of NO_x

The concentration of oxygen in the exhaust flow during regeneration can influence the release of NO_x as well as the reduction of NO_x. The formation of N_2O and NH_3 during regeneration of the LNT followed a similar trend to that shown in Figure 6.8. The peak N_2O and NH_3 concentrations during regeneration are shown in Figure 6.16 and Figure 6.17, respectively.

The peak concentration of N_2O slip and NH_3 released during n-butanol regeneration appeared to be largely influenced by the quantity of reductant injection. As the quantity of n-butanol injection increased, so did the peak N_2O and NH_3 concentration. This relationship was also true for the total mass of NH_3 formed. As for the diesel regeneration, the concentration of N_2O and NH_3 appeared fairly constant regardless of the quantity of reductant.
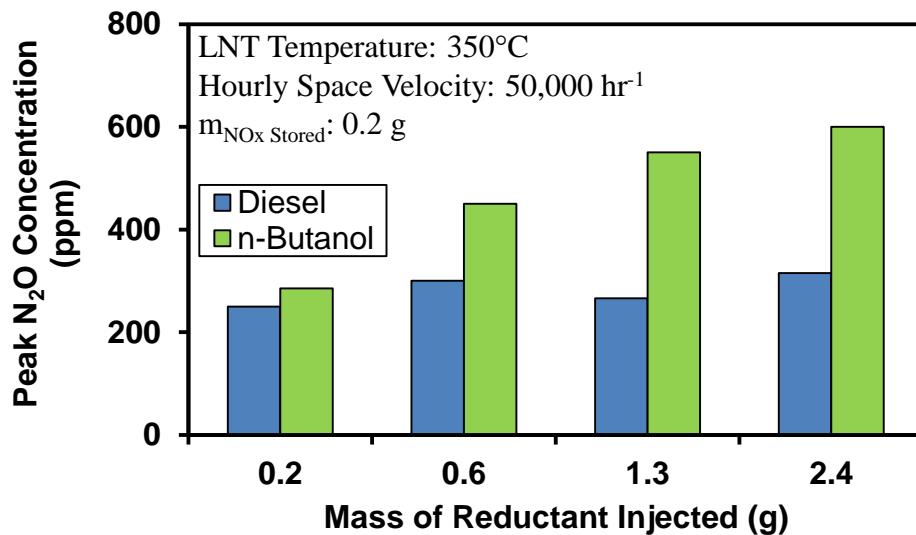
Figure 6.16 – Peak N$_2$O During LNT Regeneration (0% Exhaust O$_2$)
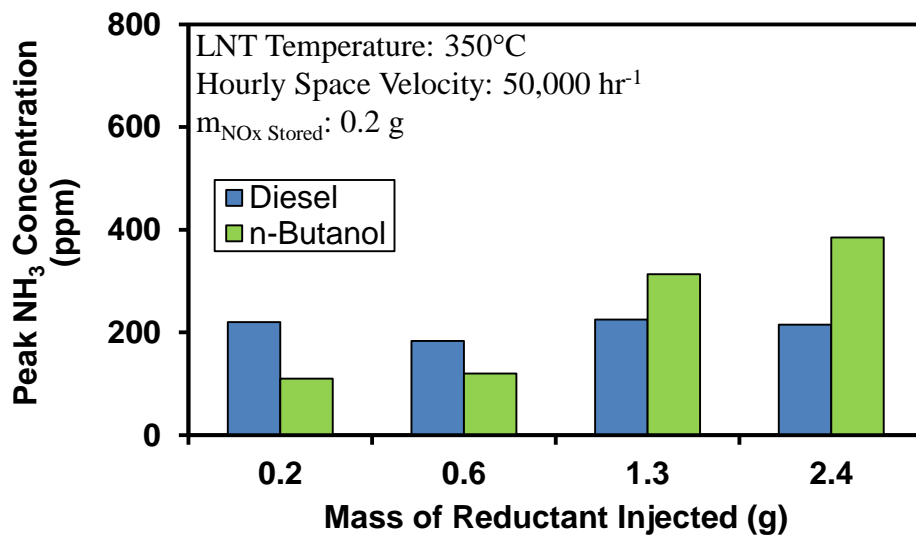
Figure 6.17 – Peak NH$_3$ During LNT Regeneration (0% Exhaust O$_2$)

The selectivity to N$_2$ for diesel and n-butanol regeneration conducted at 0% O$_2$ is given in Figure 6.18. The selectivity to N$_2$ with regeneration using diesel, was higher than regeneration using n-butanol, except for the lowest reductant quantity regeneration. The diesel selectivity to N$_2$ remained relatively constant, with a peak of 84% and the lowest

selectivity to N_2 being about 82% at the lowest reductant quantity. The n-butanol regeneration selectivity to N_2, however, decreased with increasing reductant injection. This was attributed to the high amount of N_2O and NH_3 formed during regeneration with n-butanol, as well as the slightly higher NO_x release with n-butanol. This could be attributed to the significantly higher H_2 generated with n-butanol compared to diesel.
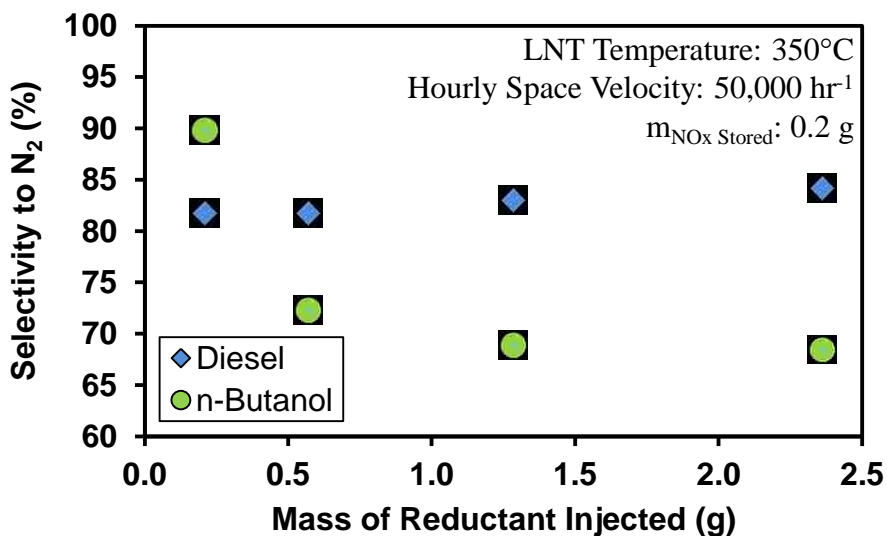
Figure 6.18 – Selectivity to N_2 (0% Exhaust O_2)

Thus, diesel was much more effective in the conversion of NO_x into N_2, than n-butanol, during 0% O_2 LNT regeneration. However, at the lowest reductant quantity regeneration, n-butanol regeneration resulted in over 90% selectivity to N_2, while diesel regeneration resulted in less than 85% selectivity to N_2.

6.3   Summary of LNT Regeneration Test Results

The effectiveness of regeneration for both the 3% O_2 regeneration tests and the 0% O_2 regeneration tests is shown in Figure 6.19. n-Butanol proved to be slightly more effective in regenerating the LNT at 3% O_2, although, both the regeneration effectiveness with diesel and n-butanol initially decreased, then subsequently increased with the

reductant injection. For the 0% O_2 regeneration tests, the diesel and n-butanol regeneration was very effective and relatively independent of the quantity of reductant. Diesel was slightly more effective in regenerating the LNT, however, n-butanol was over 98% effective in regenerating the LNT for each case tested at 0% O_2.
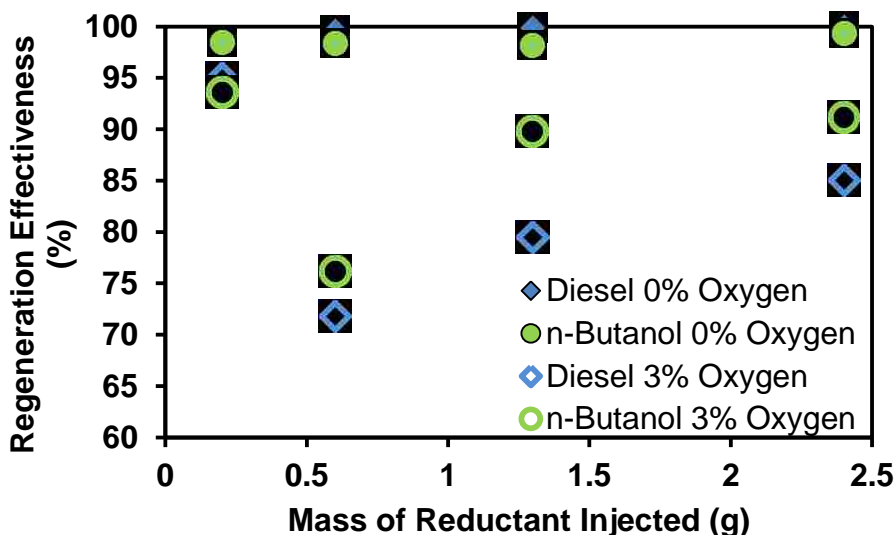
Figure 6.19 – Regeneration Effectiveness at 0% and 3% Exhaust O_2

Comparing the regenerations conducted at 0% O_2 concentration and 3% O_2 concentration, the conversion of NO_x to N_2 was much more efficient with the presence of oxygen. Even though oxygen can contribute to the formation of N_2O from NH_3, the selectivity to both N_2O (Equation 6.3) and NH_3 (Equation 6.4) during regeneration was higher for both diesel and n-butanol regeneration at an O_2 concentration of 0%.

$$N_2O \text{ Selectivity} = \frac{2[N_2O]_{regeneration}}{[N]_{in}} \qquad \text{(Equation 6.3)}$$

$$NH_3 \text{ Selectivity} = \frac{[NH_3]_{regeneration}}{[N]_{in}} \qquad \text{(Equation 6.4)}$$

The selectivity to N_2O is shown in Figure 6.20. The N_2O formed was quite low for both n-butanol and diesel at the lowest reductant quantity of regeneration, at both 3%

86

and 0% O_2. An increase in the N_2O was then noticed as the regeneration reductant quantity increased to 0.6 g. The total N_2O formed then remained relatively constant as the reductant quantity increased further, for all cases. The 0% O_2 regeneration with n-butanol resulted in a higher selectivity to N_2O than all other cases, when the amount of reductant was 0.6 g or greater. For the 3% O_2 tests, the N_2O selectivity was relatively similar with diesel and n-butanol as the reductant, although slightly higher during the diesel regeneration.
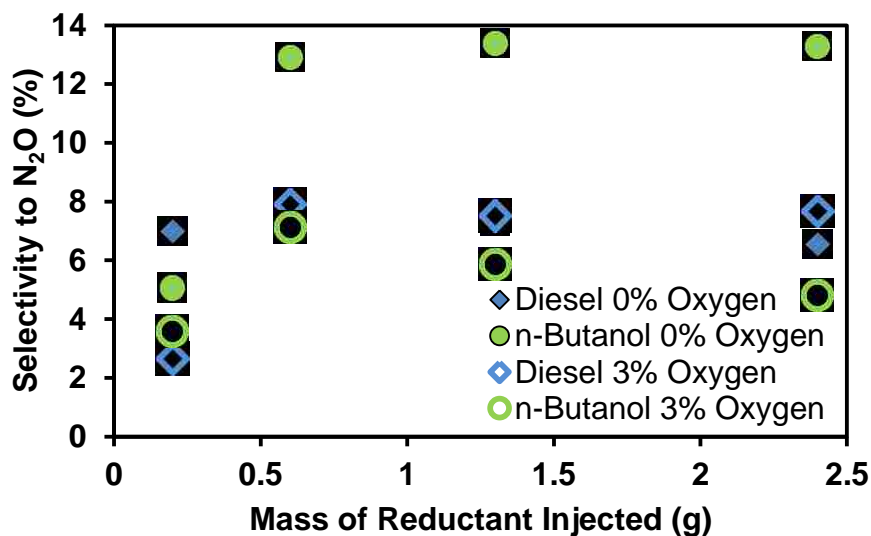
Figure 6.20 – Selectivity to N_2O at 0% and 3% Exhaust O_2

The selectivity to NH_3 is shown in Figure 6.21. The 0.2 and 0.6 g of reductant regeneration did not produce a high quantity of NH_3 for both diesel and n-butanol regeneration at 0% and 3% O_2 concentration. As the regeneration reductant quantity increased to 1.3 g however, the quantity of NH_3 formed increased substantially (as much as double). Finally the NH_3 remained relatively constant as the regeneration reductant quantity increased to 2.4 g. n-Butanol as a reductant for regeneration in the absence of oxygen resulted in a significantly higher selectivity to NH_3. The greatest reductant

regeneration of n-butanol at a 0% O_2 concentration, resulted in 9% selectivity to NH_3, while for every other case, the selectivity to NH_3 was below 6%.
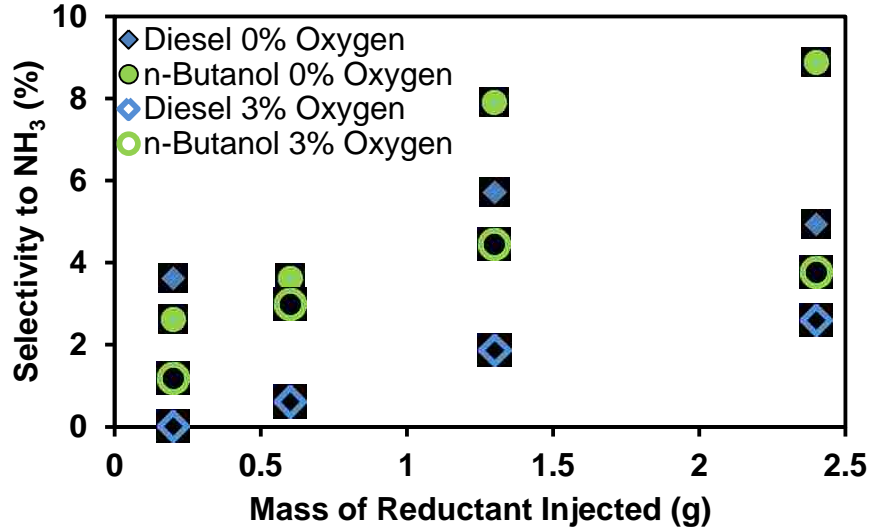
Figure 6.21 – Selectivity to NH_3 at 0% and 3% Exhaust O_2

6.4 Fuel Penalty Analysis

Since the main purpose of the long breathing strategy is to reduce NO_x emissions while also minimizing the fuel penalty associated with an LNT, a comparison of the fuel penalty of a conventional diesel LNT, a low NO_x diesel LNT, and an n-butanol long breathing LNT was conducted. The parameters of each LNT operational strategy are outlined in the following subsections. The fuel penalty associated with the LNT was determined by Equation 6.5 [52].

$$\text{Fuel Penalty} = \frac{\text{Fuel Regeneration (kJ/h)}}{\text{Engine Fuel (kJ/h) - Fuel Regeneration (kJ/h)}} \qquad \text{(Equation 6.5)}$$

6.4.1 Conventional Strategy

The operation of a conventional LNT is largely reliant on driving conditions. Rather than implementing a set time for lean adsorption and rich regeneration, conventional LNTs often apply an adaptive control strategy. This is due to the largely fluctuating exhaust temperatures and engine-out NO_x emissions generally observed during conventional diesel combustion. For this study, a fairly modest mid-load engine-out NO_x emission value of 750 ppm, coinciding with a low EGR level at an engine load of 10 bar, was assumed. Adsorption tests reported in Chapter 4 that an adsorption time of about one minute 20 seconds would thus be required, resulting in approximately 40 regenerations per hour. If a 10 second injection of 0.8 g of diesel (equivalent to a 30 second injection of 2.4 g of fuel) is used for regeneration, the total fuel consumption of the LNT amounts to 32 g of diesel fuel per hour, or over 1300 kJ of lost fuel energy per hour. This amounts to a total fuel penalty of around 3.15% for this research engine at the targeted conditions. This fuel penalty value is in agreement with literature [52, 70].

6.4.2 Diesel LNT with Moderate EGR

Engine-out NO_x emissions can be reduced by applying EGR. At medium load, DI diesel combustion was able to reduce NO_x emissions below 100 ppm, however, PM emission levels were often quite high. In Chapter 4, it was determined that the lowest achievable engine-out NO_x emission concentration was around 200 ppm before the DPF filtration efficiency would need to increase. According to adsorption flow bench tests, this amounted to an adsorption time of around 5 minutes 45 seconds, resulting in about 10 regenerations per hour at 30 seconds per regeneration. Assuming a mass of 2.4 g of diesel fuel is used for regeneration, the total fuel consumption of the LNT amounts to

26.4 g of diesel fuel per hour, or a loss of over 1000 kJ of fuel energy. This amounts to a total fuel penalty of about 2.11% for this research engine at the targeted conditions.

6.4.3   n-Butanol Long Breathing LNT

With DI n-butanol combustion, the application of EGR can reduce engine-out NO_x emissions, without a significant increase in PM emissions. Engine test results in Chapter 4 showed that at a medium engine load of 10 bar, engine-out NO_x emissions were successfully reduced below 100 ppm with the application of EGR. Adsorption flow bench tests showed that with a NO_x inlet concentration of 60 ppm, the adsorption time exceeded 18 minutes, resulting in a total of about three 30 second regenerations per hour. Assuming a mass of 2.4 g of n-butanol fuel is used for regeneration, the total fuel consumption of the LNT amounts to 7.2 g of n-butanol fuel per hour. This amounts to an LNT energy consumption of about 240 kJ per hour and a fuel penalty of 0.39% for this research engine at the targeted conditions.

The total fuel penalty of each strategy is given in Table 6.2. Thus for the given test conditions, the long breathing LNT is able to significantly reduce the fuel penalty associated with NO_x reduction in an LNT, and can potentially be a viable option for NO_x reduction in heavy-duty CI engines.

Table 6.2 – Fuel Penalty Analysis of Various LNT Strategies

Strategy	Engine-Out NO_x (ppm)	IMEP (bar)	Regenerations per hour	LNT Energy Consumption (kJ/hr)	LNT Penalty (%)
Conventional LNT	750	10	40	1376	3.15
Low NO_x Diesel LNT	200	10	11	1032	2.11
Long Breathing n-Butanol LNT	60	10	3	238	0.39

CHAPTER 7: CONCLUDING REMARKS

7.1 Summary of Results

The use of n-butanol for a long breathing LNT strategy was investigated in this study. The main areas of investigation were: n-butanol direct injection engine experiments to determine the suitable operating region for long breathing LNT strategy (i.e. 100 pm of NO_x and 0.036 g/kW·hr of PM), the adsorption characteristics of the selected LNT under long breathing operation, LNT hydrogen reforming with n-butanol, and regeneration of an LNT with n-butanol as a reductant. The experiments were conducted separately using an engine test bench, and an after-treatment flow bench. The results were divided into three parts, and are summarized below.

Long breathing LNT enabling and adsorption tests:

- At low load, DI n-butanol combustion produced low engine-out NO_x and PM emissions suitable for the long breathing strategy; while the low load diesel engine test required EGR to lower the exhaust NO_x to long breathing LNT conditions.

- At medium load, for the conditions tested, the tested diesel engine was not able to achieve low engine-out NO_x and PM emissions simultaneously, which was not suitable for the long breathing LNT strategy. Medium load DI double shot n-butanol required EGR to reduce NO_x emissions in order to use the long breathing LNT strategy, while PM emissions remained ultra-low.

- The LNT storage experiments were conducted on an off-engine after-treatment flow bench. The NO_x adsorption time was increased substantially when the concentration of inlet NO_x was decreased. An adsorption time of over 11 minutes

was observed with an inlet NO_x concentration of 100 ppm, and an adsorption time of over 18 minutes was reached when the inlet NO_x concentration was reduced to around 60 ppm.

- The total NO_x slip downstream of the LNT decreased as the concentration of feed NO_x decreased, even though the period of NO_x slip was longer. Moreover the storage efficiency was enhanced when the NO_x inlet concentration was reduced. A storage efficiency of over 99% was achieved at a NO_x inlet concentration of 60 ppm.

LNT hydrogen reforming tests on the after-treatment flow bench:

- At 3% O_2 concentration, n-butanol produced a greater mass of H_2 compared to the same reductant injection of diesel. With both diesel and n-butanol, the mass of H_2 generated increased, with increasing reductant injection. The mass of hydrogen produced per kJ of reductant reached a peak at the second richest reductant mixture tested with a reductant quantity of 1.3 g. n-Butanol produced a higher mass of H_2 compared to diesel, even though a lower total energy was injected due to the lower heating value of n-butanol.

- At 0% O_2 concentration, n-butanol produced a greater mass of H_2 compared to the same injection of diesel. At the lowest reductant injection, diesel resulted in a higher peak H_2 yield than n-butanol. The mass of H_2 produced per kJ of reductant, decreased with increasing reductant injection, however the magnitude was greater with n-butanol.

LNT regeneration tests on the after-treatment flow bench:

- n-Butanol typically released a higher peak concentration of NO_x during regeneration, however the total mass of NO_x slip during regeneration was lower compared with diesel, for the 3% O_2 regeneration.

- The 3% O_2 regeneration was typically more effective for n-butanol with a regeneration effectiveness of 91% with 2.4 grams of reductant injected, while diesel had a regeneration effectiveness of 85% at the same reductant quantity.

- n-Butanol regeneration resulted in a significantly greater quantity of NH_3 slip, although it still produced a slightly higher selectivity to N_2 than diesel regeneration, with the richest regeneration achieving a selectivity to N_2 of 89%, compared to 87% for diesel.

- At an O_2 concentration of 0%, the amount of NO_x released during regeneration was higher with n-butanol than diesel. Each reductant quantity tested was over 98% effective in regenerating the LNT.

- n-Butanol had a lower selectivity to N_2 compared to diesel, due to the higher amount of NH_3 and N_2O produced during n-butanol regeneration, which was potentially associated with the higher H_2 yield of n-butanol.

- Selectivity to N_2 was greater when oxygen was present in the exhaust flow for both n-butanol and diesel regeneration.

7.2   Recommended Future Work

The following investigations are recommended for future work related to this research:

- The use of EGR with DI n-butanol in a CI engine at high engine loads, i.e. above 12 bar IMEP should be investigated so as to determine whether the long breathing LNT exhaust conditions can be achieved at higher loads with n-butanol fuel.

- Regeneration of an LNT with n-butanol should be tested with more conditions, such as various temperature ranges, greater reductant quantities, shorter or longer regeneration durations, as well as gasoline and n-butanol blends, for lean burn SI engines in order to further validate its potential for future vehicles.

- A combination after-treatment system featuring an SCR downstream of a long breathing n-butanol LNT should be investigated for ultra-low NO_x emissions, and utilization of the NH_3 produced from n-butanol regeneration.

- Various alternative fuels such as ethanol, and biodiesel are of interest for future ICEs and therefore, their use as a reductant for LNT regeneration should be investigated.

- The use of an LNT should be investigated directly on an n-butanol CI engine exhaust system, for a more thorough assessment on its feasibility.

REFERENCES

1. Heywood, J.B., "Internal Combustion Engine Fundamentals", McGraw-Hill Singapore, 1988.

2. United States Environmental Protection Agency, "EPA Emission Standards for Heavy-Duty Highway Engines and Vehicles", https://www.epa.gov/emission-standards-reference-guide/epa-emission-standards-heavy-duty-highway-engines-and-vehicles, 2016.

3. Bailey, R., Clark, H., Ferris, J., Krause, S., Strong, R., "Chemistry of the Environment – 2nd Edition", Academic Press, San Diego, California, 2002.

4. United States Environmental Protection Agency, "NO$_x$ – How Nitrogen Oxides Affect the way we Live and Breathe", EPA-456/F-98-005, 1998.

5. California Environmental Protection Agency Air Resources Board, "Draft Technology Assessment: Lower NO$_x$ Heavy-Duty Diesel Engines", https://www.arb.ca.gov/msprog/tech/techreport/diesel_tech_report.pdf, 2015.

6. California Environmental Protection Agency Air Resources Board, "Mobile Source Strategy", https://www.arb.ca.gov/planning/sip/2016sip/2016mobsrc.pdf, 2016.

7. Environmental Protection Agency, "Greenhouse Gas Emissions and Fuel Efficiency Standards for Medium- and Heavy-Duty Engines and Vehicles – Phase 2", https://www.gpo.gov/fdsys/pkg/FR-2016-10-25/pdf/2016-21203.pdf, 2016.

8. Zheng, M., Reader, G., Hawley, G., "Diesel Engine Exhaust Gas Recirculation – A Review on Advanced and Novel Concepts", Energy Conversion and Management, 45(6), pp. 883-900, 2004.

9. Akagawa, H., Miyamoto, T., Harada, A., Sasaki, S., Shimazaki, N., Hashizume, T. and Tsujimura, K., "Approaches to Solve Problems of the Premixed Lean Diesel Combustion", SAE Technical Paper 1999-01-0183, 1999.

10. Alriksson, M. and Denbratt, I., "Low Temperature Combustion in a Heavy Duty Diesel Engine Using High Levels of EGR," SAE Technical Paper 2006-01-0075, 2006.

11. Asad, U., Zheng, M., Han, X., Reader, G.T. and Wang, M., "Fuel Injection Strategies to Improve Emissions and Efficiency of High Compression Ratio Diesel Engines", SAE Int. J. of Engines, 1 (1), pp. 1220-1233, 2008.

12. Zheng, M., Asad, U., Han, X., Wang, M., Reader, G., "Hydrocarbon Impact on NO_x survivability during diesel low-temperature combustion cycles", Journal of Automobile Engineers: Part D, 224 (2), pp. 271-284, 2010.

13. Han, X., "Study of Fuels and Fuelling Strategies for Enabling Clean Combustion in Compression Ignition Engines", Electronic Theses and Dissertations, University of Windsor, Paper Series 5103, 2014.

14. Zheng, M., Tan, Y., Mulenga, C., Wang, M., "Thermal Efficiency Analyses of Diesel Low Temperature Combustion Cycles", SAE Technical Paper 2007-01-4019, 2007.

15. Fayaz, H., Saidur, R., Razali, N., Anuar, F., Saleman, A., Islam, M., "An Overview of Hydrogen as a Vehicle Fuel", Renewable and Sustainable Energy Reviews, 16(8), pp. 5511-5528, 2012.

16. Hesterberg, T., Lapin, C., Bunn, W., "A Comparison of Emissions from Vehicles Fueled with Diesel or Compressed Natural Gas", Environmental Science and Technology, 42(17), pp. 6437-6445, 2008.

17. Cummins, L., "Internal Fire", Society of Automotive Engineers, Warrendale PA, 1989.

18. U.S. Energy Information Administration, "Today In Energy – Almost all U.S. Gasoline is Blended with 10% Ethanol", http://www.eia.gov/todayinenergy/detail.php?id=26092, 2016.

19. Miller, G. L., Smith, J. L., and Workman, J. P., "Engine performance Using Butanol Fuel Blends", Transactions of the American Society of Agricultural and Biological Engineers, 24 (3), pp. 538-540, 1981.

20. Kinoshita, E., Hamasaki, K., and Imabayashi, R., "Diesel Combustion Characteristics of Biodiesel with 1-Butanol," SAE International Journal of Fuels Lubricants, 5(1), pp.558 – 565, 2011-32-0590, 2012.

21. Chen, G., Yu, W., Li, Q., and Huang, Z., "Effects of n-Butanol Addition on the Performance and Emissions of a Turbocharged Common-Rail Diesel Engine", SAE Technical Paper 2012-01-0852, 2012.

22. Yanai, T., Aversa, C., Dev, S., Reader, G., Zheng, M., "Investigation of Fuel Injection Strategies of Neat n-Butanol in a Compression Ignition Engine", SAE Int. J. Engines, 9(3) pp. 1512-1525, 2016-01-0724, 2016.

23. Jin, C., Yao, M., Liu, H., Lee, C. F., and Ji, J., "Progress in the production and application of n-butanol as a biofuel", Renewable and Sustainable Energy Reviews, 15(8), pp. 4080-4106, 2011.

24. Vertès, A., Qureshi, N., Blaschek, H., Yukawa, H., "Biomass to Biofuels – Strategies for Global Industries", New York, Wiley, ISBN: 978-0-470-51312-5, 2009.

25. Rickeard, DJ., Thompson, ND., "A Review of the Potential for Bio-Fuels as Transportation Fuels", SAE Technical Paper 932778, 1993.

26. U.S. Department of Energy, "Alternative Fuel Data Center – Fuel Properties Comparison",http://www.afdc.energy.gov/fuels/fuel_comparison_chart.pdf, 2015.

27. Granger, P., Parvulescu, V., "Catalytic NO_x Abatement Systems for Mobile Sources: From Three-way to Lean Burn After-Treatment Technologies", Chemical Reviews, 111, pp. 3155-3207, 2011.

28. Budi, P., Howe, R., "Steam Deactivation of CoZSM-5 NO_x Reduction Catalysts", Catalysis Today, 38(2), pp. 175-179, 1997.

29. Shimizu, K., Satsuma, A., Hattori, T., "Catalytic Performance of Ag-Al_2O_3 Catalyst for the Selective Catalytic Reduction of NO by Higher Hydrocarbons", Applied Catalysis B: Environmental, 25(4), pp. 239-247, 2000.

30. Epling, W., Campbell, L., Yezerets, A., Currier, N., Parks II, J., "Overview of the Fundamental Reactions and Degradation Mechanisms of NO_x Storage/Reduction Catalysts", Catalysis Reviews, 46(2), pp. 163-245, 2004.

31. Hachisuka I, Hirata H, Ikeda Y, Matsumoto, S., "Deactivation Mechanism of NOx Storage-Reduction Catalyst and Improvement of Its Performance", SAE Technical Paper 2000-01-1196, 2000.

32. de Ojeda, W., Zheng, M., Han, X., Jeftic, M., Wang, M., "Diesel Engine NO_x Reduction", US Patent 20150113961 A1, 2015.

33. Singh, N., Rutland, C., Foster, D., Narayanaswamy, K., He, Y., "Investigation into Different DPF Regeneration Strategies Based on Fuel Economy Using Integrated System Simulation", SAE Technical Paper 2009-01-1275, 2009.

34. Jeftic, M., "Strategies for Enhanced After-Treatment Performance: Post Injection Characterization and Long Breathing with Low NO_x Combustion", Electronic Theses and Dissertations, University of Windsor, Paper Series 5737, 2016.

35. Park, S., Choi, B., Oh, B., "A Combined System of Dimethyl Ether (DME) Steam Reforming and Lean NO_x Trap Catalysts to Improve NO_x Reduction in DME Engines", International Journal of Hydrogen Energy, 36, pp. 6422-6432, 2011.

36. Mahzoul, H., Brilhac, J., Gilot, P., "Experimental and Mechanistic Study of NO_x Adsorption over NO_x Trap Catalysts", Applied Catalysis B: Environmental, 20(1), pp. 47-55, 1999.

37. Svedberg, P., Jobson, E., Erkfeldt, S., Andersson, B., Larsson, M., Skoglundh, M., "Influence of the Storage Material on the Storage of NO_x at Low Temperatures", Topics in Catalysis, 30(1), pp. 199-206, 2004.

38. Lindholma, A., Currier, N., Fridell, E., Yezerets, A., Olsson, L., "NOx Storage and Reduction over Pt Based Catalysts with Hydrogen as the Reducing Agent: Influence of H_2O and CO_2", Applied Catalysis B: Environmental, 75(1-2), pp. 78-87, 2007.

39. Jeftic, M., Zheng, M., "Lean NO_x Trap Supplemental Energy Savings with a Long Breathing Strategy", Journal of Automobile Engineering: Part D, 227(3), 2012.

40. Abdulhamid, H., Fridell, E., Skoglundh, M., "The Reduction Phase in NO_x Storage Catalysis: Effect of Type of Precious Metal and Reducing Agent", Applied Catalysis B: Environmental, 62(3-4), pp. 319-328, 2006.

41. Theis, J., Ura, J., Li, J., Surnilla, G., Roth, J., Goralski, C., "NO_x Release Characteristics of Lean NO_x Traps During Rich Purges", SAE Technical Paper 2003-01-1159, 2003.

42. Fridell, E., Skoglundh, M., Westerberg, B., Johansson, S., Smedler, G., "NO_x Storage in Barium-Containing Catalysts", Journal of Catalysis, 183(2), pp. 196-209, 1999.

43. Liu, Z., Anderson, J., "Influence of Reductant on the Thermal Stability of Stored NO_x in $Pt/Ba/Al_2O_3$ NO_x Storage and Reduction Traps", Journal of Catalysis, 224(1), pp. 18-27, 2004.

44. Balcon, S., Potvin, C., Salin, L., Tempere, J., Djega-Mariadassou, G., "Influence of CO_2 on Storage and Release of NO_x on Barium-Containing Catalyst", Catalysis Letters, 60(1), pp. 39-43, 1999.

45. Clayton, R., Harold, M., Balakotaiah, V., "NO_x Storage and Reduction with H_2 on $Pt/BaO/Al_2O_3$ Monolith: Spatio-thermal Resolution of Product Distribution", Applied Catalysis B: Environmental, 84(3-4), pp. 616-630, 2008.

46. Wang, J., Yaying J., Easterling, V., Crocker, M., Dearth, M., McCabe, R., "The effect of regeneration conditions on the selectivity of NOx reduction in a fully formulated lean NOx trap catalyst" Catalysis Today, 175(1), pp. 83-92, 2011.

47. Clayton, R., Harold, M., Balakotaiah, V., "Performance Features of Pt/BaO Lean NO$_x$ Trap with Hydrogen as Reductant", American Institute of Chemical Engineers Journal, 55(3), pp. 687-700, 2009.

48. Kočí, P., Plát, F., Štěpánek, J., Bártová, Š., Marek, M., Kubíček, M., Schmeißer, V., Chatterjee, D., Weibel, M., "Global Kinetic Model for the Regeneration of NO$_x$ Storage Catalyst with CO, H$_2$ and C$_3$H$_6$ in the Presence of CO$_2$ and H$_2$O", Catalysis Today, 147S, pp. S257-S264, 2009.

49. Cumaranatunge, L., Mulla, S., Yezerets, A., Currier N., Delgass, W., Ribeiro, F., "Ammonia is a Hydrogen Carrier in the Regeneration of Pt/BaO/Al$_2$O$_3$ NO$_x$ Traps with H$_2$", Journal of Catalysis, 246(1), pp. 29-34, 2007.

50. Jozsa, P., Jobson E., Larsson, M., "Reduction of NO$_x$ Stored at Low Temperatures on a NO$_x$ Adsorbing Catalyst", Topics in Catalysis, 30(1), 2004.

51. Poulson S., Rajaram R., "Regeneration of NO$_x$ trap catalysts", Catalysis Today, 81(4), pp. 603-610, 2003.

52. Kong, Y., Crane, S., Patel, P., Taylor, B., "NO$_x$ Trap Regeneration with an On-Board Hydrogen Generation Device", SAE Technical Paper 2004-01-0582, 2004.

53. Burch, R., Shesov, A., Sullivan, J., "A Transient Kinetic Study of the Mechanism of the NO+H$_2$ Reaction over Pt/SiO$_2$ Catalysts: 1. Isotopic Transient Kinetics and Temperature Programmed Analysis", Journal of Catalysis, 186(2), pp. 353-361, 1999.

54. Yuejin, L., Roth, S., Dettling, J., Beutel T., "Effects of Lean/Rich Timing and Nature of Reductant on the Performance of a NO$_x$ Trap Catalyst", Topics in Catalysis, 16(1), pp. 139-144, 2001.

55. Amberntsson, A., Fridell, E., Skoglundh, M., "Influence of Platinum and Rhodium Composition on the NO_x Storage and Sulphur Tolerance of a Barium Based NO_x Storage Catalyst", Applied Catalysis B: Environmental, 46(3), pp. 429-439, 2003.

56. Epling, W., Yezerets, A., Currier, N., "The Effects of Regeneration Conditions on NO_x and NH_3 Release from NO_x Storage/Reduction Catalysts", Applied Catalysis B: Environmental, 74(1-2), pp. 117-129, 2007.

57. West, B., Huff, S., Parks, J., Swartz, M. et al., "In-Cylinder Production of Hydrogen During Net-Lean Diesel Operation", SAE Technical Paper 2006-01-0212, 2006.

58. Lutz, A., Bradshaw, R., Bromberg, L., Rabinovich, A., "Thermodynamic Analysis of Hydrogen Production by Partial Oxidation Reforming", International Journal of Hydrogen Energy, 29(8), pp. 809-816, 2004.

59. Wang, W., Cao, Y., "Hydrogen-Rich Gas Production for Solid Oxide Fuel Cell (SOFC) via Partial Oxidation of Butanol: Thermodynamic Analysis", International Journal of Hydrogen Energy, 35(24), pp. 13280-13289, 2010.

60. Houseman, J., Hoehn, F., "A Two-Charge Engine Concept: Hydrogen Enrichment", SAE Technical Paper 741169, 1974.

61. G. Hoogers, "Fuel Cell Technology Handbook", CRC Press, Boca Raton, Fl, USA, 2003.

62. Harjua, H., Lehtonena, J., Lefferts, L., "Steam- and Autothermal-Reforming of n-Butanol over Rh/ZrO2 Catalyst", Catalysis Today, 244, pp. 47-57, 2015.

63. Kang, I., Bae, J., "Autothermal Reforming Study of Diesel for Fuel Cell Application", Journal of Power Sources, 159(2), pp. 1283-1290, 2006.

64. Sorensen, B., "Hydrogen and Fuel Cells", Elsevier Ltd., Oxford, UK, 2005.

65. Asad, U., Kumar, R., Han, X., Zheng, M., "Precise Instrumentation of a Diesel Single-Cylinder Research Engine", Measurement, 44(7), pp. 1261-1278, 2011.

66. Forzatti, P., Lietti, L., "The Reduction of NO_x Stored on LNT and Combined LNT-SCR Systems", Catalysis Today, 155(1-2), pp. 131-139, 2010.

67. Theis, J., Gulari, E., "A LNT + SCR System for Treating the NO_x Emissions from a Diesel Engine", SAE Technical Paper 2006-01-0210, 2006.

68. Snow, R., Cavatatio, G., Dobson, D., Montreuil, C., Hammerle, R., "Calibration of a LNT-SCR Diesel Aftertreatment System", SAE Technical Paper 2007-01-1244, 2007.

69. Parks, J., Prikhodko, V., "Ammonia Production and Utilization in a Hybrid LNT + SCR System", SAE Technical Paper 2009-01-2739, 2009.

70. Majewski, W., "NO_x Adsorbers", DieselNet Technology Guide, https://www.dieselnet.com/tech/cat_nox-trap.php, 2016.

APPENDIX A: GAS MIXER OPERATION

The gas mixer used for this study was an Environics Series 2000 Multi-Component Gas Mixer. Each of the six ports of the gas mixer features an industry standard mass flow controller (MFC) device, which can accurately control the mass flow of each gas. These MFCs operate on a closed loop system which measures the thermal loss of a cross section to the gas flowing through the individual MFCs. The MFC rating for each port is given in Table A.1. Each port was calibrated with a different gas in order to determine the maximum error in measurement, for each port. The calibration curve for port 1 is given in Figure A.1.

Table A.1 – Gas Mixer Port Specifications

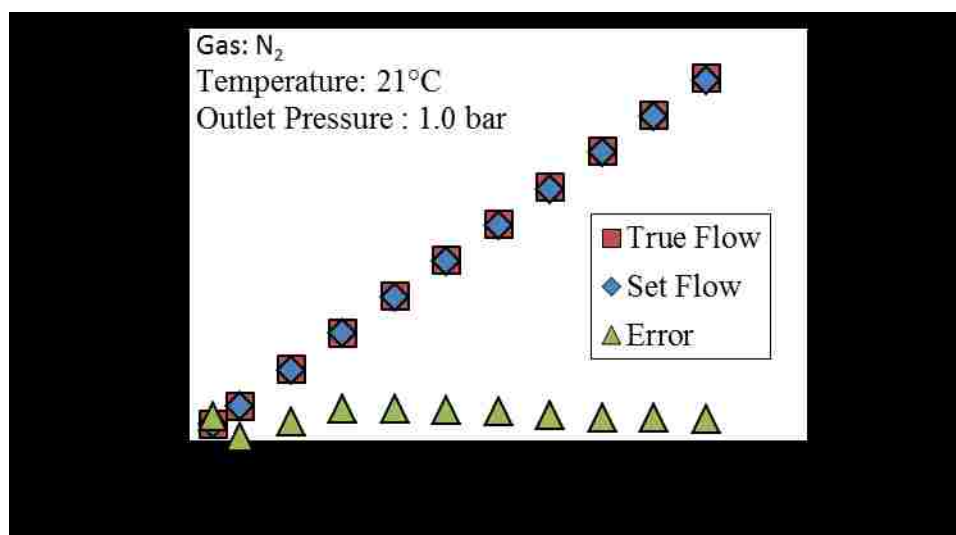| Port	Calibrated Gas	Maximum Flow Rate
1	N_2	350 L/min
2	O_2	120 L/min
3	CO_2	90 L/min
4	C_3H_6	30 L/min
5	CO	30 L/min
6	NO	15 L/min

Figure A.1 – Port 1 Calibration Curve

The tests conducted in this study only utilized the first port of the gas mixer in order to accurately control the flow of balance air through the after-treatment flow bench. The gas mixer is shown in Figure A.2 and the front control screen is shown in Figure A.3.
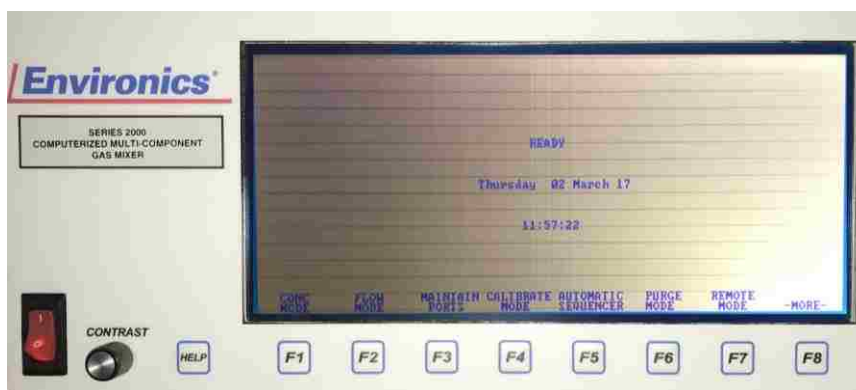

Figure A.2 – Photograph of the Gas Mixer

Figure A.3 – Front Panel of the Gas Mixer

The gas mixer can be controlled through either the in-built front panel keyboard, or via a personal computer connected through the RS-232 serial port in the back of the gas mixer.

For this study an open-source software implemented terminal emulation program called "Tera Term", was used for serial control of the gas mixer. In order to enable communication through the RS-232, the serial communication was activated by selecting remote mode (button F7 on the front of the gas mixer) to access the serial communication settings screen. -Com1- was turned on, and the terminal type was set as VT100.

The terminal emulation program displayed the front display of the gas mixer, and allowed for serial control of the 8 buttons listed as "F1 – F8" in Figure A.3. This program allowed for two different types of communication: TCP/IP for communication through the internet or a private network, and serial (Figure A.4).

Figure A.4 – Tera Term Connection Settings

Once the appropriate mode of communication is selected, the terminal will display the front screen of the gas mixer, with each of the selectable button labels (Figure A.5). The display screen font size and colour scheme can be altered through the setup drop down menu at the top of the window.
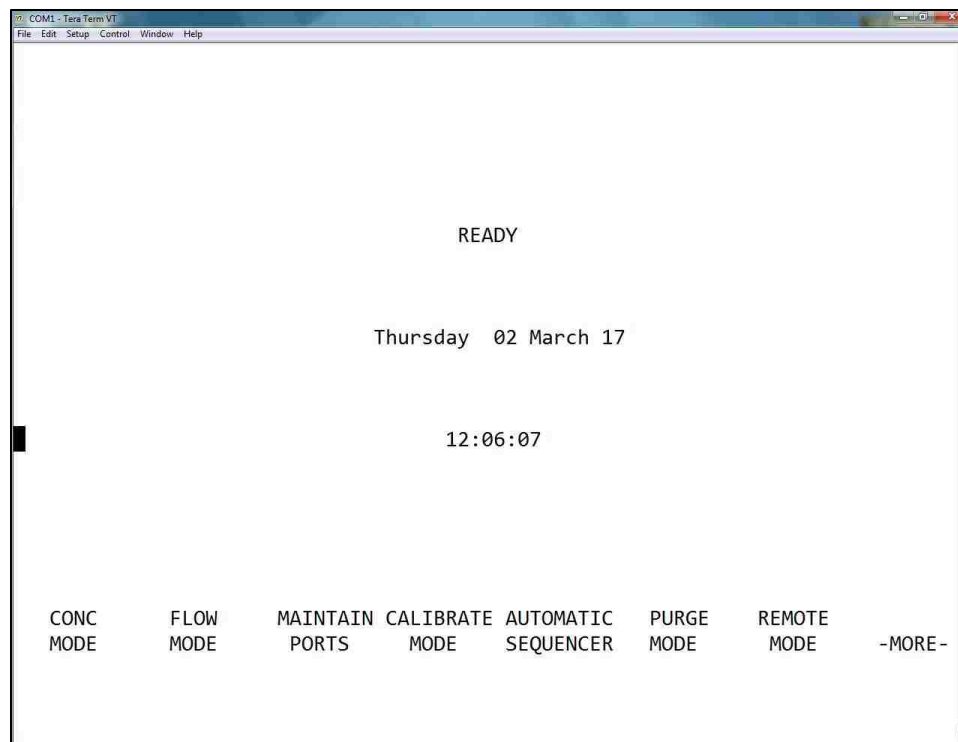
Figure A.5 – Gas Mixer Main Menu

The eight buttons on the front panel of the gas mixer can be triggered by pressing the "F" key on the computer keyboard, followed by the key "1" to "8" for the number button that is to be selected (i.e. 1 – 8 moving left to right).

Although each port was calibrated for specific gases, the gas entering each port can be changed according to the user's requirements. The use of lighter gases such as H_2, or helium (He), however, require special MFCs not found on the standard Series 2000 gas mixer. In order to alter the gases for each port, "maintain ports" must be selected. To select maintain ports, the user must press the "F" key and the "3" key (hereby signified as F-3) on the keyboard in succession. The maintain ports screen is shown in Figure A.6.

Figure A.6 – Gas Mixer Port Maintenance

The user can then use the arrow keys on the keyboard to select the port which requires a different gas. By pressing F-5 (select gas) on the port that is to be changed, the user can select a name from the system library of gases (Figure A.7). F-2 and F-3 can be used to navigate from page to page of the system library. The user can also enter the name of the gas manually by pressing F-3.

Figure A.7 – Gas Mixer Gas Selection

If any of the cylinders entering the gas mixer is a blend of gases, then the concentration of the gas specified must be input by the user. The concentration of the gas and the type of gas used as a balance can affect the K-factor which in turn will affect the mass flow measurement. Thus, compute K (F-1 from the maintain ports screen) should be selected (Figure A.8). In the example shown, the gas cylinder contains 10% nitric oxide, with balance nitrogen. If lower concentrations or more types of gas are required, the concentration can be changed to a ppm scale (F-1), and the gas type can be selected from the gas library by pressing F-1. The K-factor is computed by using a conversion factor table within the gas mixer computer.
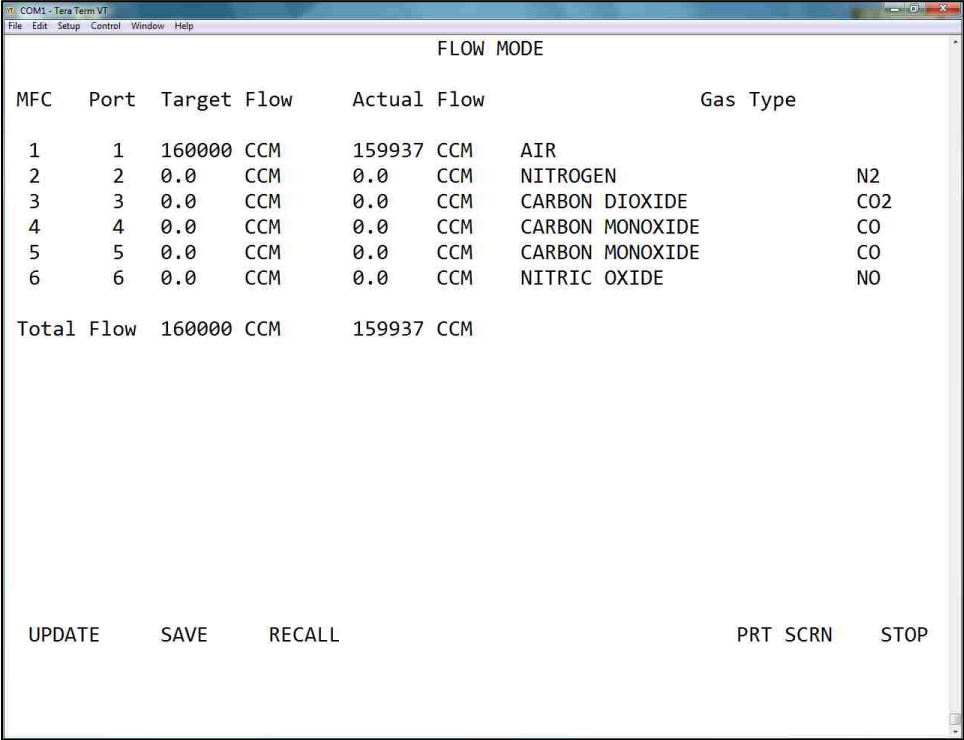
Figure A.8 – Gas Mixer Compute K-Factor

Before operating the gas mixer, each gas must be pressurized above the minimum specified pressure (30 psig for port 1 and 10 psig for every other port) and below the maximum specified pressure of 100 psig for each port. The pressure at each port inlet must be stable for proper operation of the MFCs.

The gas mixer has two main modes of operation: concentration mode and flow mode. To select concentration mode, the user must press the F-1 key combination from the home screen. In concentration mode the user can specify the desired concentration of each gas using the numbers on the keyboard, in either % or ppm. During mixing the actual output gas concentration will be displayed on the screen. Environics specifies an accuracy of ±1.0%. To begin flow the user must press the F-1 keys, and to stop flow the user can press the F-8 keys.

Flow mode (F-2 from the home screen) can also be used to control the output gas flow rate, by specifying the target flow of each port in cubic centimetres per min (CCM). After the flow of each port is specified, the actual flow will be displayed (Figure A.9). The flow rate can be updated periodically by entering a new desired flow rate, and pressing F-1. If at any time, the actual flow of any port is less than 50% of the commanded flow rate, a low flow warning message will be displayed, and all MFC will be shut down. Again, to stop flow the F-8 keys should be pushed in succession.

Figure A.9 – Gas Mixer Flow Mode

LIST OF PUBLICATIONS

Refereed Journals

1. Yanai, T., **Aversa, C.,** Dev, S., Reader, G., Zheng, M., "Investigation of Fuel Injection Strategies for Direct Injection of Neat n-Butanol in a Compression Ignition Engine", SAE International Journal of Engines, 9(3), 2016-01-0724, 2016.

2. Yang, Z., Dev, S., Jeftic, M., **Aversa, C.**, Ravi, A., Ting, D., Zheng, M., "Preliminary Investigation of Exhaust Pressure Waves in a Single Cylinder Diesel Engine and the Impacts on Aftertreatment Sprays", SAE International Journal of Engines, 10(2), 2017-01-0616, 2017.

Non-Refereed Conference Proceedings

3. **Aversa, C.**, Yang, Z., Tan, Q., Yu, X., Yu, S., Zheng, M., "Preliminary Investigation on the Ignition Characteristics of a Three-Pole Spark Plug Under Lean or CO_2 Diluted Conditions", Proceedings of Combustion Institute – Canadian Section, 2016.

4. Yang, Z., **Aversa, C.**, Ives, M., Divekar, P., Ting, D., Zheng, M., "Hydrogen as a By-Product of Diesel Engine Low Temperature Combustion", Natural Gas and Hydrogen Storage Symposium, 2015.

5. Bryden, G., **Aversa, C.**, Divekar, P., Zheng, M., "Preliminary Investigation of the Influence of Low Temperature Combustion on Diesel Heat Release Profiles", Proceedings of Combustion Institute – Canadian Section, 2013.

Poster Presentations

6. **Aversa, C.**, Divekar, P., "Engine Efficiency Improvement for Biofuels in Low Temperature Combustion Application", BioFuelNet Canada, Advanced Biofuels Symposium, Vancouver, BC, 2016.

7. Divekar, P., **Aversa, C.**, "Advanced Ignition Systems for Biofuel Combustion", BioFuelNet Canada, Advanced Biofuels Symposium, Vancouver, BC, 2016.

8. Ives, M., **Aversa, C.**, Jeftic, M., "Biofuels for Advanced Engine Technologies", NSERC CREATE Program in Clean Combustion Engines, Combustion Summer School, Toronto, ON, 2016.

9. **Aversa, C.**, Ives, M., "Biofuels for Advanced Engine Technologies", Auto21 Final Conference, Ottawa, ON, 2016.

VITA AUCTORIS

NAME:	Christopher Aversa
PLACE OF BIRTH:	Windsor, Ontario, Canada
YEAR OF BIRTH:	1992
EDUCATION:	B.ASc Mechanical Engineering University of Windsor 2010-2014
	M.ASc Mechanical Engineering University of Windsor 2014-2017